DEGRADATION STUDIES OF PPV & CN-PPV THIN FILMS

By

Debju Ghosh

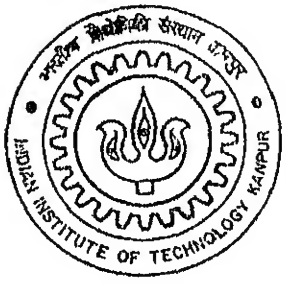

MATERIALS SCIENCE PROGRAMME

Indian Institute of Technology Kanpur

MARCH, 2003

DEGRADATION STUDIES OF PPV & CN-PPV THIN FILMS

A Thesis Submitted in
Partial Fulfilment of the Requirements
For the Degree of

Master of Technology
in
Materials Science Programme

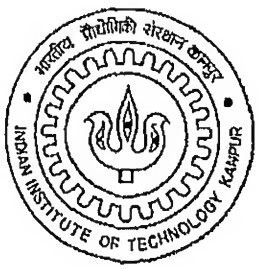

By
Debju Ghosh

to the
Materials Science Programme
INDIAN INSTITUTE OF TECHNOLOGY
Kanpur
March, 2003

CERTIFICATE

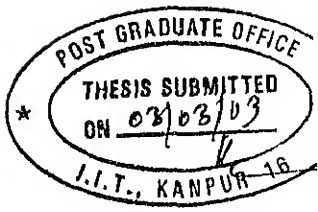

This is to certify that the work presented in this thesis entitled **"Degradation Studies of PPV & CN-PPV Thin Films"**, by **Debju Ghosh**, has been carried out under my supervision and has not been submitted elsewhere for a degree

Dr Y. N. Mohapatra
Professor
Materials Science Programme,
SAMTEL Centre for Display Technologies
& Department of Physics
Indian Institute of Technology, Kanpur

March 2003

ACKNOWLEDGEMENT

I would first of all like to thank my supervisor, Dr Y. N Mohapatra for his valuable guidance, critical discussions, timely help and continuous encouragement throughout my thesis work. I am also very grateful to Dr J. Narain, Dr R.Sharan and Dr. R. S. Anand along with Dr Asha for their help in device preparation during my thesis Specifically this work would not have been possible without the supply of materials synthesized by Mr. Anand Biswas and others in the Chemistry Group of Samtel Centre for Display Technologies, IIT Kanpur.

I also like to express my deep gratitude to other faculty members of Materials Science who taught me during my coursework and helped in proper understanding of my subjects.

I also specially like to thank Mr. Girija Samal for his kind help throughout my thesis work I would also like to thank Rahul Dubey, Vishal Varshney, Samarendra Pratap Singh, Vineet Rao and Vibha Kumar for their help from time to time. I am also thankful to Amitesh for his help

I am thankful to my friends especially Pradip, Arindam, Shiladitya and to all my batch mates whose encouragement and continuous interaction led to successful completion of my course and thesis work

The love, care and constant encouragement from my family are invaluable support that I got throughout the course of study.

Debju Ghosh

TABLE OF CONTENTS

LIST OF TABLES

LIST OF FIGURES

Abstract

Degradation of active polymer materials in presence of light, oxygen and moisture is known to be the most important reason limiting the lifetime of devices fabricated using light emitting polymers. In this thesis, we focus on monitoring of degradation of two most popular light emitting polymers PPV and CN-PPV We develop a procedure for accelerated laser induced degradation and quantify degradation rate by monitoring loss of photoluminescence (PL). We use this procedure to optimise thin film preparation conditions in terms of ambient and heat treatment schedule.

Polymeric thin films of PPV and CN-PPV were spin-coated on glass substrate under different baking conditions. PL and degradation was studied using 442 nm line of He-Cd laser with 0.5mW/mm^2 power Laser induced degradation in air of PPV films show second order exponential decay along with changes in components of PL spectra, which has four Gaussian peaks at 508, 543 1, 581, 604 nm. The rates of decay of individual components are different Similar experiments with laser irradiation for vacuum dried PPV films show PL enhancement in vacuum, in contrast to PL decay in air Degradation in air is slower for vacuum dried samples compared to oven dried samples in nitrogen atmosphere demonstrating efficacy of vacuum drying in reducing oxygen content of processed films No peak shift occurs when laser irradiation is carried out under vacuum clearly indicating absence of production of quenching centres, which affect conjugation length of polymer chains

Laser induced PL degradation in air of CN-PPV films coated and baked in air show dominantly first order exponential decay for baked samples, while the decay is second order for unbaked samples. No peak shift is observed in CN-PPV with decrease in PL intensity showing that degraded chains do not give rise to PL, most probably owing to diffusion of carriers from degraded to undegraded chains. Degradation rate for samples baked in nitrogen ambient is slower compared to air baked samples indicating role of trapped oxygen or moisture in the film. For unbaked samples, decay of PL intensity is seen initially and then enhancement is observed at longer times suggesting competition between degradation and in-situ drying. First order exponential decay is observed for baked CN-PPV samples in contrast to second order for unbaked CN-PPV samples and PPV samples in all cases. Laser irradiation in vacuum for CN-PPV films prepared under nitrogen ambient show PL enhancement Significant resistance to photo-degradation is observed even in air after laser irradiation under vacuum.

Some of the common instabilities observed in electrical characteristics of single layer devices are described. The electroluminescence decay measurements on double layer encapsulated PPV-CNPPV device show that at the present stage of our device development effort in the Laboratory, the lifetime is limited by faster process than material degradation due to photo-oxidation.

In short, we demonstrate the importance of laser induced accelerated degradation tests, and also show that the resistance to degradation of light emitting polymers can be increased by UV laser irradiation under vacuum.

1. Introduction

Displays are crucial to all man-machine interactions including information and entertainment industry. Cathode Ray Tubes has been so far the most used device However, today many alternatives flat display devices to bulky, power hungry cathode ray tube (CRT) as are being developed Technology based on Liquid Crystal Display is so far the best entrenched of flat panel technologies. But the problem still persists regarding the cost and the low efficiency of these displays. LCDs suffer from many disadvantages. Not being self-emissive, they require backlighting and hence are not efficient They are not bright and have severe viewing angle limitations The developments in the last decade in organic and polymeric light emitting diodes has led to tremendous possibilities in terms of cheap, flat, true colour and bright emissive displays. Organic light emitting diodes is likely to emerge as major flat panel technology

Light emitting diodes are about the production of light under application of forward bias, the basic mechanism being the conversion of electrical energy to light There is injection of electrons and holes from cathode and anode respectively resulting in recombination and successive emission of light The wavelength of the light emitted depends on the band gap of the semi-conducting materials between the electrodes. Organic light emitting diode differs from conventional inorganic light emitting diode by incorporating either a polymer layer or a layer of small molecules between the electrodes One of the electrodes needs to be transparent to facilitate the light output and hence typically ITO (Indium Tin Oxide) is chosen to be the anode, which is both conducting and transparent. For injection of holes the electrode needs to be a high work-function material (ITO 4.5-5.3 eV) compared to low work-function metals (Al 4.3 eV, Mg 3.7 eV, Ca 2 9 eV) for cathode to inject electrons. Since the first announcement of OLED by Tang and VanSlyke (1987) using small molecule Alq_3, there has been a significant advances in this area with the promise of emerging technology having several advantages such as wider viewing angle, better resolution and faster response time.

The light emitting devices fabricated using polymer material (PLED) instead of small molecules have added advantage of ease of fabrication using spin-coating, inkjet

printing and screen printing (Padro *et al*, 2000; Birmstock *et al*, 2001). These methods of fabrication can easily be adapted to large area applications

The light emitting property of polymers under application of bias arises from the conjugation of alternate single and double bonds resulting in a delocalized pi-electron system along the polymer backbone, which supports negative and positive charge carriers along the chain These charges are transported and they recombine to give luminescence from the material Among the most popular group of materials introduced were PPV (poly-para-phynylene-vinylene) with band gap of nearly 2 4eV and cyano substituted PPV (CN-PPV) with band gap of 2 1 eV and then MEHPPV with bandgap of 2.2eV PPV has the luminescence in the greenish yellow region with CNPPV & MEHPPV in the red and orange region respectively. Properties of these polymers can be tuned through chemical design methods of changing the backbone or sidegroups

The potential for making large-area flat panel displays (Onada *etal*, 1995) from easily processable polymers has driven much of the recent research in the area of Polymeric Light Emitting Diodes(PLEDs) Parker (1994) first reported systematic investigation of the charge injection properties of different metal contacts in a single layer device. For OLED the materials should be chosen by following criteria:

(a) Emitting region mainly near the visible range of spectrum.

(b) Electronic band-matching of organic and metallic layers (Roman *et al*, 1996; Ishii *et al*, 1997), i.e. harmonious charge injection (Watanabe *et al*) from the metal electrode into the organic layer, and charge confinement in the emitting zone (Hamaguchi *et al.*, 1996)

(c) Charge carrier mobility in organic layers and determination of exact emitting zone (Antoniadis *et al*, 1997)

(d) Mechanism of interfacial reaction between organic and metallic layers and the solution of contact problem

The polymeric materials PPV and CN-PPV both are conventionally used as PPV acts as a hole transport layer and CN-PPV as electron transport layer. In such a multilayer recombination occurs in the CNPPV region as the mobility of electrons in CN-PPV is less

as compared to mobility of holes in PPV. The injection of electrons forming a bottleneck in efficiency of device. But the main problem hindering full commercialization is the lifetime of PLED devices. On encapsulation, there is increase in the device lifetime. With careful fabrication practices, lifetimes in the order of 10,000 – 40,000 hrs have been reported in the literature. However issues controlling degradation and lifetime are not well understood. Even on controlling the contact degradation by encapsulation, there is problem of photo-oxidation under the ambient light and also from the light generated from within the device itself. The remnant oxygen present in PPV itself in its precursor used for spin-coating can be responsible for degradation. Also there are reports of diffusion of oxygen from ITO. Hence, the photo-degradation of the material itself restricts the lifetime even in an encapsulated device

On the road to widespread commercialization of PLED technology, there is a urgent need for studies on the factors affecting degradation, and specifically steps which can be taken to control the photo-degradation in the material to improve the lifetime of devices

1.1 ORIGIN OF THIS WORK

Keeping in view international developments in this filed, organic and polymeric diode based displays are being developed at Indian Institute of Technology, Kanpur by an interdisciplinary group at Samtel Centre of Display Technologies (SCDT). Basic materials needed for this research are being synthesized and tested for suitability of devices. In the course of development of this work, deposition of thin polymer films and their characterization as regards their suitability has become an important component

1.2 STATEMENT OF PROBLEM

Among the chief concerns of material and device development in Polymeric LED technology is degradation of luminescence in presence of light and air ambient. Though there have been many studies on the degradation of specific polymer called MEH-PPV. Of the two most important materials for PLED application, photodegradation of PPV has been studied to some extent whereas CN-PPV is yet to be studied. A coherent understanding of photodegradation is yet to emerge.

In this work, we specifically want to develop a method of accelerated photo-degradation so that degradation resistance of materials and thin films grown in the technology development effort can be studied Such studies besides giving insight to material degradation mechanism, can be fruitfully be used to quantify degradation resistance and hence can be used to optimize process parameters while depositing thin films.

We seek to study degradation of PPV and CN-PPV films spin-coated in different ambients (nitrogen, air and vacuum) and baking conditions. We use photoluminescence as a chief measurement tool in order to focus on material degradation issues as separate from device degradation issues The problem of degradation of PLEDs is very wide in its scope. Hence we limit ourselves to material degradation under UV laser irradiation, and to an enumeration of some of the problems encountered in monitoring electrical degradation of devices used in the early stage of their development

1.3 ORGANIZATION OF THE THESIS

In Chapter 2, background and perspective of technologies being used for flat panel displays are described to bring out principles and advantages of Organic Light Emitting Diodes. In Chapter 3, principles of some of the important characterization techniques are described Chapter 4 is a brief review of the degradation studies related to photo-oxidation of light emitting polymers Chapter 5 describes the materials and methods along with the experimental setups used for this work. The main results and conclusions are detailed in the following two chapters

2. Background & Perspective

2.1 LCD-Liquid Crystal Displays

2.1.1 Background

LCDs are based on the unique properties of liquid crystals. Liquid crystals are an intermediate form between disordered molecules in a liquid and the ordered molecules in a crystalline solid form, yielding a liquid with a crystalline behaviour. The phenomena of the liquid crystals have been known for over 50 years but were not used in displays until the discovery of the properties of *twisted nematic* in 1971, which lead to the start of a new display era The advantages compared to CRT are lower power consumption, thinner structure and less flickering The disadvantages on the other hand consist of a poor viewing angle, more expensive manufacturing and unreliable colour performance

2.1.2 Working Principle

LCD works as a light modulator by affecting the polarization angle of a liquid crystal using an electrical field. The display does not emit any light by itself and must therefore be illuminated reflectively or by background lighting. LCD consists of a number of liquid crystal cells forms the display. The thin glass layers encapsulating the liquid have a very thin row like patterns allowing the rods only to be placed in the same orientation as the patterning. On placing the glass layers with a 90° difference, they affect the rods in the liquid to be twisted by 90°. This configuration is called *Twisted Nematic* (TN) and can be seen in Figure 2.1.2.1

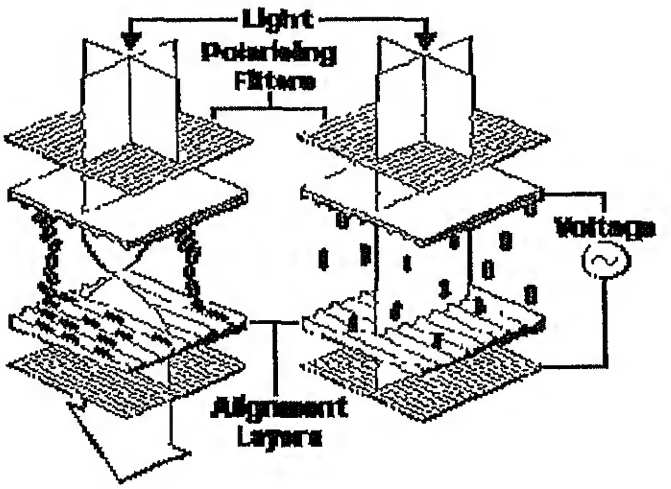

Fig 2.1.2.1: A typical schematics of LCD operation (Thesis Stark *et al*)

When an electrical field is applied to the liquid crystal cell the rods orient randomly and no twist of the polarizing angle is achieved. Two polarization filters are placed at each side of the liquid crystal layer that can be arranged in a parallel or a crossed manner depending on function desired. If they are placed parallel, the LCD is in black mode and only allows light to pass if a voltage is applied. In white mode, the display allows the light to emit through if there is no voltage and block the light when a voltage is applied. Due to the parallel filter arrangement a small light leakage is apparent even when the display should be dark. This leading to a lower contrast ratio for black mode displays compared to white mode displays Different grayscale levels are achieved through modulating an analog driving voltage to change the amount of twist of the rods

2.1.3 Types of LCD

LCDs can be also classified as reflective and transmissive displays. The transmissive LCD is illuminated by a backlight behind the display panel, which is often a fluorescent tube, or a panel of LEDs that is positioned in such arrangement that it covers as large area as possible. A prism can also be used to enhance the distribution of light. One common method to display full-colour is achieved by splitting each pixel into three side by side placed sub pixels, one for each *RGB* colour, red, green and blue. The sub pixels contain band pass filters usually dyes that are filtering the white light from the backlight to achieve the right wavelength. But a reflective LCD uses the light from an external light source, which the panel reflects. It is also possible to use reflective display without an external light source in environments with a high surrounding illumination, e g. mobile phones and hand calculators.

One drawback for reflective LCDs is that the field-sequential colour representation results in a three times faster refresh rate needed, compared to transmissive LCDs. To avoid this a rotating colour scheme can be used. This works by dividing the screen into three equal parts for each colour, which continuously moves over the display surface resulting in a three times faster frame rate (Shimizu, 2000). Another drawback is that the position of the reflective light source can limit the viewing angle, allowing the display only to be used in near-eye or projection applications. But the pixels do not have to be that tight patterned compared to transmissive displays, where the pixels must be three times tighter patterned due to the sub pixel colour representation.

2.2 OLED – Organic Light Emitting Diodes

2.2.1 Device Structure

2.2.1.1 Single Layer Structure

The device structure consists of anode and cathode with polymer in-between The anode injects hole and hence should have a higher work function compared to cathode material to inject holes The anode ITO (Indium Tin Oxide) and cathode metal are on two sides of the polymer material in device configuration The reason for using ITO in light emitting devices is requirement for one of the electrodes to be transparent so that the emitted light is able to come out. ITO serves both purpose as a transparent & electrically conducting material. The ITO sputtered thin film glass plates are available commercially. The polymer is spin coated above the ITO film and then subsequently cathode material deposited at the top. The schematic of device structure is shown in Figure 2.2 1 1 1

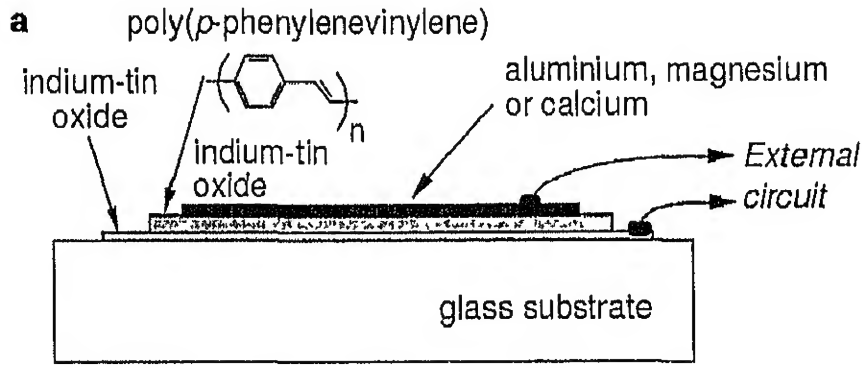

Fig 2.2..1.1.1: OLED device structure (Friend *et al*)

But ITO films on glass cannot be used for fabrication of flexible displays due to inflexible glass. For the purpose of flexible displays, Al-doped zinc oxide (AZO) (Zhao *et al.*, 2001) below ITO can be used as anode. Polyaniline (Karg *et al*, 1996) is also reported to be viable as anode material for hole injection. There are also reports of indium contamination from ITO and the resulting degradation (Chao *et al*, 1996, Schlatmann *et al*, 1996). To avoid this problem, conductive polymeric layer is inserted in between the ITO and the luminescent polymer layer. The layers used are polypyrole (PPY) (Vaz *et al*, 2001) and PEDOT. Polyfluorenes (Sainova 2000) used before the cathode results in pronounced increase of luminescence efficiency. Oxygen plasma (Milliron *et al.*, 2000) treatment of ITO results in increase of workfunction resulting in better injection of holes

2.2.1.2 Double Layered Structure

The single layer device layer used has lower efficiency as PPV has lower barrier for holes compared to that for electrons Hence PPV transports holes more effectively than electrons and hence the injection of electrons limits the efficiency. Similarly for CNPPV the case is just opposite where the injection of electrons is easier So if a double layer structure with ITO-PPV-CNPPV-Al is used then PPV acts as hole transport layer and CNPPV as electron transport layer resulting in balance and higher efficiency of the device due to better injection and charge confinement (Greenham *et al*, 1993). Also there is less quenching of electrons and holes due to better balance and the device is also brighter In the double-layered device the recombination mostly takes place in the CNPPV region as it has a lower bandgap (2.1eV) compared to PPV (2 4eV) and also because the mobility of holes through PPV is higher compared to that for electrons in CNPPV. Hence if a very thin layer of CNPPV is used compared to PPV then the recombination may take place in the PPV region Also the recombination zone depends on the applied voltage and also on temperature of operation as the mobilities are dependants on temperature. A figure of the structure is shown in Figure 2 2.2.2 1

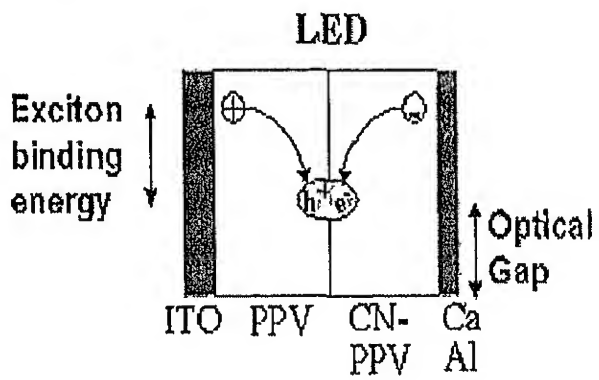

Fig 2.2.1.2.1: The electrons and holes then travel through the polymer layer, combine to form an exciton, and emit a photon of visible light (Greenham *et al.)*

2.2.1.3 Multi-layered Device Structure

To further improve the efficiency of the device, three or multi-layered structures are used. In the three-layered structure, a desired electroluminescent material is used in between the hole and electron-transporting layer. . Typical structures of an OLED cell are shown in Figure 2.2.1 3.1

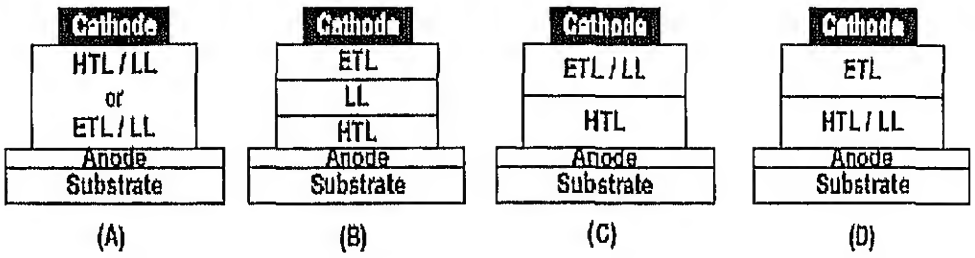

Fig 2.2.1.3.1: ETL-Electrons Transport Layer, LL-Luminescence layer, HTL-Holes Transport Layer

Further transporting layers are also used to improve the efficiency by increasing the probability of the electron-hole recombination. In the recombination electron hole pairs called excitons are formed, which may decay radiatively or phononically depending on the spin of electrons and holes. If the spins are in opposite directions then radiatively decaying singlet exciton is formed, otherwise triplet exciton is formed which decays as thermal energy or heat.

2.2.2 Organic Semiconductors

2.2.2.1 Semiconducting polymers and their applications

Traditionally polymers have been associated with insulating properties in the electronic industry and are applied as insulators of metallic conductors or photoresists Since the serendipitous discovery in 1977 of the doping of polyacetylene, which resulted in increase of the conductivity of polyacetylene by eleven orders of magnitude (Shirakawa *et al.,* 1977; Chiang *et al*, 1995), many research laboratories initiated projects in the field of conducting polymers. Although the initial emphasis was on the conduction properties obtained by doping of conjugated polymers, since over a decade the research has focused on soluble and intrinsically (semi) conducting polymers. In the 25 years that have elapsed, many novel materials were designed, synthesized and developed for their specific physical or chemical properties and implemented in a variety of applications.

In arriving at a semi-conductive polymer, the majority of attention has been centered on conjugated polymers. Conjugated polymers have been found to have the necessary metallic and electrical characteristics required of a semiconductor. In comparison with a normal polymer, conjugated polymers possess a delocalized pi-electron system along the polymer backbone. It is the delocalized pi-electron system

that allows the polymer to support negative and positive charge carriers along the chain as shown Figure 2.2.2.1 1. The molecular structure of PPV is shown in Figure 2 2.2.1 2

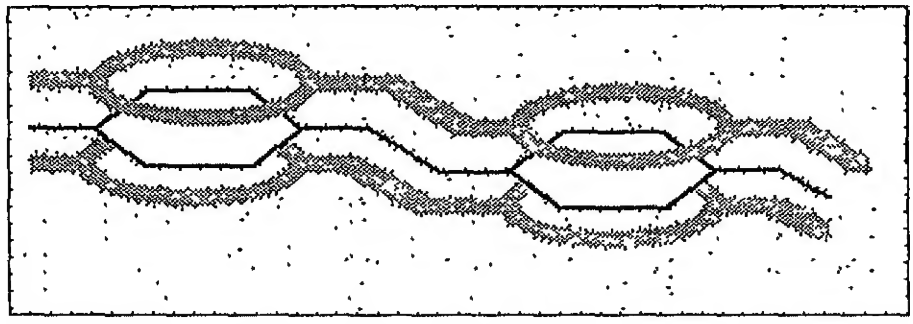

Fig 2.2.2.1.1: Delocalized conjugated polymer

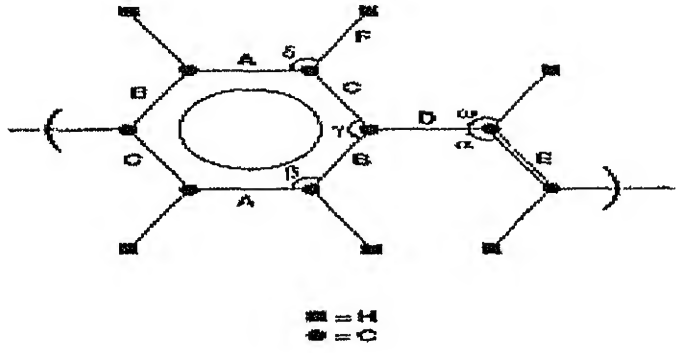

$A = B = C = 1.39^0A$
$D = 1.44^0A$
$E = 1.33^0A$
$F = 1.09^0A$

$\alpha = 128^0$
$\beta = \gamma = \delta = 120^0$
$\omega = 116^0$

Fig 2.2.2.1.2: Molecular structure of PPV

In 1990 the Cambridge group reported emission of light from a plastic sandwich that was connected to a battery. The discovery of electroluminescence (EL), i.e , the emission of light upon excitation by the flow of electric current, in conjugated polymers has provided a new impetus to the development of light-emitting diodes (LEDs) for display and other applications (May *et al.*, 1995). In LEDs, the injected holes and electrons recombine and produce luminescence with a wavelength (color) that depends on the energy difference between the excited state and the molecular ground state. For the majority of conjugated polymers, electron injection is more difficult than hole injection, since the majority of conjugated polymers are more easily oxidized than reduced. Using metals with a low work function (e.g. calcium) as the cathode material has partly remedied this problem. However, calcium is highly susceptible to atmospheric degradation as it is highly reactive metal. Therefore should be encapsulated by a metal that does not react with oxygen and moisture, like aluminum or gold. With the appropriate choice of polymer and device design, external efficiencies of

up to 4 % can be obtained, which is comparable with the best EL devices based on inorganic materials. Turn-on voltages of 5 V or below have also been achieved by the use of charge-transporting layers, enabling devices to be run from low-power sources like batteries.

Polymer-based electroluminescent displays provide a good alternative to the well-established display technologies based on cathode-ray tubes and liquid-crystal displays (LCDs) with respect to processability and viewing-angle. Especially for the application in large-area displays and flexible displays, for which the conventional methods are not well suited, polymer light-emitting diodes (PLEDs) offer great advantages.

Two years after the breakthrough in Cambridge, the Santa Barbara group reported the first results on polymer-based photovoltaic cells (Sariciftci *et al*, 1992), the principles of which can be regarded as the inverse of the EL process. In photovoltaic devices (PVDs), a bound electron–hole pair (exciton) is created upon illumination, which needs to be dissociated into separate charges that must be driven out by the built-in potential field between two electrodes with different work functions. To dissociate the exciton, the concept of electron donor and acceptor is frequently used, in which the electron affinity of the electron acceptor should be larger than the ionization potential of the donor (Bredas *et al.*, 1996). Since the first publications, most PV cells are based on blends of poly (*p*-phenylene vinylene) (PPV) derivates and C60 as light absorber/electron donor/hole conductor and electron acceptor/electron conductor, respectively, a combination which has proven promising (Brabec *et al.*, 1999) PPV-based materials are widely investigated for their opto-electronic properties (Sengura *et al*, 1998; Tessler *et al*, 1999; Friend *et al.*, 1999) and the ability of C60 to accept several electrons (Echegoyen *et al*, 1998) makes it a particularly attractive material for the use as electron acceptor. Its low solubility is a major drawback, however. A way to overcome this is the functionalization of C60 with side-chains or the incorporation of C60 into polymers, thus yielding materials that combine the physical properties of fullerene with the processability of polymers (Chen *et al*,1998; Geckeler *et al.*, 1999). Upon irradiation of an organic PVD, an exciton is created in the PPV phase, which is followed by a very rapid electron transfer (< 200 fs) to the C60 phase (photoinduced electron transfer). Since all other known competing relaxation processes in conjugated polymers occur on time scales that are orders of magnitude

larger, this ultra-fast charge transfer must have a quantum efficiency of approximately unity, i.e., nearly all excitons that are created near the donor–acceptor (D–A) junction are transferred to the C60 phase. Despite the high electron transfer efficiency, the power conversion efficiency of polymer/fullerene-based photovoltaic devices is typically still in the range of one percent due to the low mobility of holes on the conjugated polymer and the formation of a noncontinuous pathways for the charges, which results in an inefficient collection of charges at the cathode and anode, respectively (Gao *et al.,* 1997). Recently, power conversion efficiencies of 2.5–3 % were reported for mixtures of substituted PPV and C60 solution-processed from chlorobenzene (Shasheen *et al.,* 2001, Brabec *et al* , 2001).

2.2.2.2 Polymer Light Emitting Diodes (PLED)

For collection (injection) of holes in (PLEDs), indium–tin oxide (ITO) is most commonly used as the anode, which exhibits a high work function (4.5–5.3 eV) (Kim *et al* , 1998) close to the HOMO-level of the conjugated polymers. Furthermore, ITO is transparent for the visible spectrum, allowing the transmission of generated (incoming) light out of (into) the sandwiched device. For collection (injection) of electrons, a low work function metal such as Al (4.3 eV) can be used as a cathode. Electron collection (injection) can be improved to some extent by using cathodes with a lower work function (Mg, 3.7 eV; Ca, 2.9 eV), but these cathodes have the disadvantage of being more susceptible to oxidation.

Early work on PLEDs was based on sandwiching a PPV-type polymer (single layer) between dissimilar electrodes, but it became evident that electron injection was very inefficient due to the energy barrier between the work function of the metal and the LUMO of PPV. Furthermore, as a result of the high injection barrier, recombination of charges occurred close to the metal-organic interface, and, consequently, the metal could acts as a quencher of the electroluminescence. Therefore, researchers switched to a double layer device consisting of PPV with a high electron affinity or another electron transporting polymer e.g. based on oxadiazoles cast on top of a more commonly used PPV. The introduction of an appropriate electron transporting layer (ETL) not only lowers the charge injection barrier, but it can create an energy offset for holes and a barrier at the emissive layer/transport layer interface. This effectively blocks the hole current at the interface and results in a positive space-charge interfacial zone in the emissive layer. The space-charge zone will increase the field over the ETL resulting in

enhanced electron-injection from the cathode The progress of PLED is shown in Figure 2.2.2.2.1.

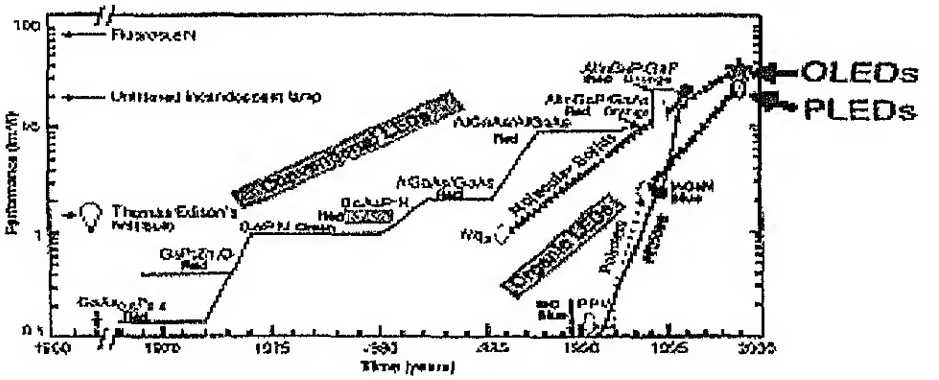

Fig2.2.2.1: Current scenario and progress of LED and OLED

Figure 2.2.2.2.2 A shows the schematic energy diagram of an organic single-layer LED in which the holes (h+) and electrons (e–) are injected in the HOMO and in the LUMO, respectively. Figure B depicts a double-layer EL device in which electrons and holes are injected from the electrodes into ETL and hole transport layer (HTL), respectively. These carriers recombine to form an exciton that may radiatively decay (emit light).

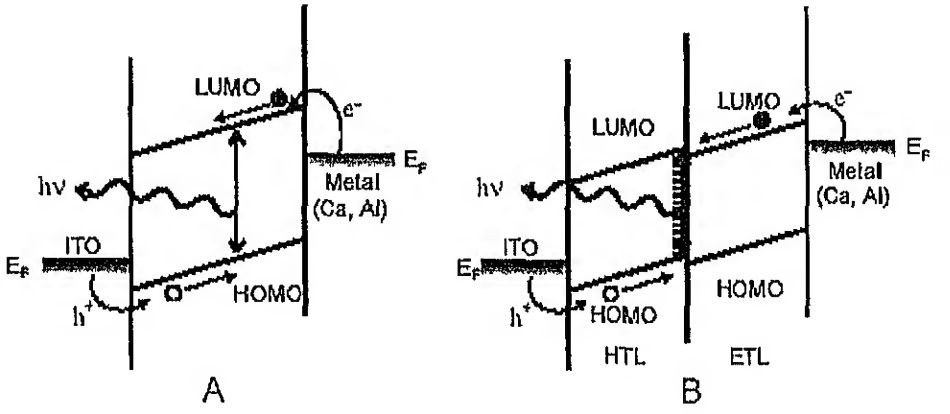

Fig 2.2.2.2.2: Energy diagram of single and double layer OLED

Controlled chemical modifications of the inorganic surfaces can improve the device performance tremendously as demonstrated by the vapor deposition of a very thin layer (< 1nm) of LiF before vapor-depositing the metal cathode (Hung *et al.*, 1997; Bao *et al.*, 2000). ITO/polymer interface can be easily modified by spin-coating a layer of p-doped conjugated polymer (PEDOT/PSS) (Ho *et al*, 2000), work function (~5.2 eV) enhances the device uniformity and lifetime due to its environmental stability.

2.2.2.3 Organic Materials

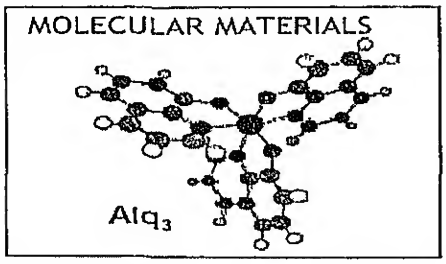

Attractive due to:
- Integrability with inorganic semiconductors
- Low cost (fabric dyes, biologically derived materials)
- Large area bulk processing possible
- Tailor molecules for specific electronic or optical properties
- Unusual properties not easily attainable with conventional materials

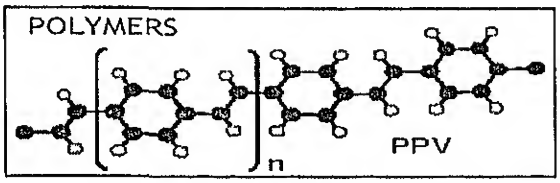

But problems exist:
- Stability
- Patterning
- Thickness control of polymers
- Low carrier mobility

Fig 2.2.2.3.1: Organic Materials

OLED devices can be divided in two classes depending on the technology used, *conjugated polymers* and *small molecules* The first approach was the small molecules and it was developed at Eastman Kodak. Together with Sanyo Electric, Eastman Kodak has formed a joint venture to produce OLEDs, mainly focusing on 1-6 inch lower resolution active matrix displays The researchers in the Cavendish Group at Cambridge University discovered the emitting properties of conjugated polymers They later formed the company Cambridge Display Technology Ltd (CDT), which is the leading research company on conjugated polymer displays today.

Small molecules in OLED has shorter chain length compared to polymers. So in small molecules the transport is usually of hopping type and the bandgap of small molecules such as Alq_3 is generally higher. The conjugated polymer such as PPV and CNPPV etc are based on this hopping type conduction. It has been observed that the PPV with higher disorder has internal quantum efficiency of 0.22% (Son *et al*, 1995) compared to 0.01% reported by Borroughes *et al*, 1990. So cis linkages are intentionally engineered into the PPV chain to increase the asymetricity and reduce the crystallinity. Work by Yan (1994) indicates that the photoluminescence efficiency can be increased in a polymer by separating the polymer chains. To afford the solubility of PPV in good spinning solvents, introducing xanthate group during polymerisation modifies Wessling method. Others polymers and organic semiconductors (Braun *et al.*, 1991) are also used for LED. Band structure (Zhao *et al.*, 2001) of PPV is shown in the Figure 2 2.2.3.2.

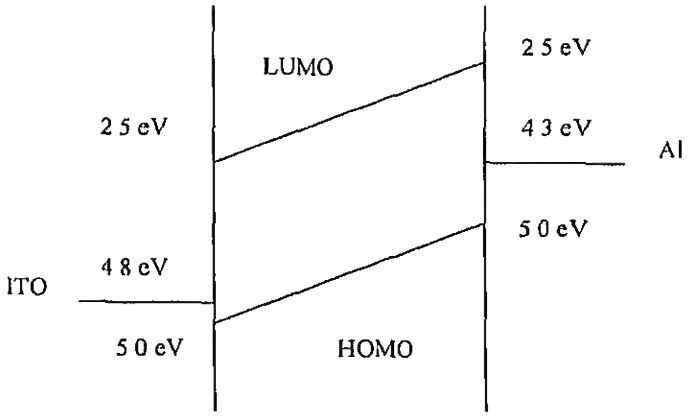

Fig 2.2.2.3.2: Band diagram of PPV

LED device performance is dependent upon the luminescence efficiency of the polymer material. The luminescence of these polymers tends to be lower in the solid-state than for isolated chain molecules because the excitons can migrate to quenching sites, such as aggregates or chemical defects. Aggregates can serve as quenching centres because inter-chain interactions can produce optically dark excited states lower in energy than the optical state that provides a non-radiative pathway to the ground state. Attaching bulky side groups to the conjugated polymer backbone, such as alkyl groups, can reduce inter-chain interactions. These side groups serve to dilute the polymer backbone, which minimizes the effects of aggregation, but they can also inhibit the transport of charges through the polymer film. More recently, in order to reduce the significance of π stacking, helical polymer (Xu *et al*, 2000; Sarker *et al*, 2002) structures have been formed by the inclusion of a biphenyl group in the unit cell structure, which has been shown to increase photoluminescence efficiencies. Luminescence is also affected by the structure of the polymer such as structural distortions along the chain and a "kink" or torsional disorder along the chain, can reduce the delocalization of the π bonds along the polymer backbone. The planarity of the polymer is affected by the nature of the substituents, temperature, and the choice of solvent. In corporation of p-Si (Zhou *et al*, 1999) in OLED decreases the turn on voltage and there is better injection of holes, but using p-si is problem as it is opaque so the purpose of using ITO as a transparent electrode is lost. But p-Si can be used for IR purpose, as Si is transparent in this region. ITO is generally used for the visible range in OLED. Several deposition techniques have been used to grow ITO thin films above glass including chemical vapor deposition (Maruyama *et al.*, 1991), magnetron

sputtering (Buchanan *et al*, 1980; Wu *et al*, 1994), evaporation (Nath *et al*, 1980), spray pyrolysis (Vasu *et al*, 1990), and pulsed laser deposition (PLD) (Zheng *et al*, 1993; Coutal *et al*, 1996). ITO is generally coated on glass by sputtering method It has been reported that ITO deposited by PLD has much lower surface roughness (Kim *at al*, 1999) and has better device performance.

2.2.2.4 Conjugated Polymers

Conjugated polymers exhibit semiconducting properties because the bonding and anti-bonding π orbitals along the polymer chain form valence and conduction bands that support mobile charge carriers. These polymers are ideal for device applications since they combine the processability and the mechanical properties of polymers with the optical and electronic properties of semiconductors. Due to their combination of photo-physical and semi-conducting properties, conjugated polymers are promising materials for the construction of devices such as OLED and solid-state lasers.

2.2.3 Advantages of OLED Based Displays

OLED is an emissive device and therefore does not suffer from the viewing angle limitation like a Liquid Crystal Display (LCD) cell. For any device to become a viable candidate for use in flat panel displays it has to be able to demonstrate high brightness, good power efficiency, good colour saturation as well as long lifetime. Reasonable lower limits (Bulovic *et al*, 2000) for any candidate device: brightness of ~ 100 cd/m^2, operating voltage of 5-15V and a continuous lifetime of at least 10,000h. Saturated-colour OLEDs have been demonstrated, spanning almost the entire visible spectrum. Moreover, the thickness of an OLED structure, which typically is less than a micrometer, allows for mechanical flexibility, leading to the development of flexible displays indicating the potential development of rolled or foldable displays. Furthermore, the recent development of vapour phase deposition techniques for OLED manufacturing process may well result in a low-cost large-scale production of OLED based flat panel displays compared to LC based displays that require extra processes such as layer alignment and tilt angle adjustment.

2.2.4 Problems of using OLED

OLED are organic devices and their environment easily affects their electrical properties. In the case of OLED, when its electrical characteristic changes, the power

efficiency degrades In addition to this, the initial I-V characteristics of OLED cells depend on a large number of factors, like local shorting and pinhole, which may be difficult to control. OLED made using Alq_3 as the active Electro Luminescence (EL) layer is driven with current of 5mA/cm², lost 50% of its initial intensity in 100h even when it is operated in dry Ar (Argon) as reported by Burrows *et al,* (1994), It was also reported that a blue OLED showed a decrease of 90% of its initial EL intensity in 130h when operated in dry N_2 (Nitrogen). Operating OLED in air resulted in 99% loss of EL intensity in as little as 150 min. It is indeed clear that such short device lifetimes, even in inert atmospheres, render OLEDs ineffective for commercial applications. In that particular paper by Burrows *et al*, (1994), an encapsulation mechanism is suggested that prolongs the lifetimes of the OLEDs device by two orders of magnitude But even with the encapsulation mechanism, the power-efficiency characteristic of the device does not remain constant during its lifetime although within an acceptable range for sufficient brightness. Figure shows the average optical power output degradation (Burrows *et al*, 1994) over time and the voltage required to maintain the same level of current through the OLED device. Present devices have the same characteristics curve although the lifetime is increased to the order of 10000-20000 hours.

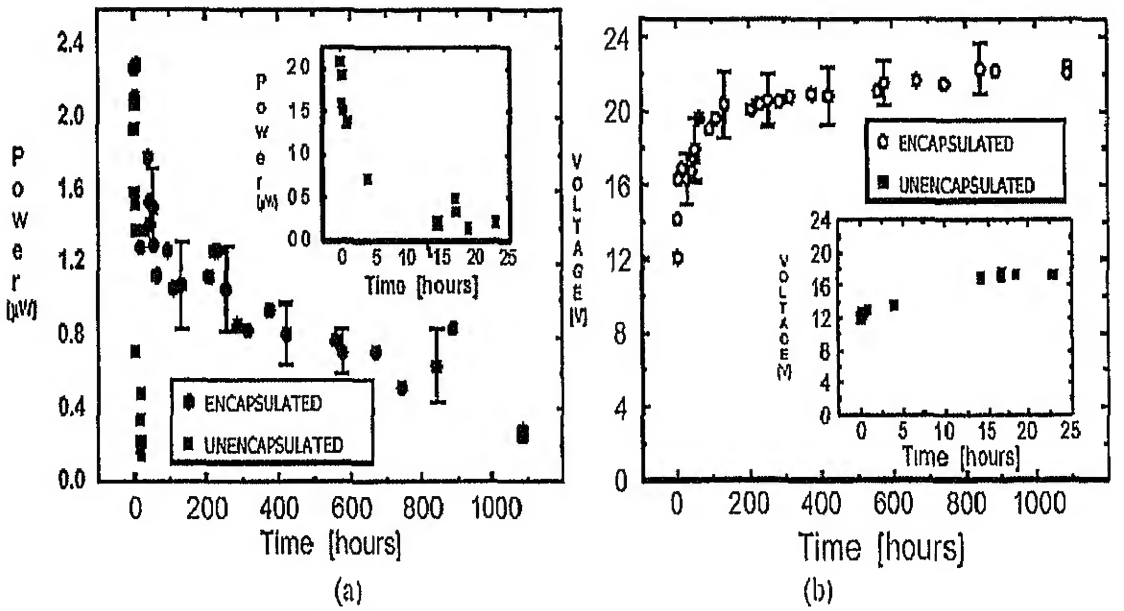

Fig 2.2.4.1: (a) Average Optical Power Variation of OLEDs with Time.
(b) Average Voltage variations required maintaining a current of 1mA through the OLEDs (Burrows *et al.)*

In addition to the power efficiency variation, the power output characteristic also changes in a non-uniform way with time. A particular level of current or voltage does not correspond to a fixed level of optical power output

2.2.4.1 Current-Voltage Characteristic Variation

Current Voltage characteristic of OLED is characterized by fluctuations. The I-V characteristics also depend on temperature, which pose another challenge in commercial use. There may be change in temperature of the device due to heating during operation. So the temperature as well as the characteristic may become unpredictable.

Besides temperature, the I-V characteristic also depends strongly on the type of anode/cathode used in the device as well as the thickness of the organic active EL layer Figure shows the I-V characteristic variation with the thickness of the organic layer

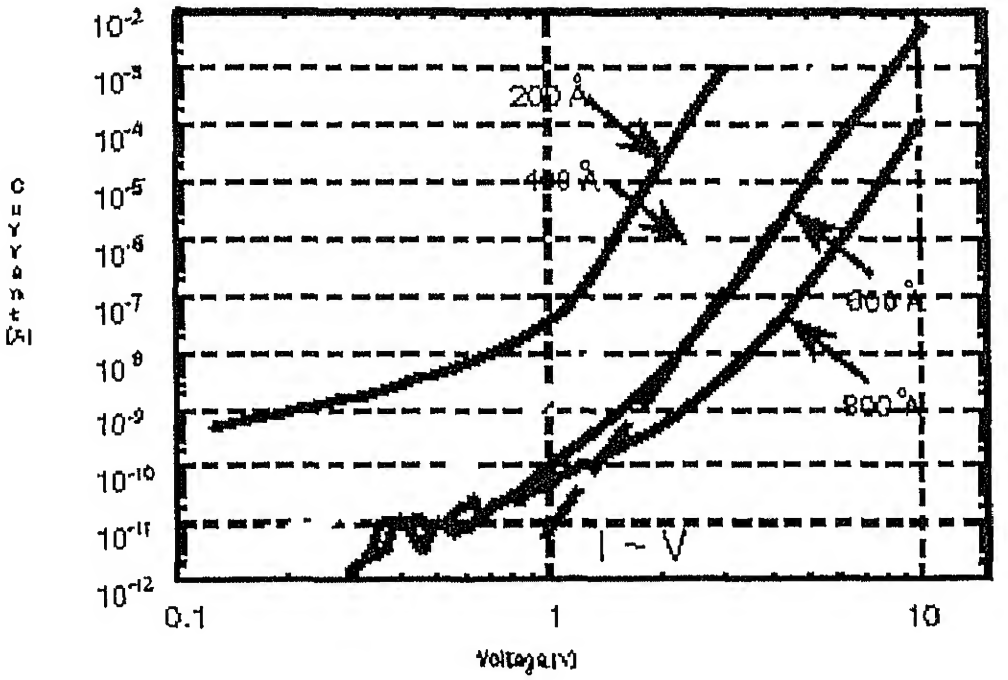

Fig 2.2.4.1.1: I-V characteristic variation with thickness of the organic EL layer (Burrows *et al.*, 1994)

3. Characterization Techniques

The characterization is the first step for determining the usefulness and salient features of any new material. The principal characterization methods can be subdivided between electrical and optical characterization for use in semiconductor device purposes. The photo characterization becomes more important for use as light emitting purpose, where the proper output of the produced light is also important factor limiting the efficiency of the device.

3.1 Electrical Characterization

3.1.1 Current-Voltage measurement

The current voltage measurement is important for any device structure and determines its usefulness. The diode behavior in the forward bias with almost exponential increase of current after cut-off voltage is seen for the organic devices But it shows almost same behavior in reverse bias unlike inorganic diodes where there is presence of depletion layer. But the magnitude of current is less in reverse bias compared to forward. Also some aspects about the transport mechanisms can be determined from the ohmic region, space charge limited region and trap assisted region. The double-logarithmic I-V plot can be divided into three distinct regions: region 1 is the non- linear region due to non-exponential behavior of diodes at low voltages (leakage currents amongst other factors); region 2 is the linear region and region 3 where the current is limited by the series resistance.

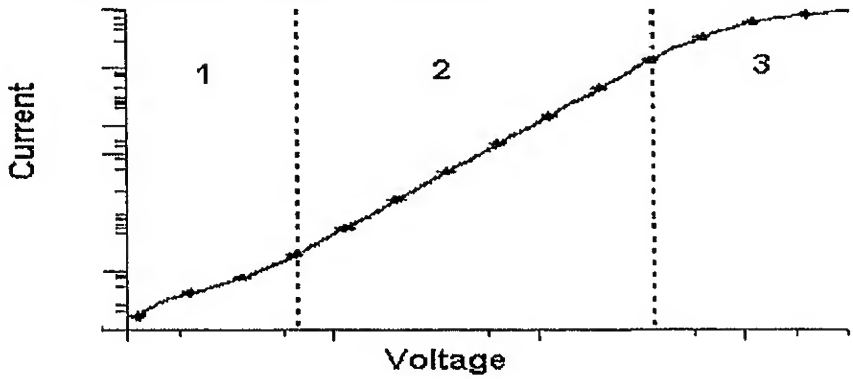

Fig 3.1.1.1: Semi-logarithmic I-V plot for a typical Schottky diode

The organic devices have been also reported to show photo-detector (Yu *et al.*, 1994) characteristics with illumination under light especially VIS-UV light. The photosensitivity increases with reverse bias voltage. Photovoltaic effects have been observed in devices fabricated from PPV (Karg *et al.*, 1993; Marks *et al*, 1994;

Antoniadis *et al.*, 1994) Recently, the dual-function characteristics of polymer devices light emission and photodetection has been demonstrated (Yu *et al.*, 1994) The illumination structure of device is shown in Figure 3 1.1.2

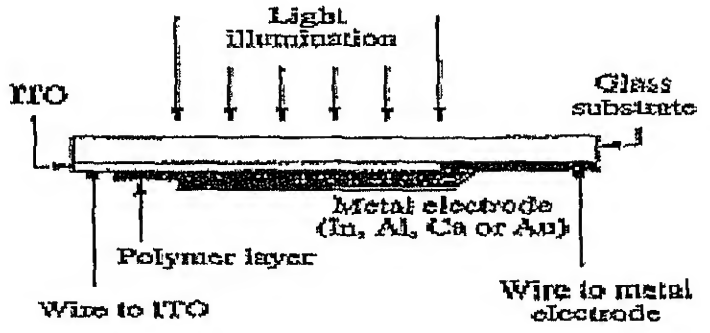

Fig. 3.1.1.2: Device arrangement for photo measurements (Yu *et al*)

The I-V characteristics varies with following factors·

- From temperature I-V the bandgap of the material can be determined. But in organic semiconductors, the bandgap itself is temperature dependant
- The I-V also depends on the type of electrodes in OLED as it determines the injection and hence the V_{bi} and the threshold voltage.
- The I-V also depends on whether it is done in dark or under light (Malliaras *et al*, 1998). Under light irradiation, there is generation of carriers that eventually increases the current. The light should be near the absorption peak for the generation of carriers and enhancement of current. The reverse bias characteristic also gets modified under light. The figure shows the dark and under light I-V behavior of MEHPPV:

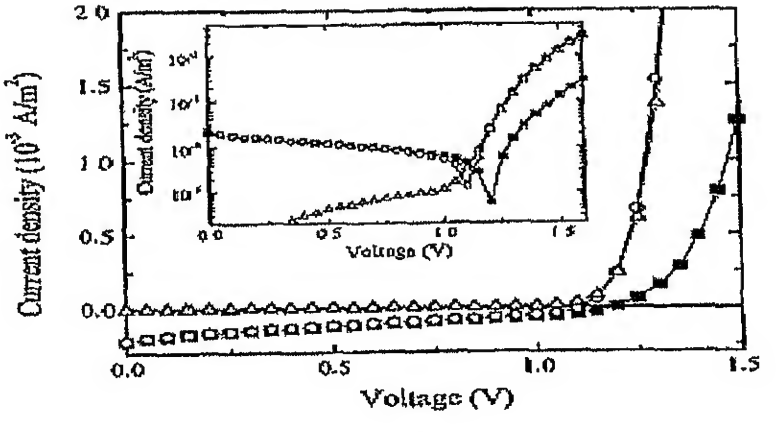

Fig. 3.1.1.3: The voltage dependence of the current densities in the dark open triangles Under illumination (Malliaras *et al.*)

The spectral response of photocurrent demonstrated that photon absorption near the electron- collecting electrode optimizes the photocurrent, indicating the device performance is limited by low electron mobilities in the bulk PPV. The photocurrent exhibits weak temperature dependence, with an activation energy that is a function of electric field in the polymer. A table with photovoltage of 120 nm PPV device is shown below.

Table 3.1.1.1: Photo-voltage of ITO-PPV-Metal device (Marks *et al.*, 1994)

Metal contact used	Measured maximum photovoltage (V)	Metal work function (eV)	Difference in work function with respect to ITO (V)
Aluminium	1.2	4.28	0.5
Magnesium	1.2	3.66	1.2
Calcium	1.7	2.87	1.9

As in the Figure 3.1.1.4 below the variation in the photocurrent with PPV film thickness is shown with the corresponding dependence of peak with temperature. The peak broadens and shifts to higher energy with higher film thickness. Below 300K photocurrent is almost insensitive to temperature, but above this temperature, the peak position shifts to higher energy and the peak broadens

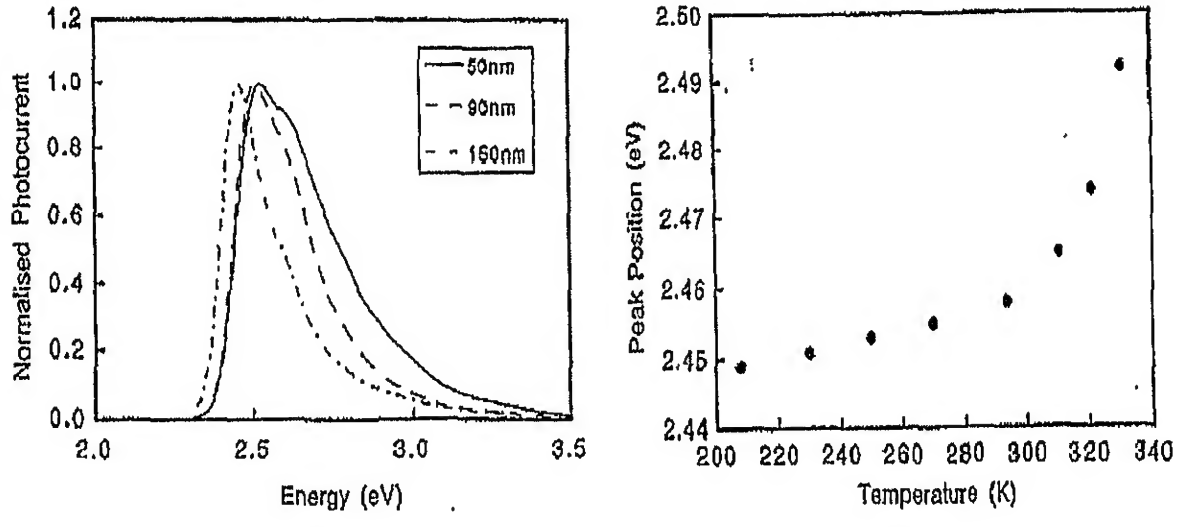

Fig. 3.1.1.4: Photocurrent variation of PPV with film thickness and temperature (Marks *et al.*)

This method can be used to find out exciton binding energy, which is found out to be about 0.4 eV for PPV.

3.1.2 Current time measurement

The current-time measurements can be used to measure the stability of the device under constant voltage. The variation in the current shows instability of the device Sometimes voltage is also measured keeping current constant.

3.1.3 Capacitance Voltage Measurements

Capacitance voltage measurement is used for the determination of traps by DLTS (Deep Level Trap Spectroscopy) method Also the characterization of fixed charges is possible by comparison with ideal behavior. The mobile charges can also be characterized by C-V measurements under different temperatures Interface traps can also be determined by distortion and streachout effect on the C-V curves. Also the interface capacitance gets frequency dependent.

3.1.4 Impedance Spectroscopy

Impedance spectroscopy is a powerful tool to determine the interface properties at contacts. The bulk and the contact factors can be separately analyzed and especially the electrical degradation mechanisms can be studied. In a degraded device to determine exactly what has degraded the polymer or the contacts, is an ideal method. Also the resistance capacitance, the variation of impedance with frequency can be used to determine the involved mechanisms.

3.1.4.1 Principle

The basic principle of impedance spectroscopy is to measure impedance as a function of frequency and bias voltage. The basic equation can be written as:

$$Z(\omega, V_o) = \delta V(\omega) / \delta I(\omega)$$

The impedance at any frequency ω is a complex number because δI(ω) contains phase information as well as magnitude - the AC current may have a phase lag θ with respect to the AC voltage. Hence if we apply $V=Vo + |\delta V| \cos(\omega t)$ and measure $I = Io + |\delta I| \cos(\omega t-\theta)$,

$$Z(\omega,Vo) = (|\delta V| / |\delta I|) \times \{\cos(\theta) + i \sin(\theta)\}$$

where $i^2 = -1$ and both magnitude and phase of the impedance, $|Z|$ and θ vary with ω

Then $Re\{Z\} = |Z(\omega)| \times \cos[\theta(\omega)]$

and $Im\{Z\} = |Z(\omega)| \times \sin[\theta(\omega)]$

An electrical layer of a device can often be described by a resistor and capacitor in parallel as shown in Figure 3.1.4.1 1

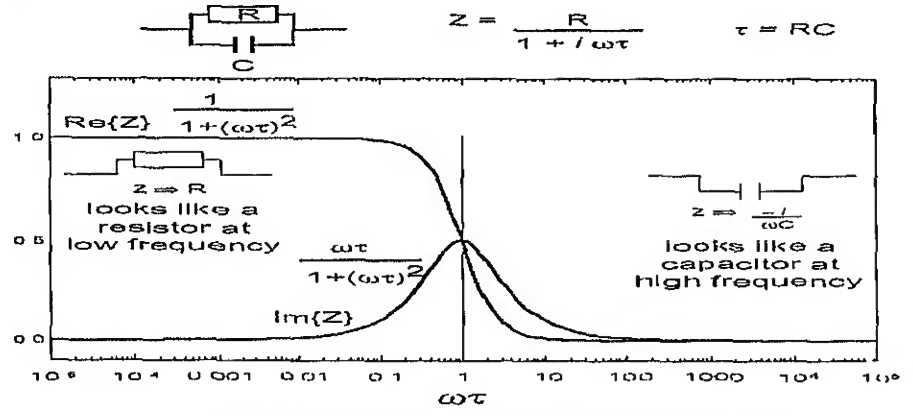

Fig 3.1.4.1.1: Typical impedance of a RC circuit

When we plot the real and imaginary components of impedance in the complex plane, we obtain a semicircle or partial semicircle for each parallel RC network. This plot is known as Cole-Cole (Cole *et al.*, 1941) plots as shown in Figure 3 1 4 1.2

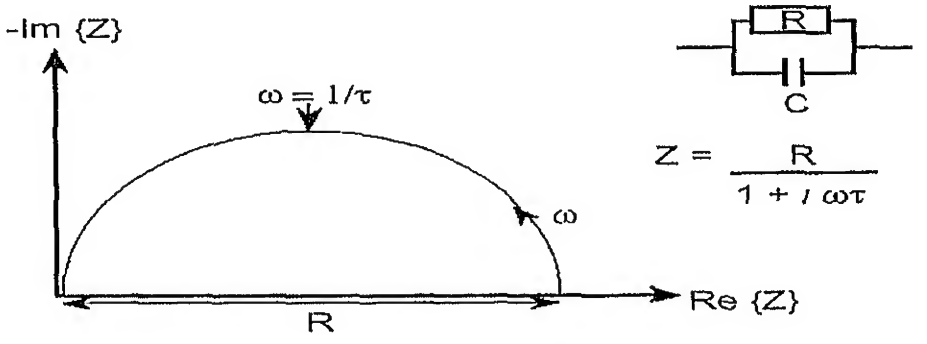

Fig 3.1.4.1.2: A typical impedance plot

The diameter corresponds to the resistance R and the frequency at the 90° position corresponds to $1/\tau = 1/RC$. There are also two related quantities:

1. Admittance $Y(\omega,Vo) = 1/Z(\omega,Vo)$

The diameter of the admittance plot usually corresponds to $1/R_{\infty}$ as shown in Figure 3.1 4.1.3.

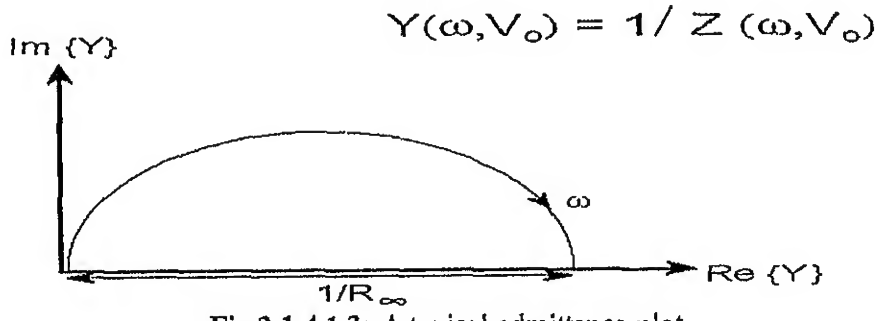

Fig 3.1.4.1.3: A typical admittance plot

2. Modulus M (ω,Vo) = iωZ (ω,Vo)

Modulus plots also give semi-circles but the diameter now corresponds to 1/C, the frequency at the 90° position is again 1/τ= 1/RC. The modulus plot is shown in Figure 3.1 4.1.4

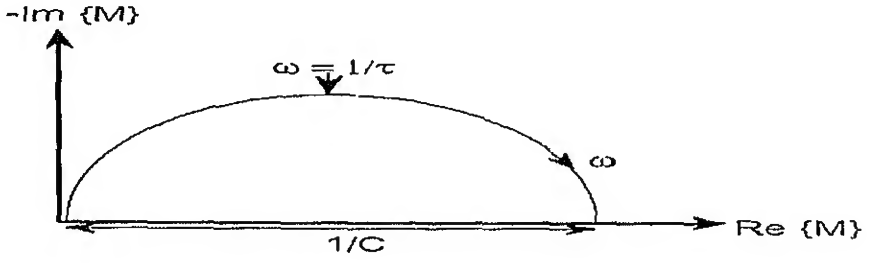

Fig 3.1.4.1.4: A typical M plot

The inferences that can be derived from impedance spectroscopy are following:

- Model of the electrical behavior of the device in terms of an equivalent circuit comprising of resistors and capacitors at different voltages and frequencies.

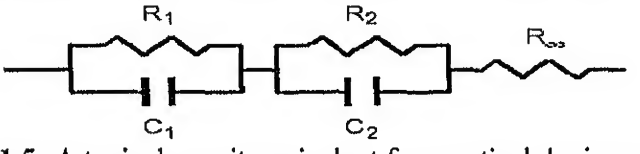

Fig 3.1.4.1.5: A typical circuit equivalent for practical device modelling

- Calculate the electric field distribution within the device
- Calculate the charge carrier concentration
- Degradation and ageing

3.1.4.2 Analysis

By using the various Cole-Cole plots of Z, M and Y, values of the elements of the equivalent circuit can be calculated for any applied bias voltage.

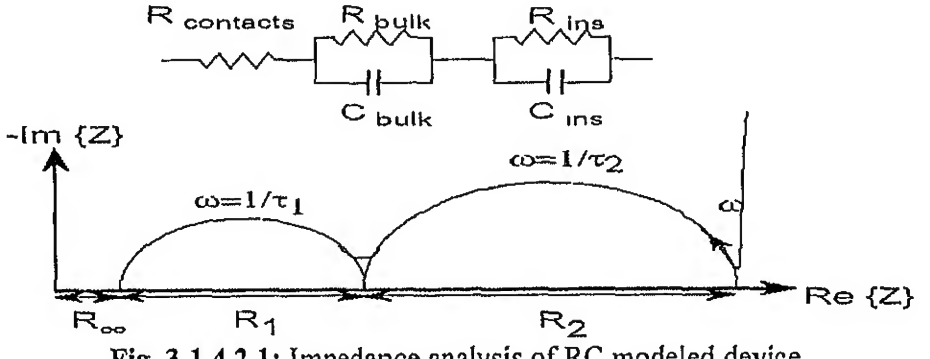

Fig. 3.1.4.2.1: Impedance analysis of RC modeled device

By doing this over a range of bias voltages, the field distribution can be obtained in the layers of the device (potential divider) and the relative widths of the layers, since C ~ 1/d Two-time constants τ_1 and τ_2 according to two sets of parallel RC circuits. The R_∞ is related to the resistance value at very high frequencies and usually

due to contact resistance. R_1 and R_2 values correspond to R_{bulk} and R_{ins} Hence the variation can be measured to find out actually which is degrading, the polymer or contacts

3.1.4.3 Problems with Impedance Analysis

- With polymer LEDs, the Mott-Schottky ($1/C^2$ vs V) plot must be used with caution! It is possible to measure a change of the device capacitance even though this is due to a change in one of the parallel resistances (change of time constant t) and not due to a change of the capacitance or width of a depletion layer! Hence the change of capacitance should be verified
- The Cole-Cole plots do not always give perfect semi-circles. Diffuse interfaces can give rise to other features - depressed semi-circles, constant-phase elements
- More variation may be seen between notionally 'identical' devices than between devices where it may seem that an experimental parameter varied. In particular, the impedance spectra are rather sensitive to oxygen and moisture.

3.2 Photo-characterization

3.2.1 Photoluminescence

Photoluminescence (PL) is an important physical phenomena used to characterize semiconductors which depicts a sample's energy structure while possibly revealing other important material features. In brief, PL occurs when a sample absorbs light of some frequency and emits light at a specific frequency corresponding to the material's specific structure, composition and quality. It involves a system excited by electromagnetic (EM) radiation, is classified as an optical luminescence technique.

As the incident light (EM radiation) impinges on the sample, it causes electrons to be elevated into excited states, as depicted in Figure 3.1.1.2, a typical energy diagram for this process. Since lasers can provide "power sufficient to excite an adequate signal, the incident light typically comes from a laser source with energy of hw_{laser}. When the excited electron returns to its initial state, it may generate a photon with energy hw_{PL} (and possibly multiple phonons with combined energies of $h\Omega_{phonon}$. The energy conservation, can be expressed as Equation:

$$hw_{laser} = hw_{PL} + h\Omega_{phonon}$$

Laser is irradiated having energy higher than the bandgap of the material, and then the material gives luminescence spectrum according to the bandgap of the

material. In this the electron hole pair generated by the laser recombines in the process emitting a photon with energy of the bandgap and other secondary levels. The various methods are shown in Figure 3.2.1 1

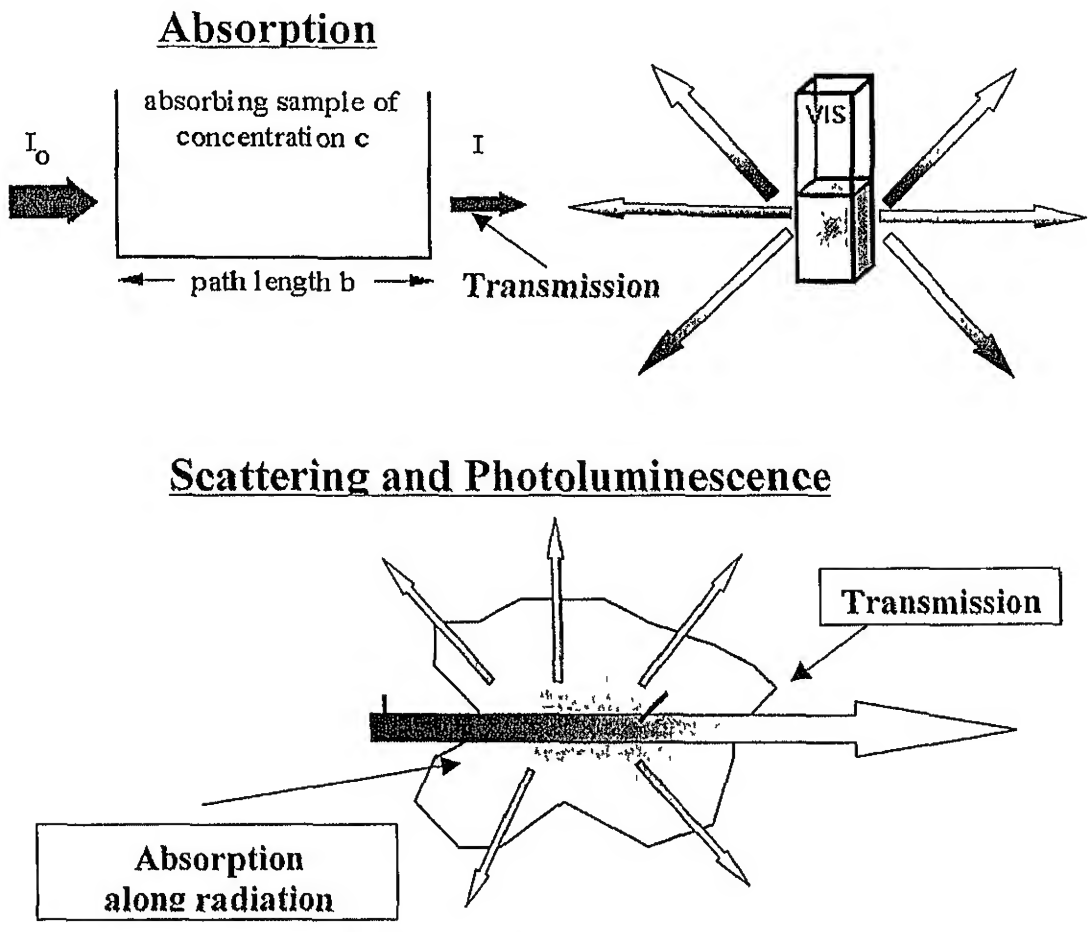

Fig 3.2.1.1: Different photo processes

Although the time-dependence of these effects can be examined and yield further details of the transition rates. PL as such can be considered as a steady-state phenomena; the sample interacts with the excitation source and emits light continuously.

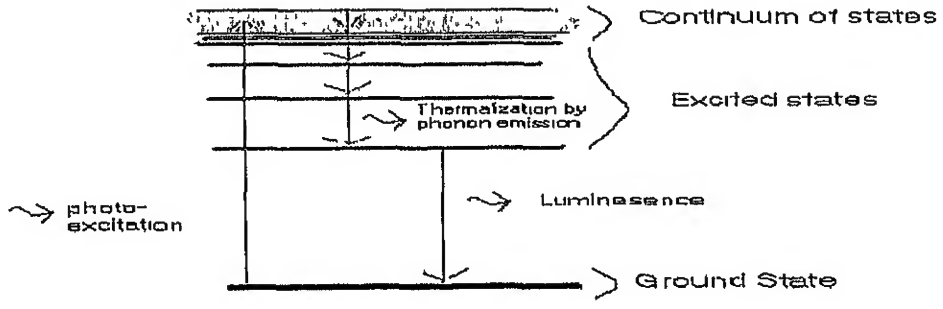

Fig. 3.1.1.2: The Electron Picture: A Simplified energy diagram of Photoluminescence.

The material's absorption depends on the wavelength of the excitation source Equation shows the theoretical dependence the absorption coefficient (α) for a direct bandgap semiconductor.

$$\alpha = A(\hbar\omega - E_{gap})^p = A(\frac{hc}{\lambda} - E_{gap})^p$$

In this equation, A and p are constants determined by the particular material hv is the photon energy of the laser light, and E_{gap} is the energy of the bandgap of the structure. The comparison of optical absorption and photoluminescence is shown in Figure 3.1.1.3

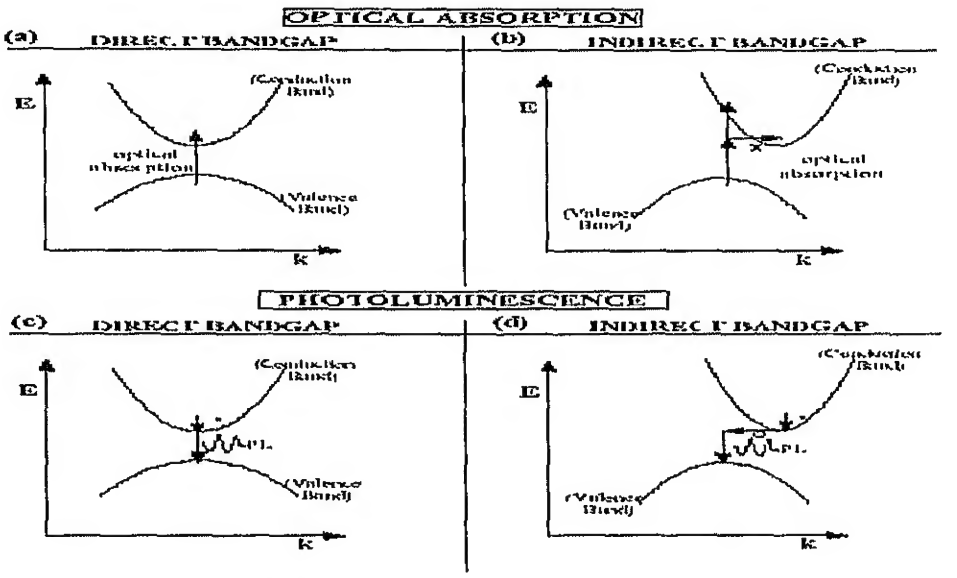

Fig. 3.1.1.3: Absorption and Photoluminescence

PL can be observed on samples with structures that are more complicated in composition than just a bulk semiconductor material. It can investigate how well the samples were grown, and verify the growth composition. This is because the energy differences measured by PL change with impurities and structures, as illustrated in figure 3.1.1.4.

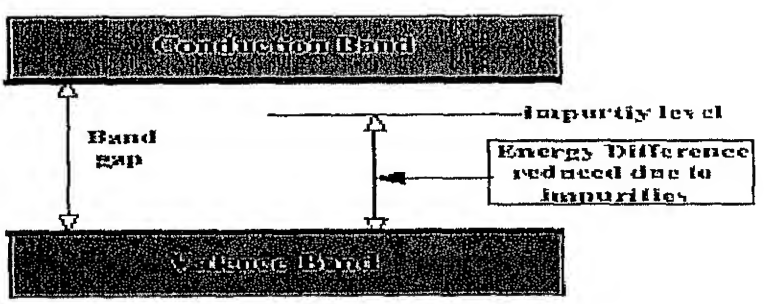

Fig. 3.1.1.4: Band Diagram

Some of the possible luminescence transitions, including those due to defects, are shown in Figure 3.1.1.5.

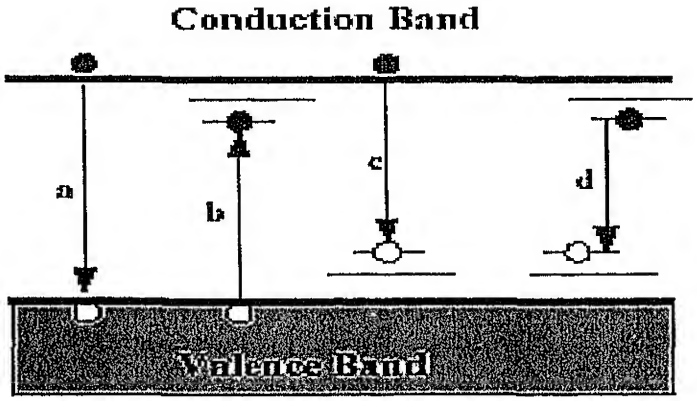

Fig. 3.1.1.5: Radiative Transitions (a) simple electron-hole recombination (b) defect band involving donors, (c) defect-band involving acceptors, (d) donor-acceptor pair

3.2.2 Electroluminescence

In this technique a light emitting material is placed in-between two electrodes, where holes are injected from one side and electrons from other side under bias. In this conditions electrons and hole gets transported and recombines to give out photon. The transport phenomenon of a material is also important in addition of the requirement of being direct bandgap material to be electroluminescent. PPV shows electroluminescence peak at 510 nm (~2.4 eV) associated with radiative decay of singlet exciton Due to exciton binding energy and the lattice relaxation (Bredas *et al.*, 1996), the luminescence energy of PPV is less than the HUMO-LUMO bandgap, which is 2.7 eV.

Above some threshold voltage of 100 V, an uv-violet emission (Chayet *et al*, 1997) centered at 390 nm is observed in addition to the characteristic yellow-green luminescence of PPV. This emission can be explained as being induced by a generation of hot carriers in the strong electric field, which inhibits the formation of singlet excitons and enhances the probability for direct interband transitions of the relaxed carriers.

4. Degradation Studies

Degradation is the major problem for OLEDs and stands as a hindrance between the commercialisation of devices The degradation in the efficiency and the brightness with time is the most prominent in the OLEDs, but the quest for better materials is still on. The degradation in encapsulated and that under vacuum devices is reported to be slower compared to that under ambient conditions The degradation is also slower in inert atmosphere The degradation of luminescence of devices is reported to be due to delamination of cathode from the polymer material followed by blister and dark spot formation The dark spots then initiates the bubble formation (Yakimov *et al*, 1997; Wang *et al*, 2002) by the electrochemical reaction of the polymer materials in the presence of moisture and oxygen It has also been reported that degradation is initiated only on electrical stress or photo excitation even in inert atmospheres. There is also development of dark spots (Burrows *et al*, 1994; McElvain *et al*, 1996; Ke *et al*, 2002) on application of electrical stress for larger duration. The non-emissive spots had been attributed initially to local heating caused by short circuits, which lead to the formation of pinholes and local ablation (Burrows *et al*, 1994) or local fusion of the metallic cathode (Scott *et al*, 1996)

Typical degradation processes of organic EL devices have been classified into two categories: degradation during storage before the device operation and degradation during the operation Causes of the former case include the following:

1. the deterioration of organic molecular layers themselves due to crystallization (Han *et al.*, 1994) and
2. the detachment of the organic layers from ITO electrode

Causes of the degradation during operation include·

1. the diffusion of emitting layer EML material into HTL induced by the Joule heating (Fujihira *et al.*, 1996)
2. the oxidation of Al top electrode with oxygen evolved by water electrolysis (Do *et al*, 1994), and
3. the detachment (delamination) of the contact between metal electrode and EML caused by gas evolution causing bubble formation

4.1 Bubble formation

The degradation of OLED under electrical bias is accompanied by formation of bubbles. The formations of these bubbles are slower in inert environment indicating that the ambient condition affects the device. The bubble formation is shown in Figure 4 1.1.

Fig 4.1.1: Bubble formation in device

The bubbles have following characteristics:

- Bubbles filled mostly with oxygen
- Oxygen is evolved from electrochemical & photochemical process in presence of moisture (Do *et al.*, 1994 & 1996) and electrical stress
- Bubbles originate around pinholes in metallic electrode in the presence of atmospheric humidity (McElvain *et al.*, 1996; Papadimitrakopoulos *et al* , 1996)
- Oxygen results in photo degradation
- Oxygen bubbles also form in ITO side due to local heating at bubble perimeter
- Encapsulation (Burrows *et al.*, 1994; Cumpston *et al.*, 1997) & inert environment slows down bubble formation
- Thermal treatment also leads to bubble formation
- Humidity accelerates bubble growth, but its only electrical stress which initiates bubble formation
- Formation and the growth of bubbles depends on duration and magnitude of current

Under these conditions the device lifetime is limited by photodegradation and anode degradation (Berntsen *et al*,). The photodegradation is believed to be mainly due to photo-oxidation (Kuzina *et al.*, 1993; Cacialli *et al.*, 1994; Do *et al.*, 1996; Sutherland *et al.*, 1996) by either residual oxygen in the polymer itself (Cumpston *et al.*, 1995) or

by that released from ITO (Do *et al*, 1994, Karg *et al*, 1996; Carter *et al*, 1997) It is significantly reduced when a conductive polymer layer (Salbeck *et al*, 1996) is introduced between luminescent layer and ITO. Such a prevention of contact to oxygen and water vapor enabled device operation for thousands of hours (Pichler *et al*, 1997) The Figure 4 1 2 shows the fluctuation in the light output in a PPV device due to delamination of cathode resulting in the decrease of active area and increased current densities The delamination of the cathode is shown in Figure 4 1 2.

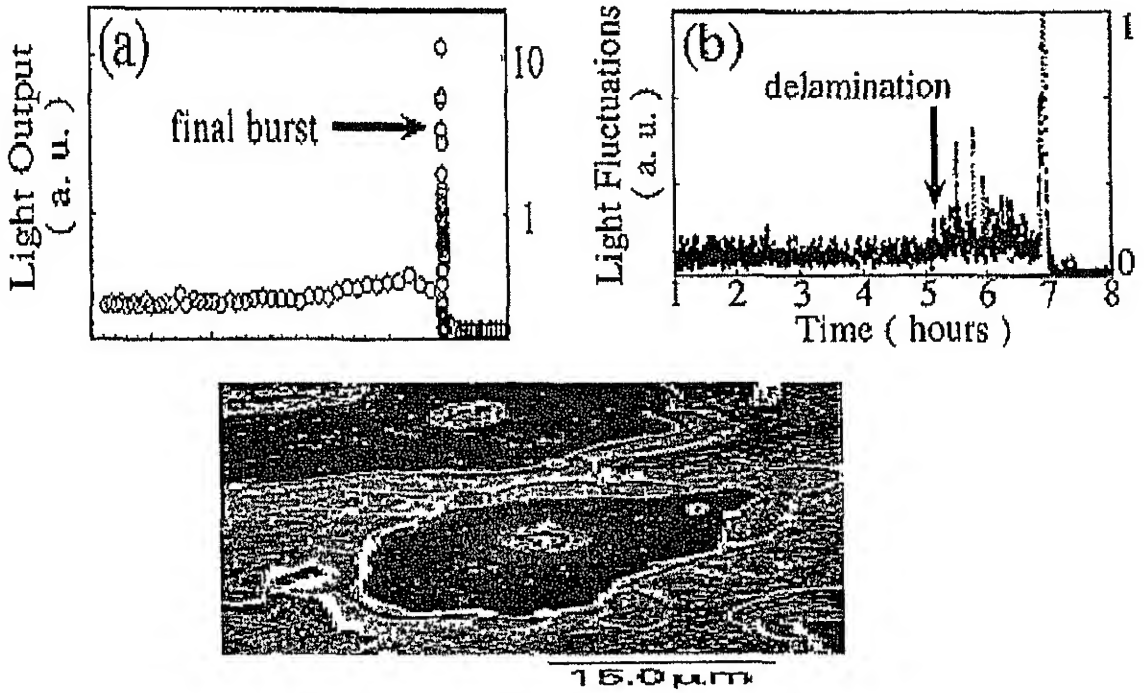

Fig 4.1.2: Light output fluctuation and delamination

The bubble formation near the cathode and the corresponding dark spot formation in PPV device is reported by Nguyen *et al.*, 1999 as shown in Figure 4.1.3

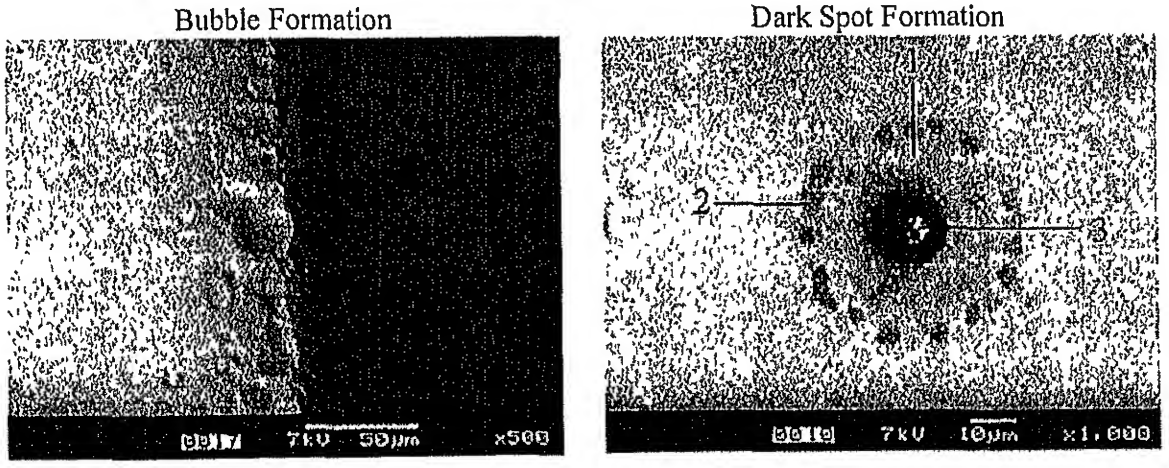

Fig 4.1.3: Bubble and dark spot formation in device

The center of the circle of dark spots shows a carbon–oxygen concentration ratio of only 80%, while in a dark point it reaches 115%. In between these points, the ratio increases to 135% The presence of a small peak of sodium was also noticed in the dark points and in the center of the circle but indium or tin was not found Therefore, oxygen is clearly identified as the main element present in the degraded zones and was found even on working in vacuum. Surface analysis of PPV films confirmed that contamination by oxygen occurred mainly on the surface of the polymer (Nguyen *et al.*, 1997). It is possible that the oxygen observed in the dark point zones could result from diffusion not through the polymer but from its surface towards particular regions, raising the concentration of oxygen there. These regions, where the dark points appear, may contain defects, which may then favor a local heating creating a temperature gradient, which in turn facilitates the diffusion. Evidence that supports the lateral diffusion hypothesis is the presence of sodium in the dark point zones. This sodium is remnant from the precursor Finally, the circular shape of the degraded zones indicates also diffusion like process toward its centre.

4.1.1 Mechanism of Bubble formation

The mechanism of bubble formation involves following regime:

- ⇨ The pinholes provide a pathway for water and/or oxygen to enter the diodes
- ⇨ Water & oxygen reacts with the organic emitter(s) and active metallic cathode
- ⇨ On application of electrical stress, the process is accelerated
- ⇨ Bubble formation near dust particles and pinholes
- ⇨ Bubbles nucleate randomly resulting in irregularly shaped features
- ⇨ Bubbles don't shrink on turning the bias off

4.1.1.1 Effect of pinholes

Pinholes help in the formation of bubbles and assist in their growth The initiation of bubble formation takes place at pinholes (Wang *et al.*, 2002) and there is linear dependence of bubble size with the size of pinholes.

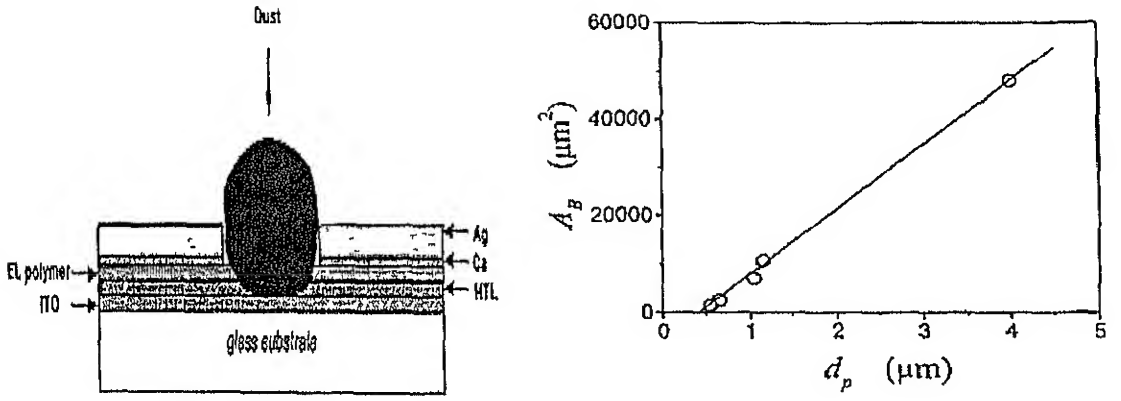

4.2 Dark Spot Formation

There is dark spot formation under higher electrical stress showing some carbonyl formation resulting in non-emitting zone formation. The reasons for the dark spot formation is given below:

- Electrical short formation & metal diffusion into the polymer
- Local heating by electrical shorts leading to formation of pinholes and damage of the polymer
- Cathodic oxidation and electrochemical reaction at metal/polymer interface
- Oxygen from ITO inducing crystallization of polymer
- Photo degradation of polymer and anodes

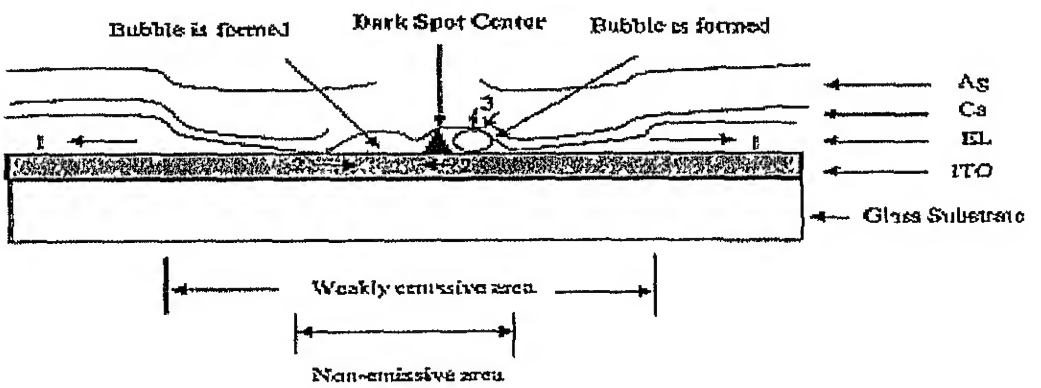

Fig 4.2.2: Dark spot formation mechanism

4.3 Photodegradation

The photodegradation of PPV polymer occurs when the film is irradiated with laser light at a wavelength corresponding to the peak wavelength of electroluminescence (EL). Degradation in photoluminescent properties was significant in an air environment but not under vacuum. This indicates that the oxygen in air aids photodegradation. This degradation may be associated with long-term stability of the electroluminescence device. Oxygen effects on PPV during the elimination reaction have been studied extensively (Shim *et al*, 1984), but there are few studies on the photodegradation reaction even though it has an important effect upon the performance of EL devices. Diphenyl (Koch *et al*, 1999) substitution in PPV is reported to reduce its photo-oxidation.

It has been reported that the PL intensity of a PPV film decrease (Zyung *et al*, 1995) drastically down to 30% of the initial intensity in a short period when the film was irradiated with 458 nm laser light (near its wavelength of EL) in air environment, as shown in Figure 4.3.1. However, the PL intensity, even when excited at 514.5 nm, where the EL peak is located as shown in the inset of Fig 4 3.1, decreases to about half of its initial intensity for fully converted PPV, which is lower, compared to the decrease for 458nm excitation.

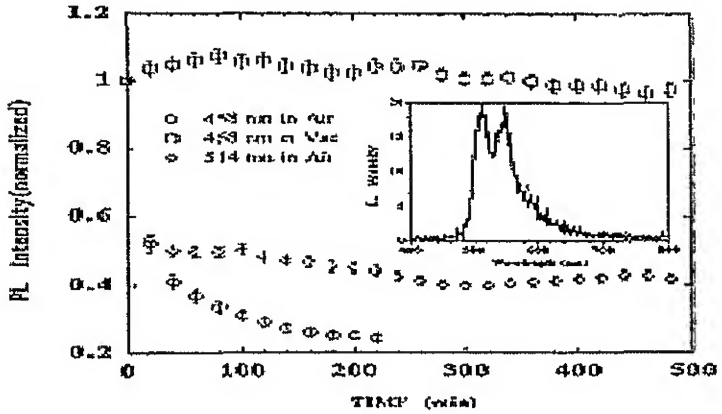

Fig 4.3.1: PL intensity with time for PPV film

This fact indicates that the polymer light emitting diode may be degraded under an air environment by its own emission. On the contrary, PL intensities show negligible change for both excitation wavelengths in a vacuum environment. These results suggest that oxygen in air may be assisting the photodegradation of PPV polymer. It is well known that oxygen affects PPV during the elimination reaction leading to low quantum efficiency due to the formation of carbonyl groups which act as quenching sites (Parker

et al., 1994). The absorption spectra are shown in Figure 4.3.2, which varies with different laser line irradiation. The decrease in absorbance shows that the material is getting more and more transparent with photo-oxidation

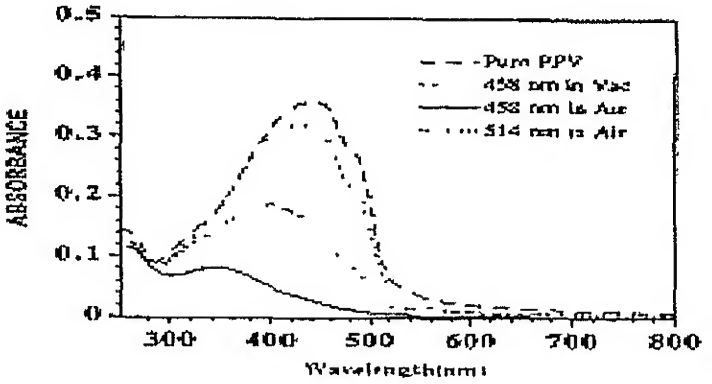

Fig 4.3.2: Absorbance of PPV with different laser lines

The original greenish yellow color of the film changes to brown after irradiation. The color is not recovered even after the sample was annealed at the elevated temperature (200 °C) in vacuum. This indicates that the chemical structure of the PPV changed during irradiation in atmospheric oxygen This can be confirmed by infrared spectroscopic measurements The photodegradation mechanism can be written as follows

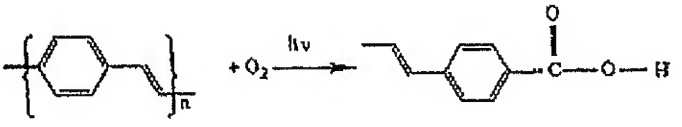

Fig. 4.3.3: Photo-oxidation Mechanism

New peaks at 1695 cm^{-1} and at 1278 cm^{-1} appear in the IR spectra of the irradiated films. They correspond to the carbonyl stretching vibrational band and C–O stretching vibrational band in a carboxyl group, respectively. This result indicates that the oxygen-sensitive electroluminescent polymers can be degraded by their own emitted light in an oxygen environment. This photodegradation of conducting polymer may seriously affect the performance of electroluminescent devices. Therefore, it is important to keep the device protected from the oxygen in air not only for protection of the easily oxidizable metal electrode but also for protection against photodegradation, resulting in enhancement of the lifetime of EL device. Carbonyl group quenching (Rothberg *et al*, 1996) of PL mechanism is shown in Figure 4.3.4. The mechanism shows that a defective carbonyl containing segment quenches the PL of neighboring segment and hence affecting more chains than actually oxidized chains.

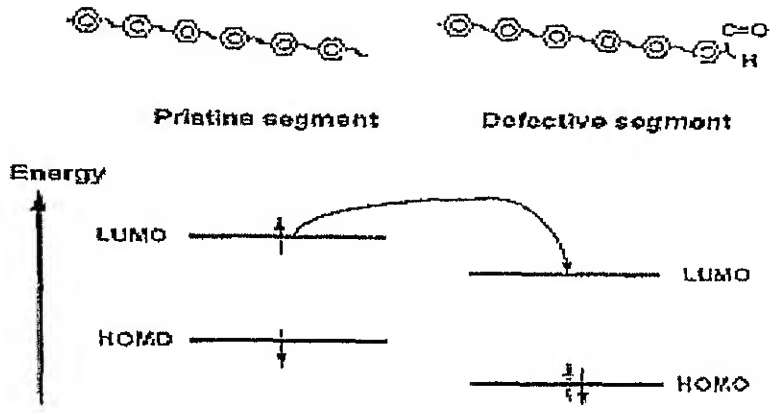

Fig. 4.3.4: Mechanism by which carbonyl containing PPV quench PL

The decay paths of excitons in PPV can be summarized as is in Figure 4.3 5.

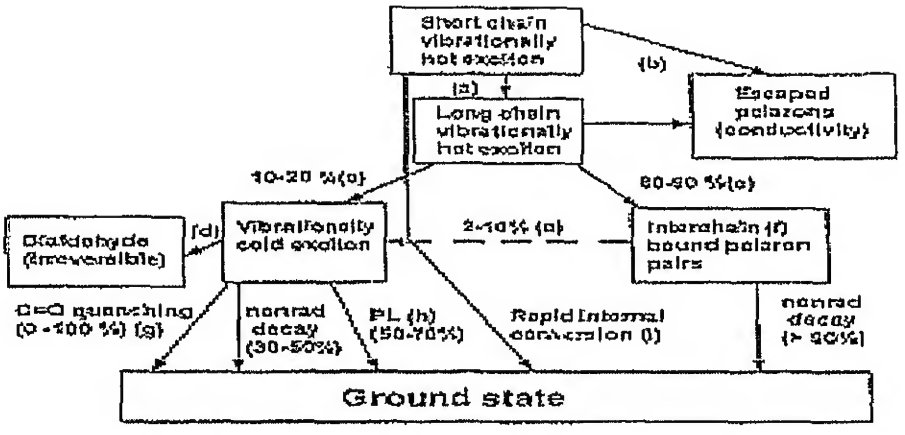

Fig. 4.3.5: *Ways of decay of exciton in PPV*

Manipulation of the chain length in the side group (Talaie *et al*, 2001) of the (PPV) based materials as well as the size of the ring located within the side group, enables to enhance PL properties of PPV related compounds. It has been found that the longer the chain length of side group and the smaller the ring size could result in much better PL. The effect of oxygen on the PL properties of these new materials was also examined and it was found that the PL intensity could be decreased more than five times than initial values over 10 min in the air compared with the same measurements in vacuum for the same period of time.

Photo-oxidation of PPV is considered to be an important cause of degradation in the performance of OLED and the consensus is that oxygen is the initiator of chain scission. The photo-oxidation is reported to decrease the refractive index and absorption coefficient along with increase in film thickness (Kumar *et al*, 2003). It is

important to understand the mechanism of photodegradation in order to improve the performance and reliability of the device. The degradation of an OLED was investigated by studying the decay of photoluminescence intensity and the change in structure by x-ray diffraction (Chen *et al*, 2002) Electrical stress also plays an important role in the photo-oxidation degradation process The photoluminescence degradation with electric field under ambient and nitrogen environment is shown in Figure 4.3.6

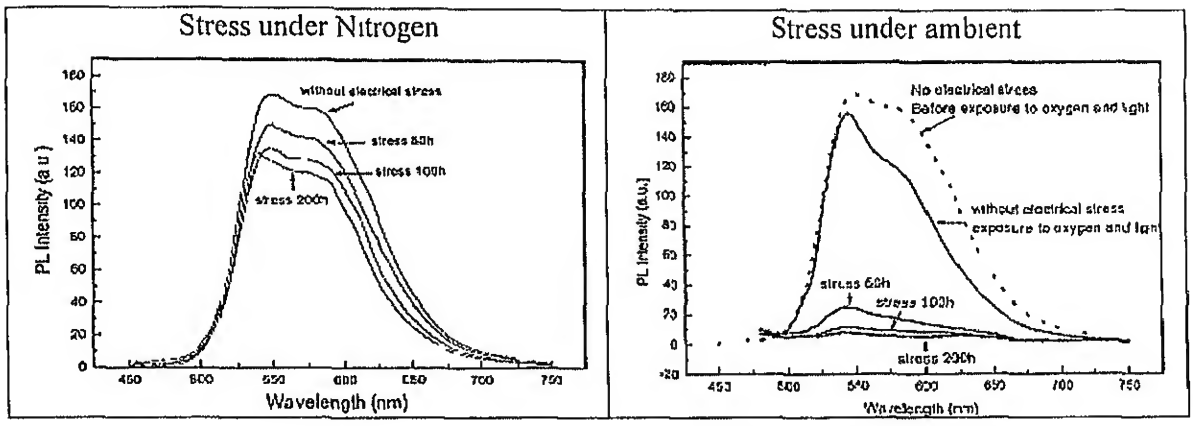

Fig 4.3.6: PL decay under stress in ambient and nitrogen

For the devices without previous electrical stress but exposed to a normal ambient for several days, the PL spectrum does not exhibit any significant change in shape and intensity. X-ray diffraction spectra for the devices after electrical stress, but without exposure to a normal ambient, shows no noticeable crystallization peak. The x-ray diffraction results from devices that were exposed to a normal ambient after the electrical stress, shows the crystallization peak at around 8°. The longer the stress time, the stronger the crystallization peak as shown below in the Figure 4 3 7.

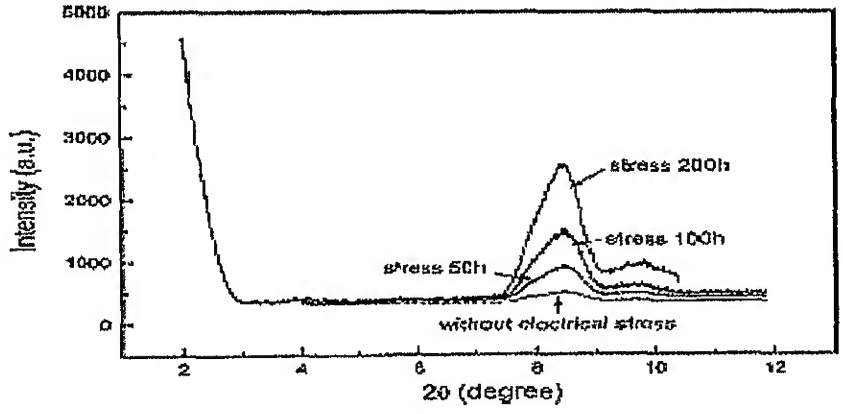

Fig. 4.3.7: XRD of devices with stress time

Extensive and systematic investigations of the polymer photo-oxidation degradation process (Shim *et al*, 1984; Scurlock *et al*, 1995; Sutherland *et al*, 1996; Cumpston *et al*, 1997) have drawn the conclusion that oxygen binds to the vinyl bond, leading to the chain scission and the formation of carbonyl groups. The effect only acts when both oxygen and light are present.

In the literature, the PL degradation with laser for MEHPPV film as a function of exposure time in air and under flowing N_2 has been compared by burrato group at Santa Barbara at California. Figure 4 3.8 a shows a decrease in the emission intensity with increasing exposure time in air, as expected Changes also occur in the shape of the emission spectrum over time.

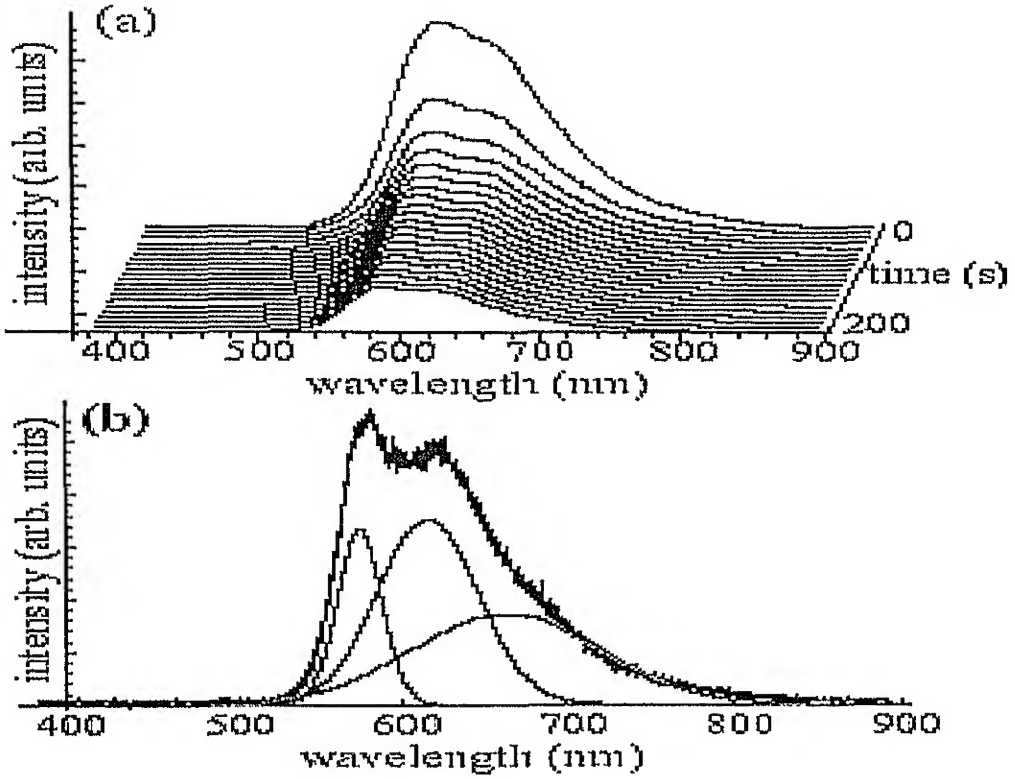

Fig. 4.3.8: Photoluminescence spectra versus exposure time.

These changes can be quantified by fitting each spectrum and plotting the fit parameters as a function of exposure time. Figure 4.3.8 b shows a representative spectrum fit to three gaussians, the individual gaussians are shown as well as the fit to the data.

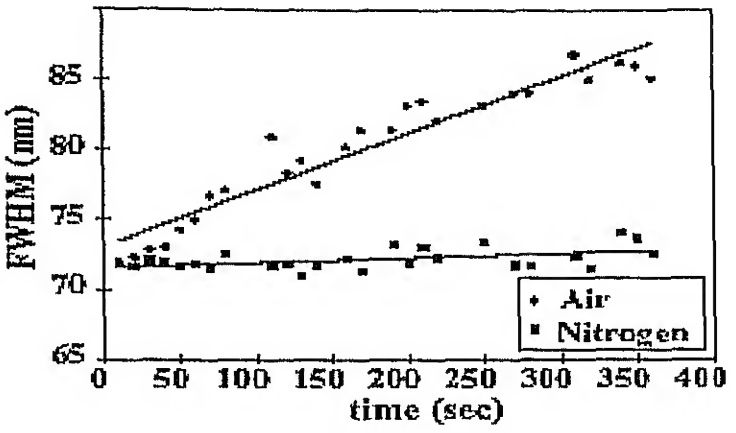

Fig 4.3.9: FWHM variation in nitrogen and ambient

Figure 4.3 9 compares the FWHM of the second gaussian versus exposure time in air and in flowing nitrogen. In air, the intensity decreases rapidly, with a 70% decrease in signal occurring after only 18 s. Accompanying the loss in signal is an increase in the FWHM of the second gaussian indicating a change in the vibronic coupling. In contrast the spectra recorded under flowing N_2 show a smaller decrease in signal and a relatively constant FWHM of the second gaussian.

This model is in agreement with a previously proposed model for photo-damage in PPV films (Papadiamitrakopoulos *et al*, 1994; Zyung *et al*., 1995). In IR experiments of films irradiated under ambient conditions, C=O stretches have been observed to grow into the IR spectra over time. The C=O groups formed by the photo-oxidation act as efficient traps of excited electrons due to their relatively high electron affinity. Once excited, electrons are trapped and relax non-radiatively, resulting in a decreased emission yield as well as heating in the polymer. It's also noted that if the film is allowed to set in air for greater than five hours, the photooxidation is the same in air or under flowing N_2, which indicates that O_2 is able to efficiently penetrate the MEH-PPV film.

As the MEH-PPV film is oxidized forming the electron trapping C=O groups, absorbed radiation is quenched nonradiatively which in turn causes a heating of the polymer film. It is likely that this heating causes the topography features observed for long exposure times as reported by Skordoulis *et al* 1999.

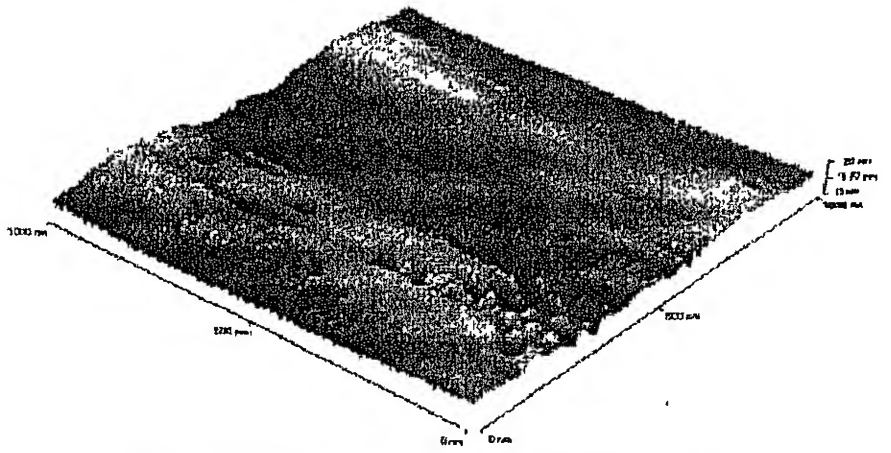

Fig 4.3.10: Surface properties after laser irradiation

PL intensity enhancement in PPV films induced by light irradiation in the presence of air has also been reported by Gobato *et al*, 2002 This effect is dependent on laser intensity and the ratio between film thickness and excitation penetration depth The results suggest that an efficient spectral diffusion of excited carriers to nondegraded PPV segments by Forster energy transfer is an important consideration in the PL efficiency of conjugated polymers light-irradiated in air The dependance of transmittance of MEH-PPV film with laser intensity is reported by Skordoulis *et al* 1999

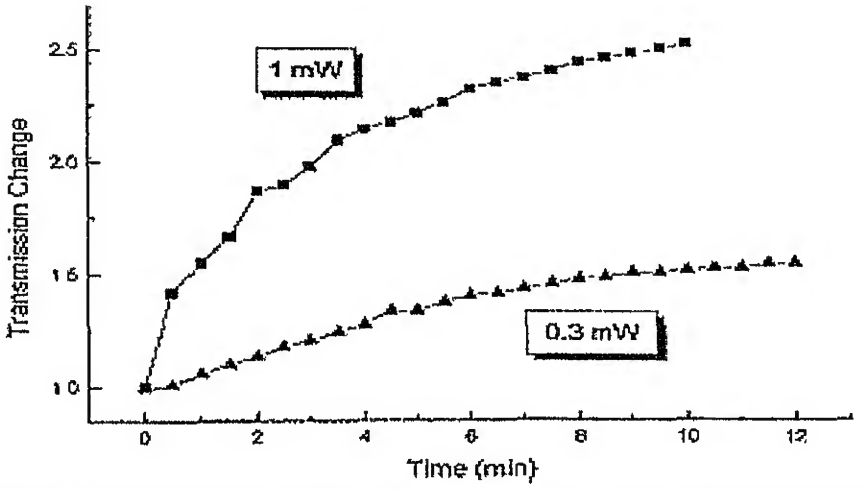

Fig 4.3.11: Transmission change with laser irradiation for different intensities

However, laser induced degradation of PPV & CN-PPV is not well studied as MEHPPV, which necessitates development for a procedure to study the parameters involved.

5. Materials and Methods

5.1 Materials

The materials used were obtained from Samtel Centre for Display Technologies at Indian Institute of Technology, Kanpur. The materials were synthesized in-house. The PPV (Poly Para Phenylene Vinylene) was synthesized by xanthate (Son *et al*, 1995) precursor route and CN-PPV (Poly{[2,5-bis(hexyloxy)-1,4-bis(1-cyanovinylene) phenylene]}) was synthesized by a Knoevengel-type condensation between hexyloxy substituted aromatic diacetonitrile and a corresponding dialdehyde (Chen *et al*, 1998) The chemical details are described in detail elsewhere (Kumar *et al*, 2003) All the glasswares used in the present study were of 'corning' quality manufactured by Borosil Glass Works Ltd De-ionised water and analytical grade chemicals were used for the device preparation.

5.2 Sample Preparation

5.2.1 Sample Cleaning

First the ITO sputtered glass sheets are checked for the direction of ITO with the help of multimeter The sheets are then cut with diamond cutter according to the desired size The samples are first marked a line with steel scale with the help of the cutter on the glass side and the sample is then broken along the cleavage plane developed. Then the samples are named with the diamond cutter on the glass side to identify the ITO side during the processing. The samples are then cleaned with tissue paper with acetone to remove dusts present at the surface of the sample Then the samples are rinsed with de-ionized water and ultrasonic cleaning is done and then they are dried. If the samples are not dried properly, then watermarks will be formed, as TCE is nonpolar so the places with water will not be wetted by TCE and hence would not be cleaned properly. They are then heated in TCE, acetone and methanol solutions one after other for around 15 min each in Teflon basket for holding the samples. The samples should be placed in the solutions and the time should be counted from that instant, otherwise the solution may become too hot and may damage ITO. The temperature should not be allowed to exceed 60^0C. Then the samples are again rinsed in de-ionized water followed by ultrasonic cleaning in de-ionized water for 10 minutes. Then RCA cleaning is done with a solution of water:ammonium hydroxide:hydrogen peroxide in the ratio of 5.1:1. The samples are again rinsed with de-ionized water The samples are then dried and put into oven for drying at around 110^0C for 1 hr.

5.2.2 ITO Patterning

The samples are taken out and cooled to room temperature. The sample is placed on the spin coating unit and the vacuum pump is turned on to hold the sample. Photo resist is then dropped above the ITO surface with the help of a syringe The sample is then rotated to spin coat the photo resist at desired speed. The photo resist is then put into oven for prebaking at around 80^0C in nitrogen environment for around 15 min. The samples are then taken out from oven and allowed to cool. The dried photo resist is then irradiated with ultraviolet light with a desired mask for the pattern so that the photo resist hardens at the place of UV irradiation Then the samples are washed in four developer solutions for 1 min each. Then the samples are again placed in oven for post baking at around 130^0C to properly dry out and harden the photo resist for around 20 min.

The samples are then cooled and the solution for etching the ITO at undesired places is prepared. The solution comprises of 20:4:1 of Water,HCl:HNO_3 respectively followed by few drops of detergent. The solution is heated to around 55^0C and the samples are placed on the Teflon basket in the solution for around 7 min. The temperature is maintained at 55^0C. The samples are taken out then checked for remnant ITO at the undesired places using multimeter after drying. If still some remnant ITO is found then the samples are again placed in the solution otherwise they are rinsed in de-ionized water. Then the samples are washed in photoresist stripping solution to wash out the hardened photo resist. The solution is first heated to 90^0C and then the samples are dipped first in used solution for 1 min followed by unused solution again for 1 min. When the photo resist layer seemed to have washed out then the samples are cleaned in hot water to remove the remaining washing solution on the sample. The samples are again cleaned with RCA solution. The samples are then ultrasonically cleaned in de-ionized water for 5 min. The samples are then dried.

5.2.3 Polymer Solution Preparation

5.2.3.1 PPV Solution Preparation

PPV (Poly Para Phenylene Vinylene) precursor films are taken and weighed according to the concentration of solution desired. The generally prepared samples are 18mg/cc, 12mg/cc and 6mg/cc solutions. The precursor film is used instead of PPV itself, as it is not as such soluble so spin coating is impossible otherwise. The vapor

deposition of PPV is not possible as PPV degrades under high temperature if vapor deposited The PPV precursor is prepared by Wessling Preccursor route (Wessling *et al.,* 1962) in which PPV is mostly trans and hence is highly crystalline. But the hydroxy group is oxidized to carbonyls (Papadiamitrakopoulos *et al.,* 1994), which limits the electroluminescence when the precursor is converted. So Xanthate route for preparation where mixture of cis and trans is formed is preferred First the desired amount of the PPV precursor is weighed and then it is transferred to bottle for solution preparation. Then the desired amount of cyclohexanone is added to the bottle Then for stirring, a plastic coated magnet is cleaned and is put inside the bottle. Then the bottle is sealed with a tube containing silica gel and placed on magnetic stirrer to properly mix the solution and absorb any remnant moisture. The solution is stirred for around 2 hours and then they are transferred to two centrifuging tubes with almost equal amount of solution in each to provide balance. Then they are put into the centrifuge and it is turned on for around 30 min If there is gel formation, then the solution above is carefully decanted to storage bottle The bottle is flushed with nitrogen and then sealed with cap and paraffin tape

5.2.3.2 CNPPV Solution Preparation

CNPPV is directly soluble in chloroform and also in toluene So there is no requirement of any precursor for CNPPV. For the purpose of spin coating, chloroform is can be used as it is volatile which is necessary for drying of the film quickly. But as it dries too quickly, so a 1:1 mixture of chloroform and toluene is used. First the desired amount of CNPPV is weighed and put into the bottle that is continuously flushed with a stream of nitrogen Then desired amount of clorofoim and toluene are poured into the bottle and then the bottle if sealed with the stopper and paraffin tape. Sealing is very important here not only for the purpose of proper storage of polymer, but also the concentration will otherwise keep on increasing with time with vaporization of chloroform.

5.2.4 Spin Coating

The dried samples are placed into oven for prebaking before the spin coating at 110^0C to dry out any remnant moisture. Then the samples are taken out and allowed to cool to room temperature. Then they are placed on ozonizing machine, which irradiates the sample with UV light under continuous flow of oxygen so that oxygen is converted

to ozone. This ozone oxidizes the surface and improves the surface properties including work function and adhesion. This is similar to oxygen plasma treatment. Then the samples are placed into the spin coating unit one by one and continuous nitrogen-hydrogen gas supply is turned on. Then vacuum in the spin coating unit is turned on so that it holds the sample at its place. Then the polymer layer is dropped on the sample uniformly and then the unit is turned on. The rpm of the unit is set according to the requirement of thickness that depends on rpm and concentration of the polymer solution. There is also dependence on temperature, but that becomes redundant, as the room temperature is kept constant. Then the samples are placed in oven at room temperature and then the temperature is increased gradually. The samples are kept under nitrogen+hydrogen ambient at 170^{0}C for PPV and 120^{0}C in nitrogen ambient for CNPPV for baking. The baking times being 6 hours and 1 hour respectively. To improve the film properties, vacuum drying of the solvent is also tried for PPV Cyclohexanone is more viscous and is difficult to vaporize So vacuum drying at 120^{0}C for 1hr before baking conversion improves the film property

5.2.5 Metallization

After baking the samples are placed properly inside vacuum coating unit above desired masks so that the side to be coated faces downward. The metal pieces are cleaned with acetone and then placed in the heating coil. Then the bell jar is closed after applying a thin layer of silicone grease below the rubber pad to check leakage and to obtain better vacuum. The bell jar is pressed against the bottom plate properly as shown in Figure 5.2.5.1.

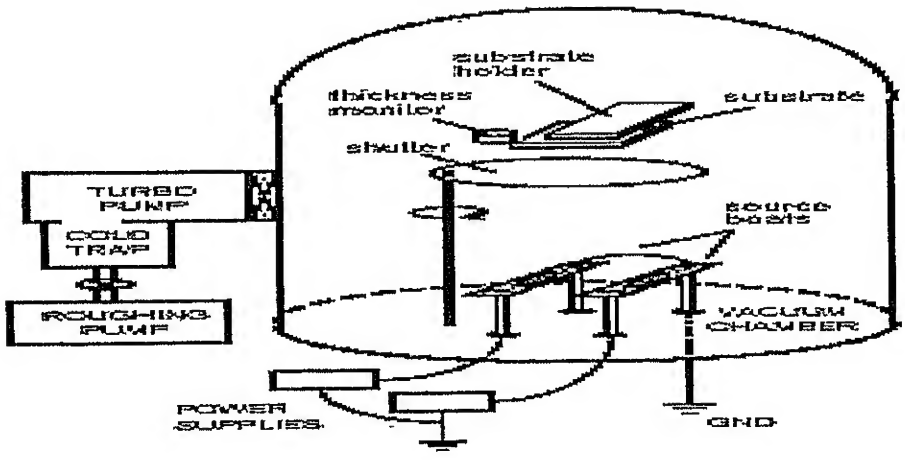

Fig 5.2.5.1: Vacuum chamber for metalization

Then the air and gas admittance valve is closed Now the rotary pump is turned on. Then the valve is placed in the backing mode to take out air within the region of diffusion pump chamber. Then after the meter shows a pressure around 10^{-3}atm is obtained, then the valve is rotated to roughing so that the air is now evacuated from inside the coating chamber. After waiting for the pressure inside the chamber to reach around 10^{-3}atm, the valve is then rotated back to backing Then the diffusion pump is turned on along with the cooling supply to the diffusion pump Then after waiting for around 25 min, the valve controlling the linkage between the coating chamber and the diffusion pump is opened. Then pressure inside the chamber starts to decrease again and when it reaches around 10^{-5}atm, the coil containing the metal in heated by passing current so that the metal just melts and remains in the coil. The shutter remains closed during the process to avoid impurities present in the metal to contaminate the samples. Then the shutter is opened and the coil is heated red-hot. Then after some time the metal gets deposited on the samples then the power supply to the coil is switched off and the system is allowed to cool with both diffusion and rotary pump on. Then the valve connecting the chamber and diffusion pump is closed. Then after 5 min, the diffusion pump is switched off Then after 15 min the coolant supply is switched off The valve is closed and the rotary pump is turned off. The samples are allowed to cool for an hour and then the samples are taken out from the chamber by allowing air inside the chamber using air-admittance valve. The samples are then transferred to vacuum desiccators.

5.3 Experimental Set-up

5.3.1 I-V Set-up

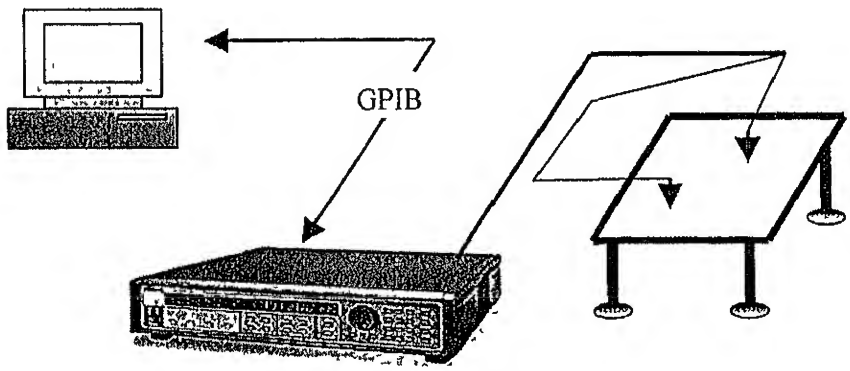

Fig 5.3.1.1 I-V Set-up

The I-V set-up comprises of table with probes to make contact with the sample having ITO and Al strips. Changing the polarity of the probes accordingly can perform the forward and reverse I-V. The probes press the sample as they are fitted with magnets at the bottom, which attracts the probes and hence creating the pressure. So the pressure is also not so much high as crocodile clips, which scratch and punch especially the Al strip The probes are connected to Keithley 236 source, which can apply a voltage and measure the corresponding current. The sweep rate and the voltage range can be programmed with a GPIB computer interface Current time measurements can also be done on this set-up to measure the stability of the device. Here constant voltage is applied and the corresponding current is monitored

5.3.2 Impedance Spectroscopy Set-up

Impedance spectroscopy is a method to separate the contact and bulk impedance and hence can be used to effectively calculate the degradation in the OLED. The degradation can be separated according to what is actually degrading, the polymer or the contact itself

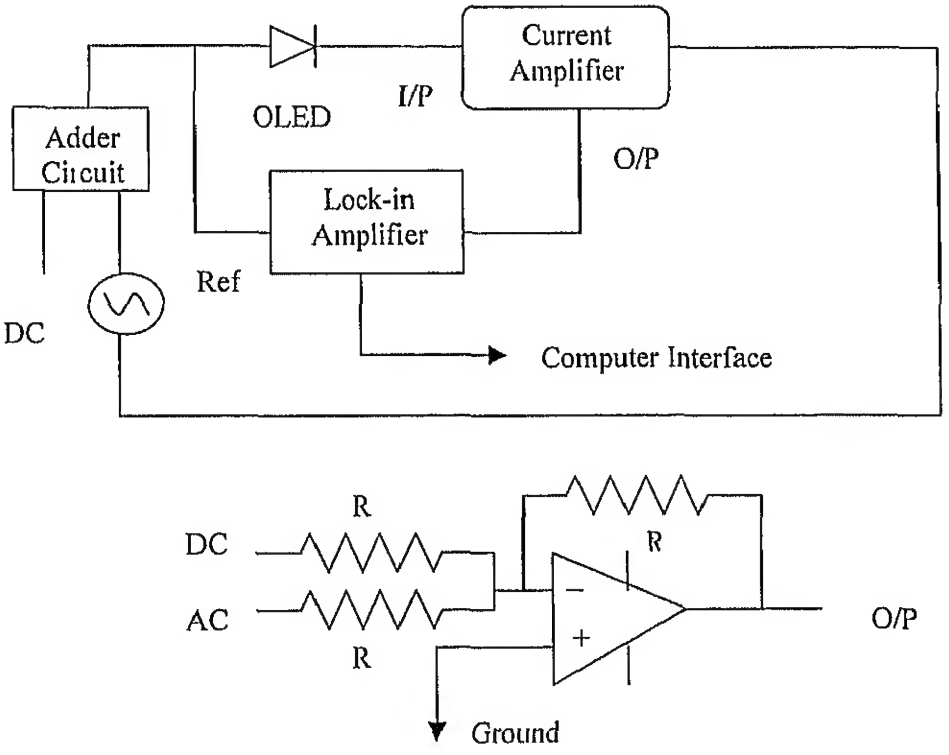

Fig.5.3.2.1: Impedance Set-up

This is a unity gain adder circuit with all the resistances R. There is optimum value for R as increasing R will reduce the loss but increase the time delay due to

increase in RC value of the circuit So optimum value is taken to be 1MΩ. The Op-Amp is taken to be UA741CN operated to V_{cc} of 13 V. Now the AC signal is applied from SRS 830 DSP Lock-In Amplifier. The DC signal is applied from the auxiliary O/P of the lock-in The lock-in is connected to computer with GPIB interface The program is made by Matlab software The commands were given by running the program The AC and DC signal are fed at the same time for measuring the impedance of the device at various biases

5.3.3 Photoluminescence Set-up

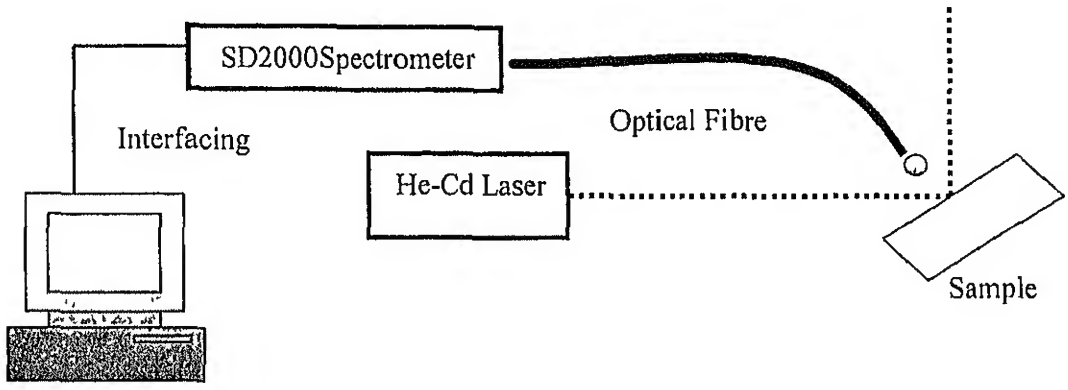

Fig 5.3.3.1: PL Set-up

The samples are placed in sample holder for air photoluminescence experiment. The sample holder comprises of two fixed ends with grooves to hold the sample. There is a movable end on one side, which moves on the base plate and can be secured by tightening screws to the base plate. So samples of different sizes can be fixed. He-Cd laser at 442 and 325 nm excited the samples. All the degradation experiments were done at 442 nm, which was near to the absorption spectrum peak for PPV. The optical fibre was fixed in front of the sample and was connected to the SD2000 Ocean Optics CCD spectrometer, which in turn was interfaced with computer with the help of ADC card and OoiBase32 software. The spectrometer has two channels, master and slave with range 180 to 820 nm and 480 to 1180 nm respectively The channels were chosen according to the PL peak position. For instance in PPV with peaks at 510 and 542 nm, master was chosen and for CNPPV with peak at 639 nm, slave was used. For Vacuum measurements, sample is mounted inside a cryostat and the light is detected though a quartz window within the cryostat.

5.3.4 Reflectance Set-up

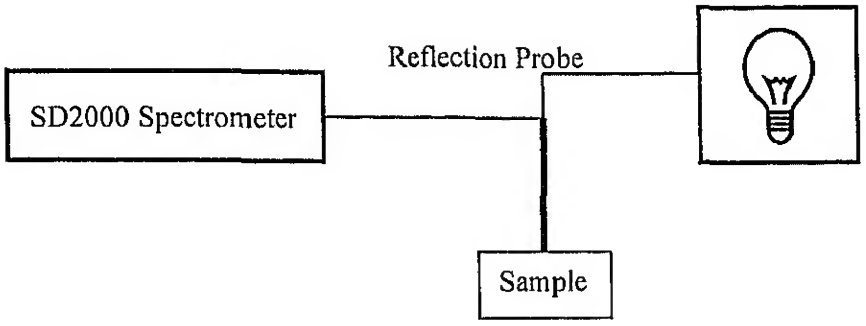

Fig 5.3.4.1: Reflectance Set-up

Reflectance was also measured with the help of SD2000 CCD Spectrometer. The light source used was tungsten halogen lamp white light and was excited with reflection probe with one central fibre and six excitation fibres surrounding the central one. First dark reference was recorded then bright reference was recorded with a cleaned glass plate. The polymer coated glass plate was taken and the intensity of the sample is recorded. Then reflectance is calculated by taking ratio of sample and reference after deducting the dark reference.

5.3.5 Transmittance Set-up

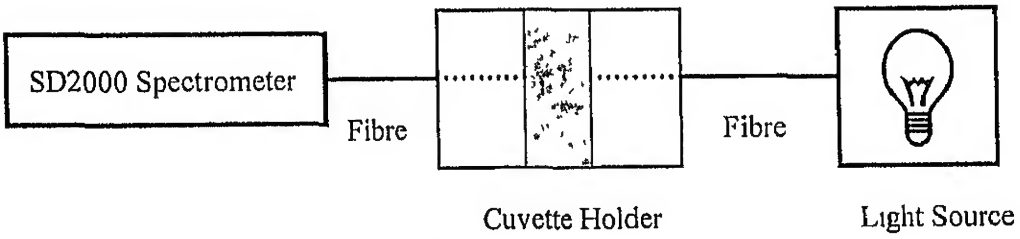

Fig 5.3.5.1: Transmittance Set-up

Transmission mode is similar to the reflectance, the only difference being that the intensity is measured in transmission mode rather than in reflection. Here two different fibres are used. The excitation fibre is of lower diameter compared to the collection one. The sample is placed in the cuvette holder. First the dark intensity is stored. Then the bright reference of only glass followed by the sample intensity is performed.

6. Results and Discussions

In the present study, attempts were made to characterize different materials for application in organic light emitting diodes. The purpose involves the study of the degradation mechanism and the causes for the degradation in OLED. The degradation occurs both in the materials and in the contacts during operation So there is a need of finding appropriate steps to check the degradation to make OLED commercially viable. Degradation was studied using accelerated laser degradation. The main motivation behind being the effect of own light of the device on degradation which can in turn restrict the lifetime of the device.

6.1 Effect of back metallization on Photoluminescence

6.1.1 Reflectance Measurements

Reflectance measurements for thin films are used as a guide for optical model of the sample prior to photoluminescence characterization. Reflectance of PPV was measured for a typical thick film to derive the film thickness in a double-coated PPV layer above glass as shown in Figure 6.1.1.1.

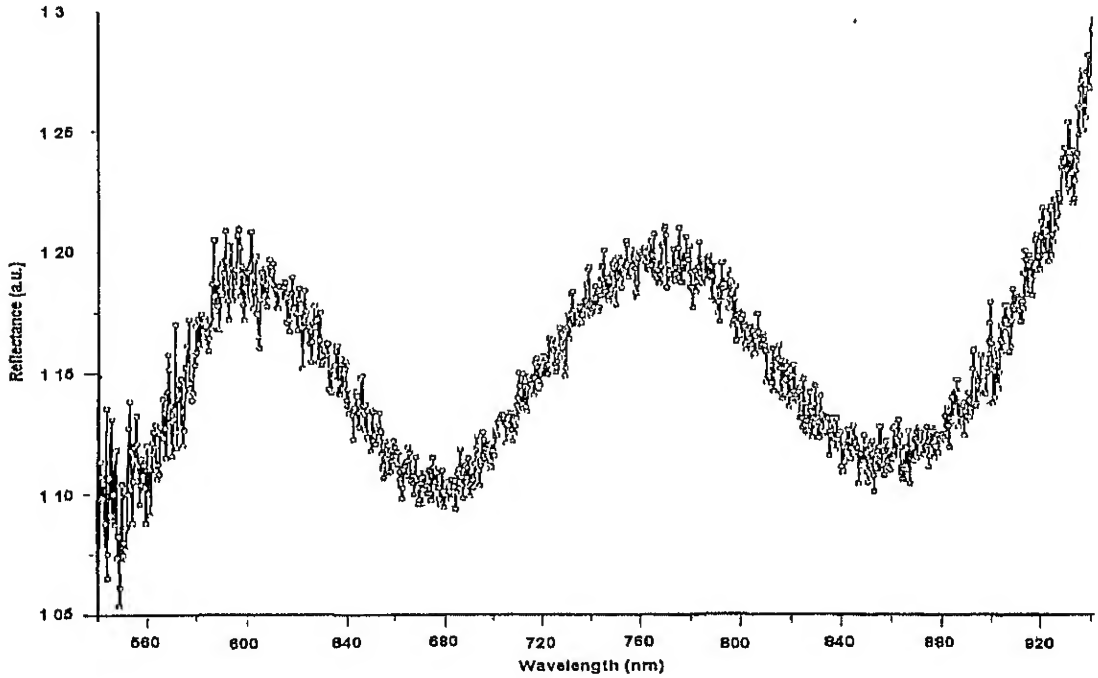

Fig 6.1.1.1: Reflectance of three layers coated thick PPV film

The thickness can be calculated from the formula as below:

$$t = \lambda_1/2\eta[1 - (\lambda_1/\lambda_2)]$$

Two peak maxima are seen at 600 82 and 769 48 nm corresponding to λ_1 and λ_2

Refiactive index for PPV vaiies from 2.3 to 2.7 and the thickness corresponding to them are.

For $\eta = 2\ 3$ $t = 0\ 6\ \mu m$

For $\eta = 2\ 7$ $t = 0.51\ \mu m$

Hence an approximate thickness can be determined. Moie accurate thickness can be deduced if the iefractive index is experimentally determined Most thicknesses used in this woik aie much smaller and are in the i ange of 1000-1200A

6.1.1 Effect of back metallization on Photoluminescence

Fig 6.1 2 1 shows PL spectia of thin films deposited on glass and on a thin film of gold coveiing the glass The PPV film on glass is shown in the Figure 6 1 2 1

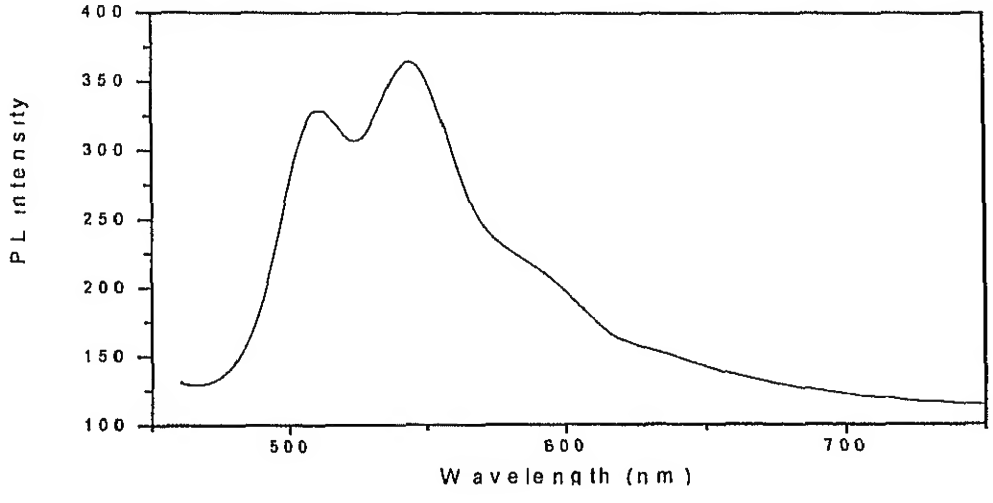

Figure 6.1.2.1: Photoluminescence spectrum of PPV film on glass

Photoluminescence peaks were obseived at 508 and 543 nm iespectively with two more peaks. The fiist peak at 508 nm is considered to be the bandgap peak corresponding to PPV. Four peaks were observed in the prepared PPV compared to the reported three peaks in the liteiature. PL is the standard chaiacterization technique for mateiial

characterization and to compare the optical properties of materials PL peak positions and the spectrum remains unchanged in a materials at a specified temperature and varies linearly with varying laser intensity hence the nature of spectrum almost independent of intensity making it a powerful tool for characterization

Photoluminescence experiments were done on PPV and the spectra were studied both above gold and above glass. The PL obtained above gold is much more intense than above glass due to reflection of PL from back and also the incident laser beam getting reflected and resulting more luminescence. So theoretically four times increase in the PL intensity is expected. The compaiative plot of PL with and without back metalization is shown in Figure 6.1.2 2

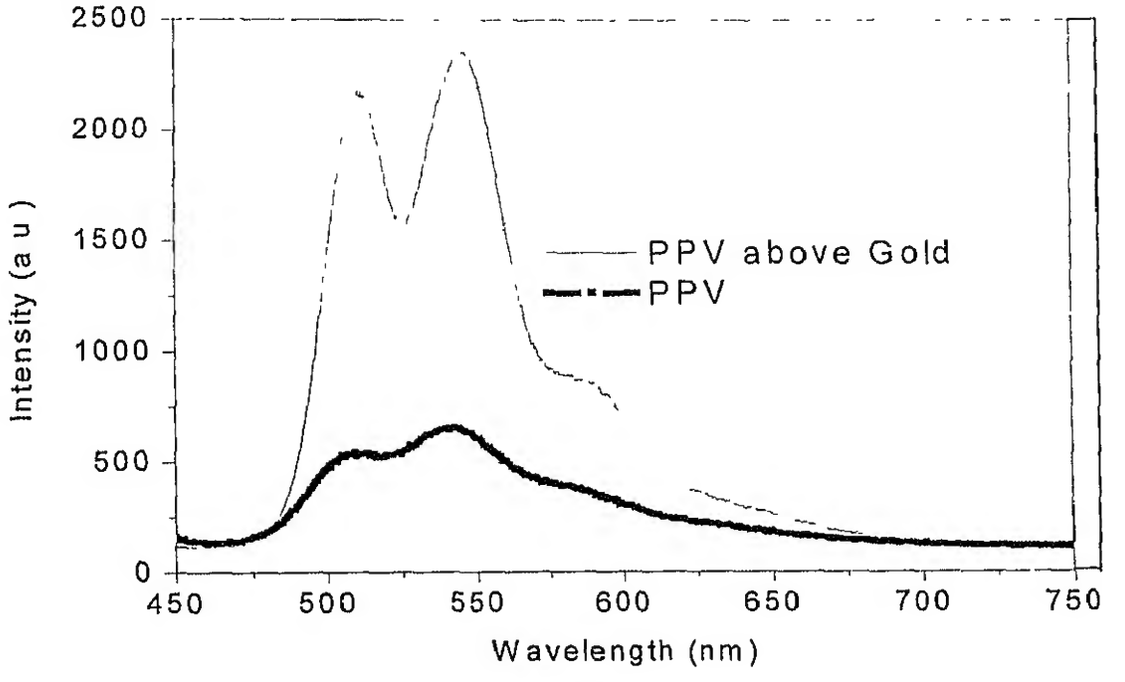

Fig 6.1.2.2: PL intensity of PPV film above glass and gold

6.1.3 Effect of laser intensity on photoluminescence

It is important to establish the relation between luminescence yield and the intensity of the excitation in the range of intensities used in this work. Figure 6.1 3 1 shows PL spectra for intensity changing over more than 500 times. The intensity of the laser is varied by putting neutral density of filters in the path of the laser beam. The photoluminescence varies almost linearly with the laser intensity.

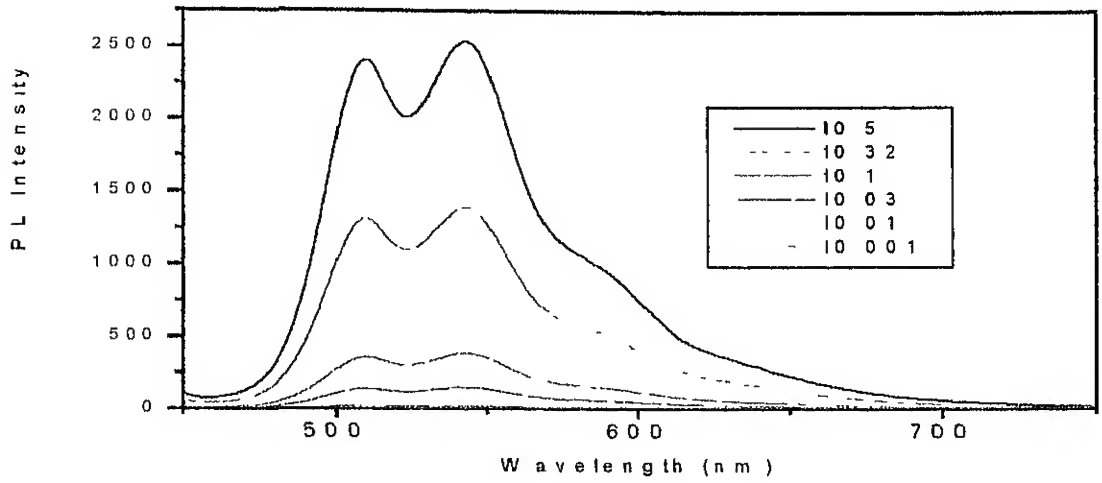

Fig 6.1.3.1: PL intensity of PPV film with different excitation laser intensities

The photoluminescence intensity is plotted as a function of transmittance of filters in double logarithmic plot in Figure 6 1 3.2

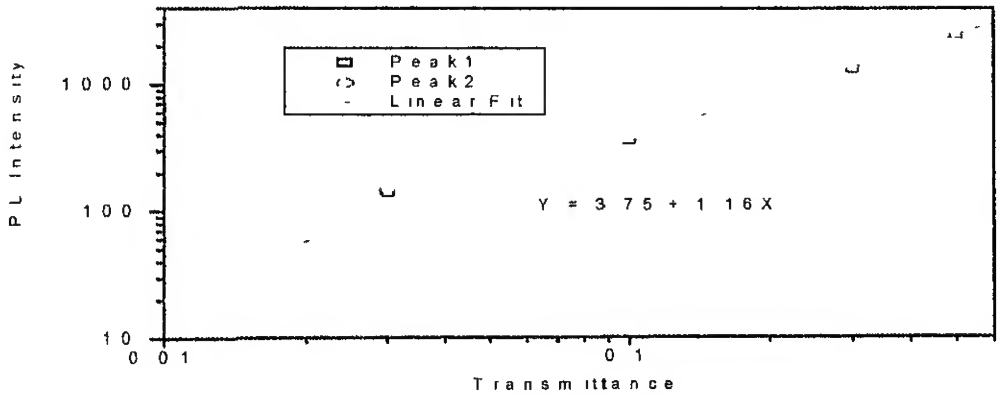

Fig 6.1.3.2: PL peak intensity of PPV film with varying transmittance of ND filters

The equation may be defined as $I_{PL} = AI^{N}_{excitation}$

So $\log(I_{PL}) = \log(A) + N\log(I_{excitation})$, here $N \approx 1$

Hence it can be inferred that $I_{PL} \propto I_{excitation}$

Transmittance = $I_{excitation}/I$

Linear dependence of PL intensity with excitation intensity ensures that arguments involving change in PL intensity with excitation is not a problem in this case

6.2 Photoluminescence degradation under laser irradiation

6.2.1 Design of Experiment

In this work, as mentioned in chapter 5, we use 442nm line of a 50 mW He-Cd laser with beam diameter of 1 5mm A typical scan of PL spectra with CCD detector takes

a fraction of second However if the laser is allowed to fall on the sample, then the laser excitation itself can degrade the material and this degradation can be monitored by observing the PL spectra intensity changes periodically during the laser irradiation We use this degradation as a means of monitoring the effect of process parameters on the quality of the material as regards their susceptibility of degradation

6.2.2 Degradation of PPV in air

There is considerable photoluminescence degradation under laser irradiation at 442 nm with power 50 mW and laser diameter of 1 5 mm It has been reported (Zyung *et al*, 1995) that laser irradiation near the absorption peak of organic semiconducting polymers causes more degradation The absorption spectrum of PPV has a peak at 400 nm and CNPPV at a higher wavelength So the degradation rate for PPV is higher compared to that for CNPPV The degradation of PPV is shown in Figure 6 2 2 1

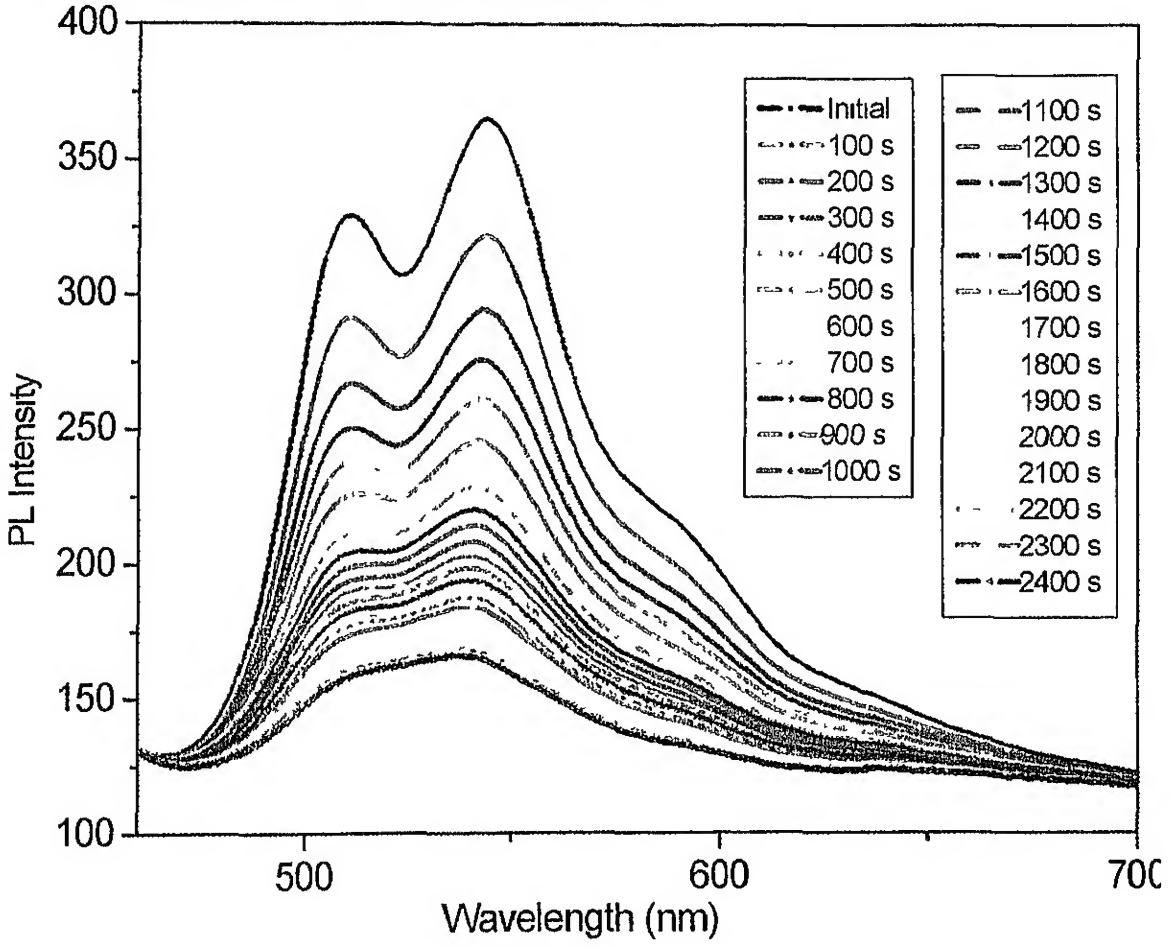

Fig 6.2.2.1: PL intensity variation of PPV film with laser irradiation time

PL spectra observed after various specified duration of laser irradiation is shown in the Figure 6 2 2.1. Note that the intensity decreases gradually for all components of the spectra with increasing duration of exposure

The intensity peaks are observed at 510.5 and 543.6nm respectively For a better appreciation of time dependence of PL intensity with exposure time, the intensity of the 543.6 peak is monitored as a function of time, in-situ as shown in Figure 6 2 2 2 where the behavior showed second order exponential decay characteristics

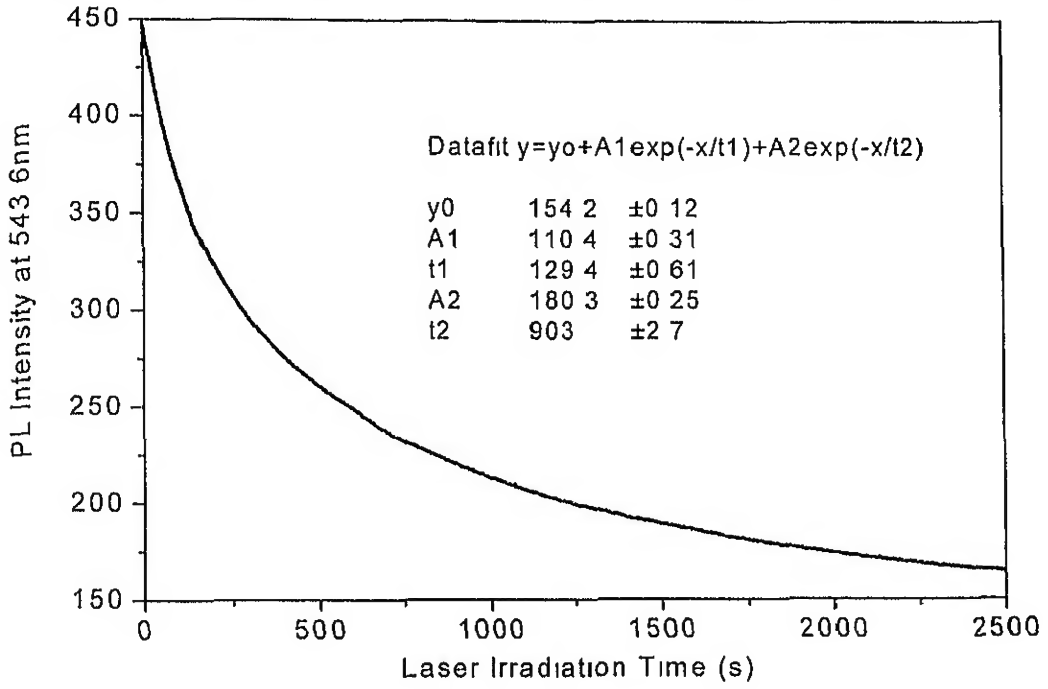

Fig 6.2.2.2: In-situ PL intensity variation of peak 2 with time

The decay shows two time constants of 129 and 903 sec respectively indicating occurrence of two distinct processes contributing to photodegradation. The picture becomes clearer by plotting log ($y-y_0$) vs. time as shown in Figure 6 2.2 3, which shows two different slopes and hence we can suspect that actually there are two processes occurring in the degradation processes giving rise to these different slopes. We subtract the contribution due to second slope and then determine the corrected shape of the faster process. In Figure 6.2.2.3 the smaller graph shows the linear fitting after this correction.

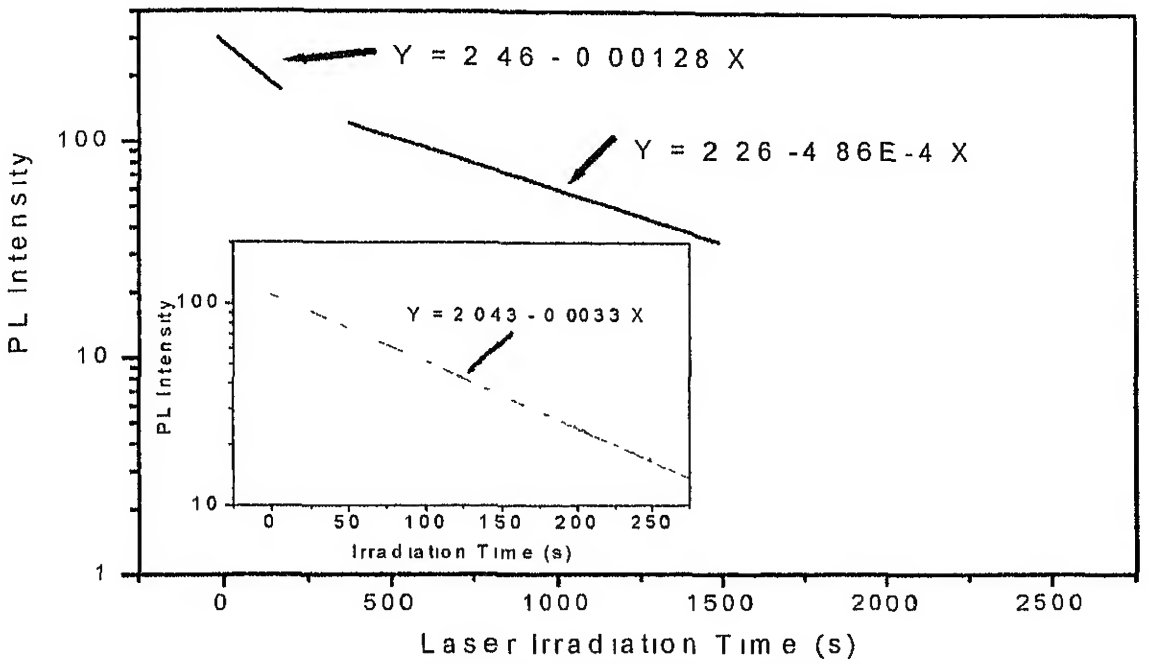

Fig6.2.2.3: Semi Logarithmic plot of PL intensity variation of peak 2 with time

All spectra are normalized and plotted in Figure 6 2 2 4 Blue shifting by about 4 nm is observed by laser irradiation especially in the 543 6 $\overset{nm}{\lambda}$ peak as seen in the Figure 6 2 2 4 Also the line shape varies widely indicating change in components of spectra

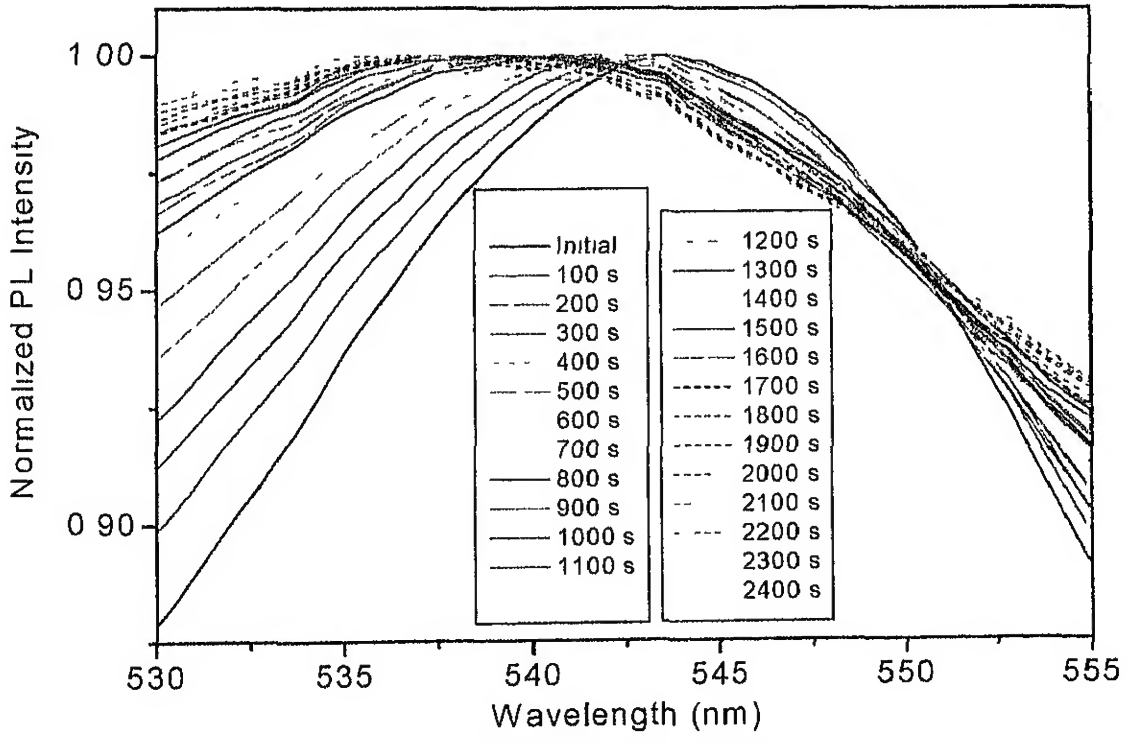

Fig 6.2.2.4: Normalized PL intensity spectrum of PPV for the peak2

In figure 6 2 2 4, there is prominent blue shifting along with the widening of the spectra with laser irradiation time In order to obtain further insight into changes in PL spectra, each of the spectra was further fitted to sum of Gaussians by automatic fitting procedure using Peakfit software It was necessary to subtract out artifactual background variation prior to fitting A typical fit of a spectrum and components are shown in Figure 6 2 2 5 The quality of the fit was very good with regression parameter greater than 99% for all curves Although the fitting quality worsened slightly for the larger irradiation time spectra We then use the results of these fitting to obtain changes in peak position, FWHM, area under the curve and intensity of the components of spectra In Figure 6 2 2 5, the red line shows the fitting of the spectra by four gaussians The black line is the main spectra The fitted peaks are shown by green, blue etc

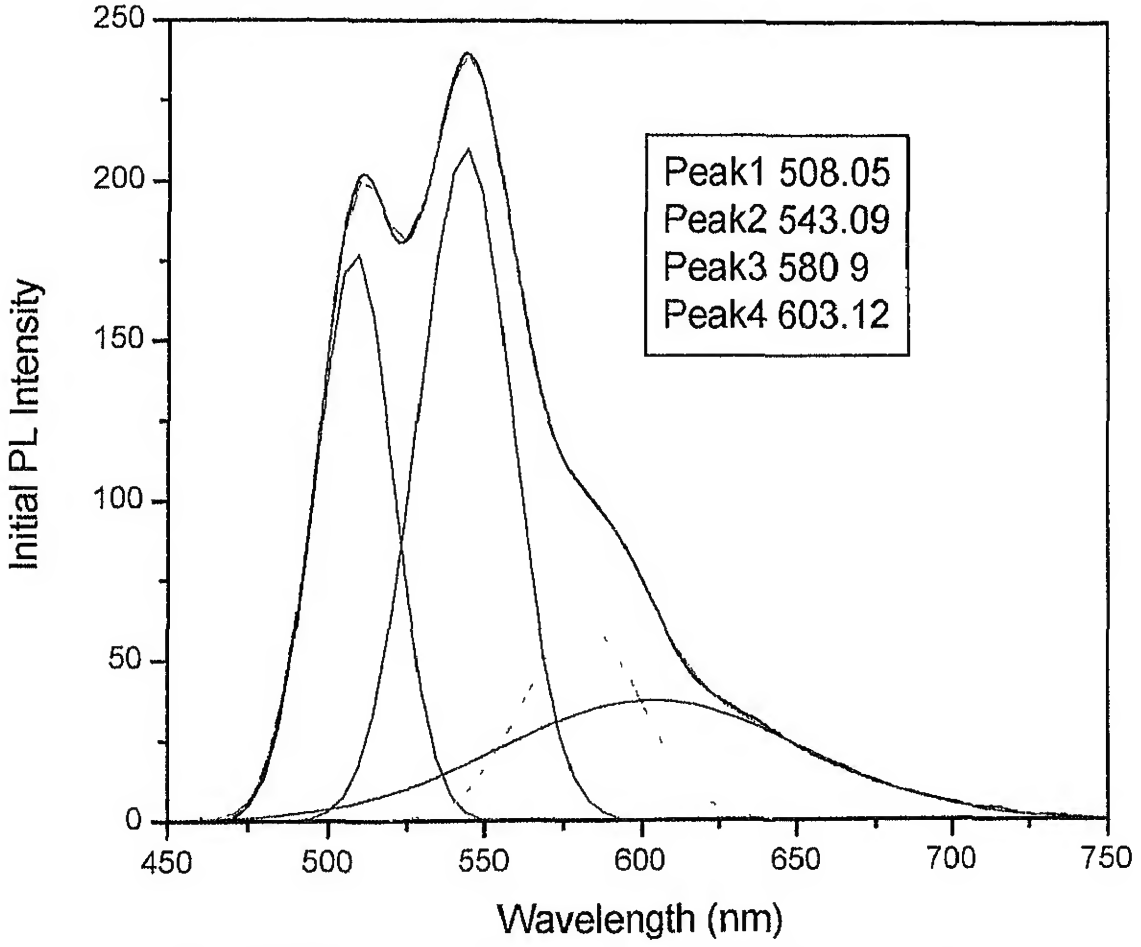

Fig 6.2.2.5: Peak fitting of the PPV spectrum by four gaussians

The PL spectrum at different time intervals on fitting with four gaussians gives the result as given in the appendix The peaks of the gaussians are plotted with time below.

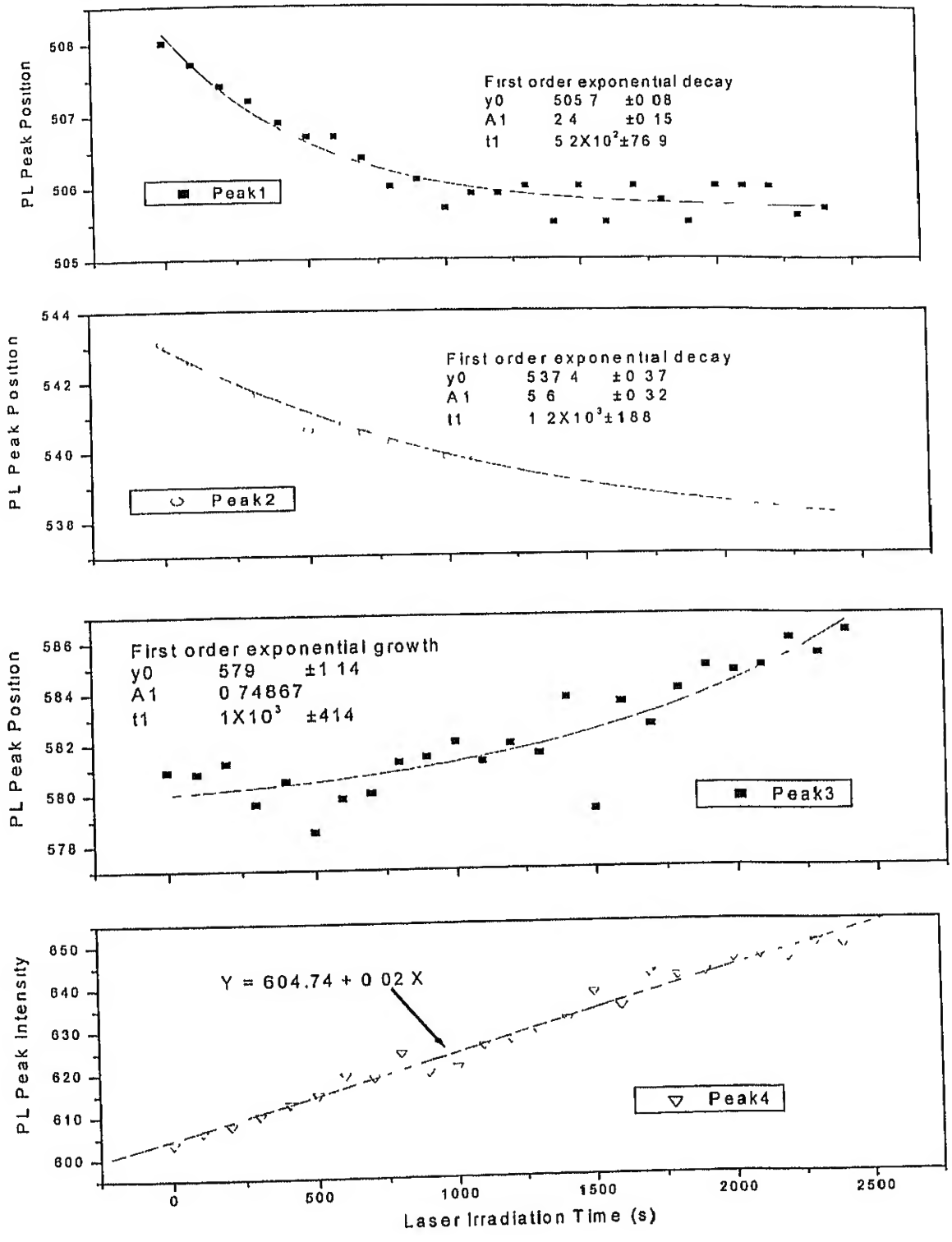

Fig 6.2.2.6: Peaks positions for PPV with laser irradiation time

The combined plot of all the peaks is shown below in Figure 6 2 2 7 Slight blue shift is observed in the first peak with more significant blue shift in the second peak Peak 3 has a minute red shift while Peak 4 has a significant red shift by about 44 nm

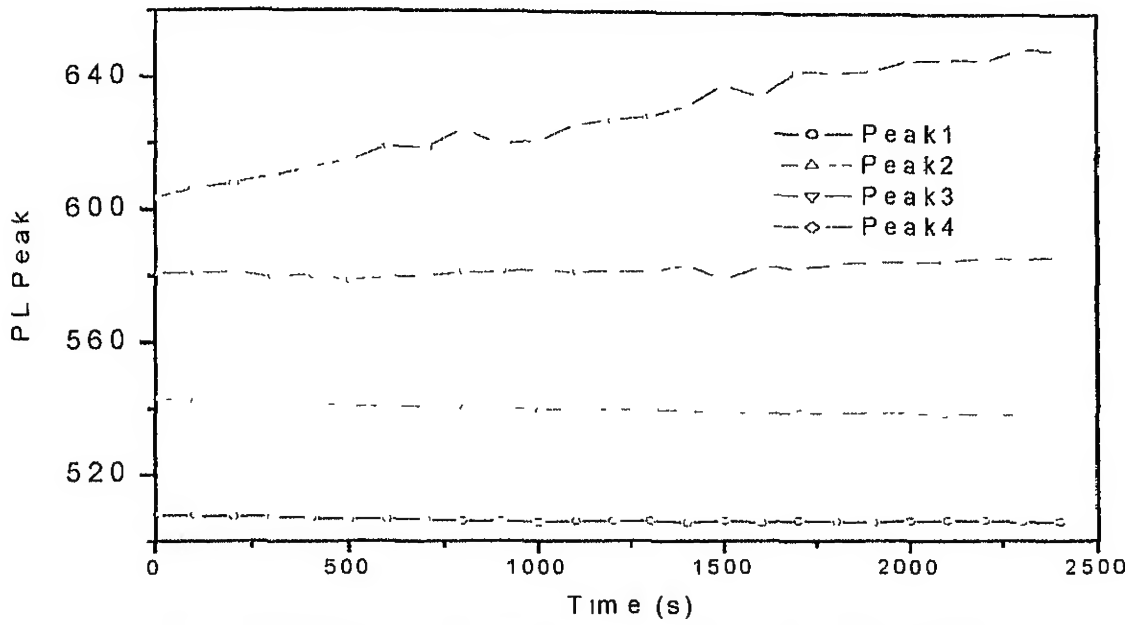

Fig 6.2.2.7: Variation of peak positions with laser irradiation time

The intensity decay plot of each peak separately obtained from the analysis is shown in Figure 6 2 2 8 The peaks decay almost with same rate, with the Peak 1 decaying fastest rate

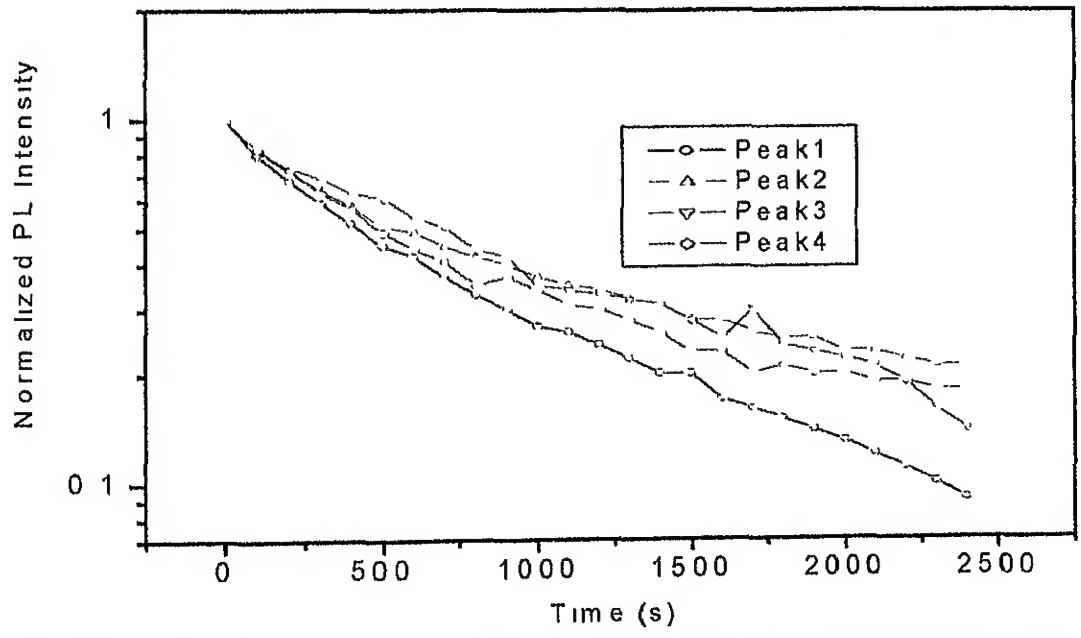

Fig 6.2.2.8: Semi logarithmic Peak PL intensity variation with laser irradiation time

The change of FWHM of the peaks with laser irradiation time is shown in Figure 6.2.2.9

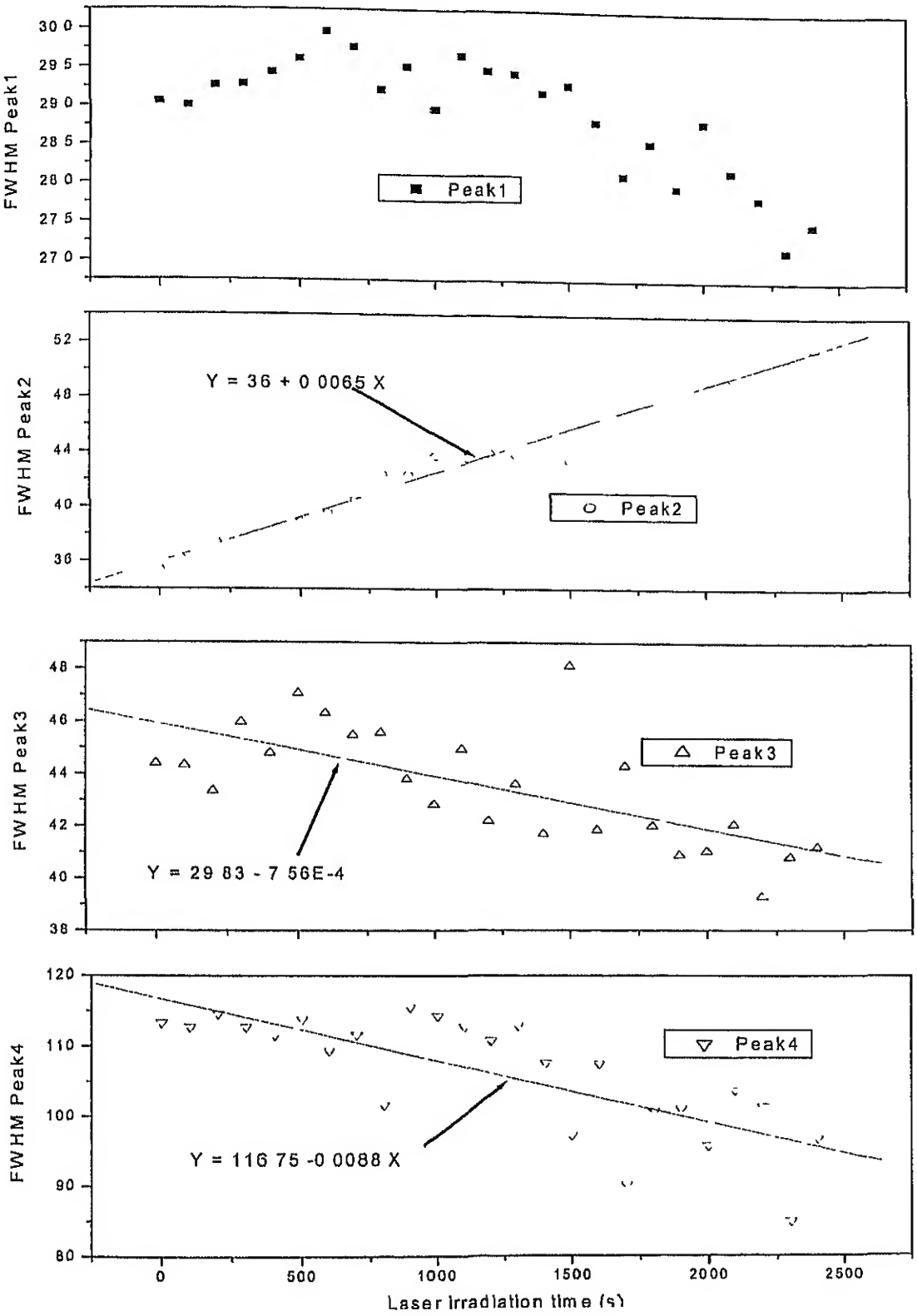

Fig 6.2.2.9: FWHM variation of peaks in PPV with laser irradiation time

The combined plots of FWHM of all the peaks are shown in the Figure 6 2 2 10

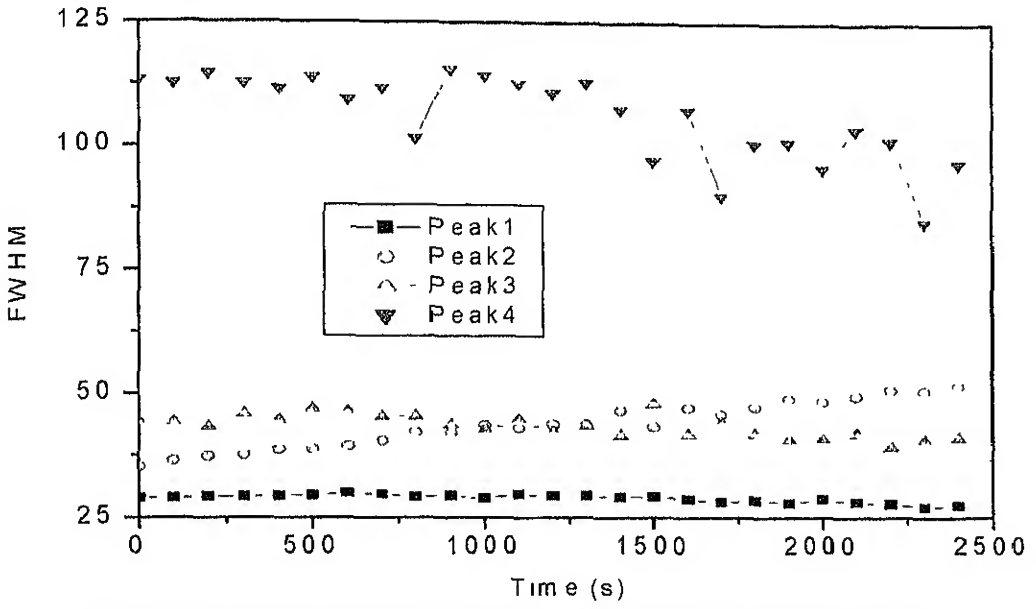

Fig 6.2.2.10: Variation of FWHM of peaks with laser irradiation time

As shown in Figure 6 2 2 10, the FWHM of all peaks except Peak 2 (corresponding to 543 nm) decreases FWHM of Peak 2 at 543 nm increases from 35 to 51 FWHM of Peak1 and Peak3 remain almost constant Clearly peak 2 is sensitive to disorder being produced in the environment of chromophores The change of area under the curve for all the peaks with time is shown in Figure 6 2 2 11, which gives better indication of degradation compared to the intensity plots for the peaks with large change in FWHM

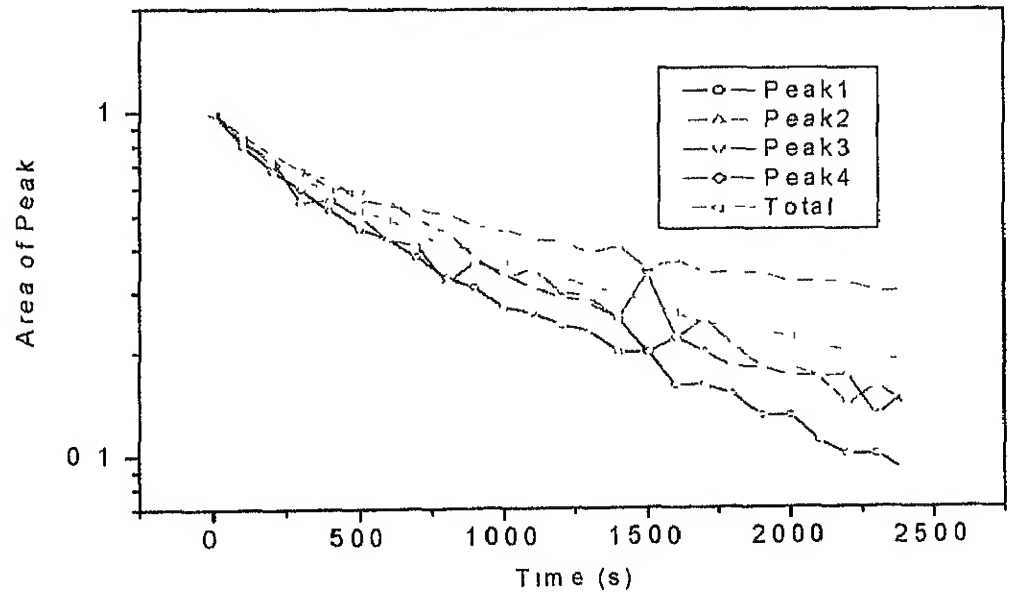

Fig 6.2.2.11: Variation of area under the peaks with laser irradiation time

6.2.3 Degradation of PPV with laser irradiation under vacuum & air

Clearly it would be instructive to compare laser induced degradation rate observed in air with that in vacuum The sample is prepared by vacuum drying to fully dry out the solvent before conversion of precursor to PPV The vacuum used for these experiments is of the order of 0 001 torr as obtained using rotary pump for small volume cryostat sample chamber The intensity of dominant bandgap related peak is monitored with exposure time of the laser under vacuum Surprisingly instead of *degradation of PL intensity, it actually increases* with time roughly displaying a logarithmic increase as shown in curve 1 (Vac505) in Figure 6 2 3 1

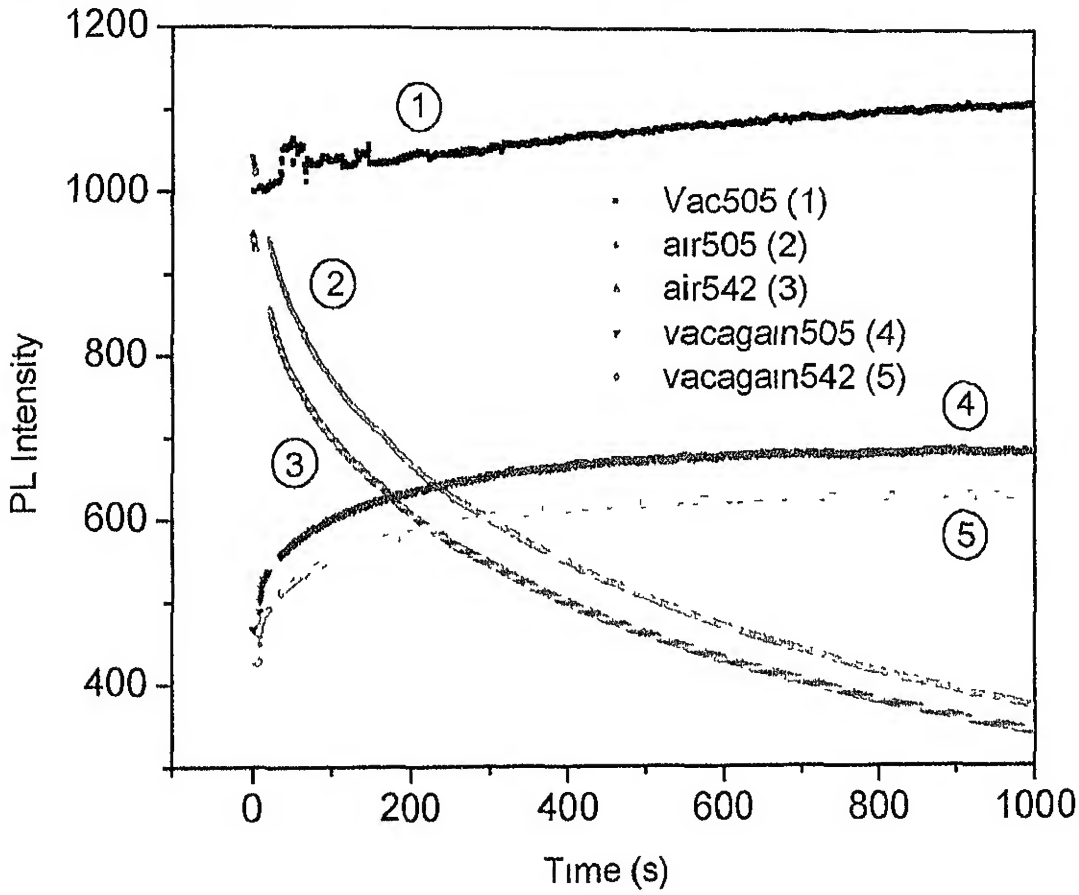

Fig 6.2.3.1: Variation of PL intensity for vacuum dried PPV with laser irradiation time

Then air is then subsequently admitted into the chamber with all other experimental conditions along with laser and sample alignment remaining the same The intensity of both the dominant peaks, peak 1 at 505nm and peak 2 at 542nm are simultaneously monitored with increase in exposure time of the excitation laser in air

ambient. PL intensity degradation similar to those reported in the last section is observed as shown in curve 2 & 3 of the Figure. This clearly indicates necessity of the presence of oxygen and moisture for the observed photoxidation At the end of the two scans in air ambient, the sample chamber is again pumped out creating vacuum while still monitoring PL intensity of the two peaks.

Again one observes PL enhancement in vacuum as shown in curves 4 & 5 During the first few seconds of pumping, we observe a clear correlation between increase of PL intensity with increase in vacuum Note that it takes only few seconds to achieve the steady state vacuum Also note that the recovery in PL intensity is only partial. This indicates that PL enhancement in vacuum is a separate process from cumulative degradation caused in air ambient.

The PL intensity decrease for the two peaks in air ambient exposure is analysed and the fittings to second order experimental decay are shown in Figure 6 2 3 2

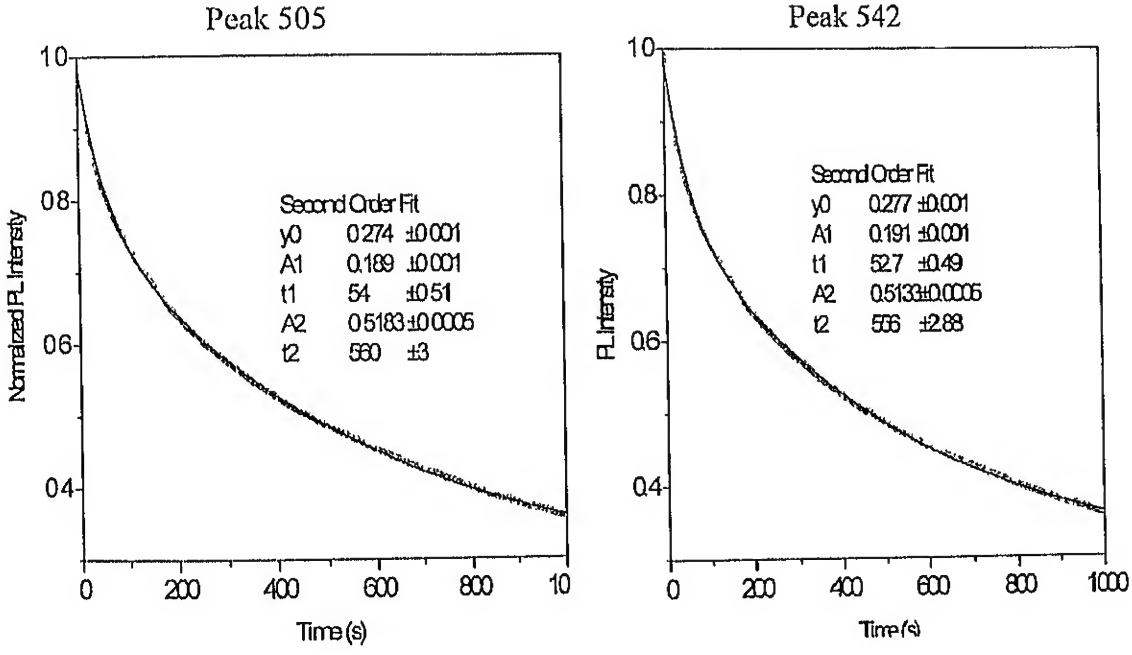

Fig 6.2.3.2: Second order exponential fit of PPV decay plot for two peaks

For the sequence of experiments described above, both normal and normalized PL spectra at different times are shown in Figure 6.2.3.3. The normalized PL plots clearly show that spectral features. The plots of PL for sample under vacuum and then in air followed by the plots under vacuum again is shown in Figure 6.2.3.3.

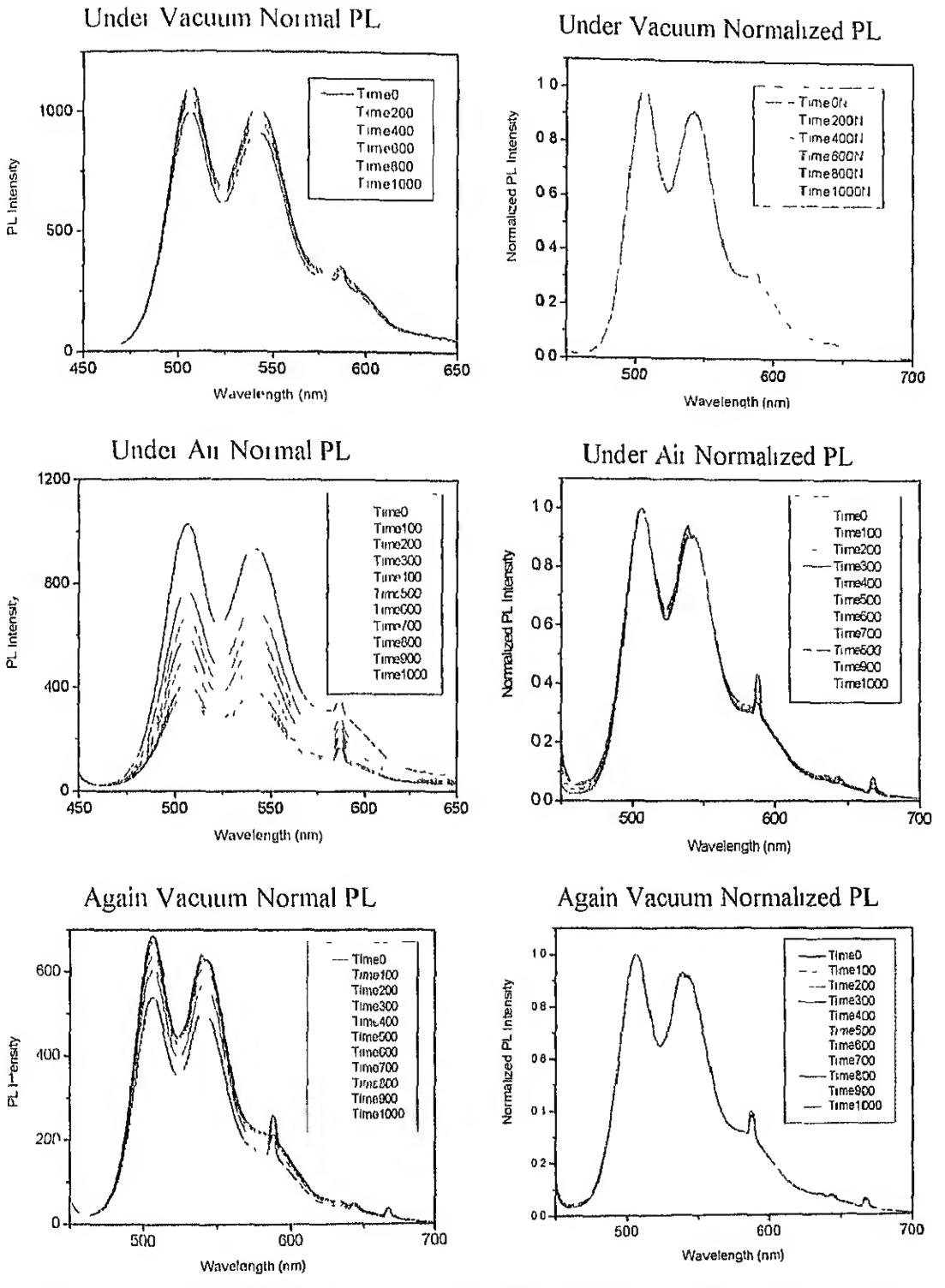

Fig 6.2.3.3: PL variation for vacuum dried PPV sample with laser irradiation time

These results show that laser irradiation under vacuum creates a degradation resistance in the sample It decreases the rate and also hinders the shifting of PL peak

position showing that the conjugation length is unchanged Peak position, FWHM and hence lineshape are not affected due to this degradation The sharp feature at around 580nm is unwanted experimental artefact originality from some background light originating from excitation source during those experiments and need to be ignored

6.2.4 Degradation of CNPPV spin coated and baked in air

In this section, we describe the results of similar experiments on CN-PPV There is one important difference however, CN-PPV being soluble in common organic solvents, the polymerisation conversion step is not required after coating Baking is drying only and involves driving out of solvent Hence baking time-temperature combination is used as another process parameter in addition to baking ambient and measurement ambient Baking is carried out for different times either in high purity nitrogen or in air The studies on an ambient processing were carried out to validate laser induced degradation as a test procedure for evaluating quality of material Most CN-PPV films are obtained from 6mg/cc CNPPV sample spin-coated at 1000 rpm

6.2.4.1 Effect of air baking on PL spectra

With baking of CNPPV, the peak red shifts by about 6 nm and the peak gets narrower than the unbaked sample The Figure 6 2 4 1 1 below shows the normalized PL spectrum The PL seems to stabilize just after 15 min of baking and showing no further change in the spectrum

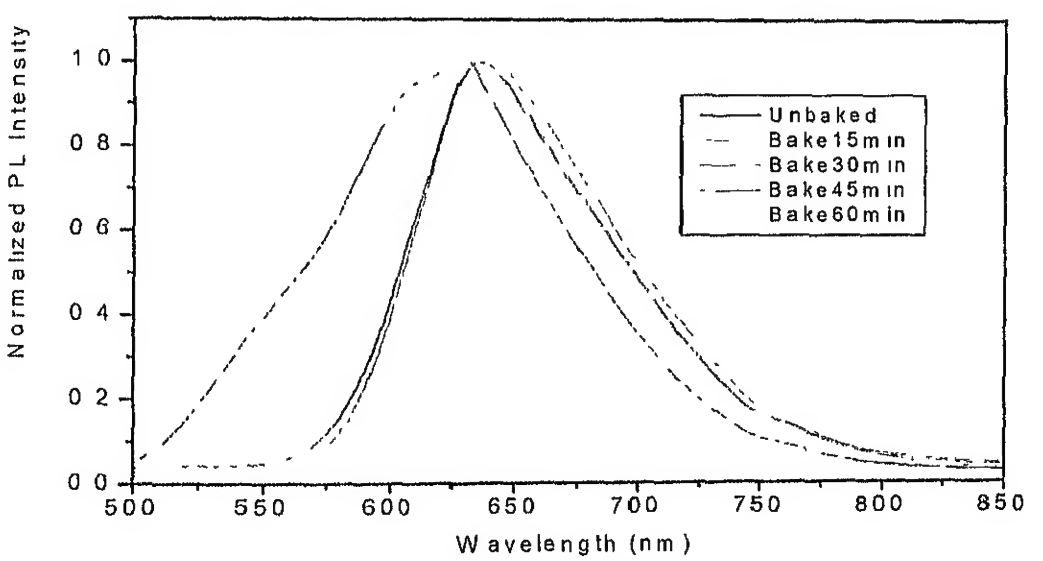

Fig 6.2.4.1.1: Normalized PL Intensity of CNPPV with different baking time

6.2.4.2 Degradability due to Processing in Air Ambient

Figure 6 2 4 2 1 shows the change in PL intensity with time of exposure to excitation laser Baking significantly improves the degradation resistance of CNPPV under laser However the rate of degradation seems higher but exposure times lower than 30 min indicating an optimum time for baking The time dependence of PL intensity for different baking times is fitted to first order exponential decay as shown in Figure 6 2 4 2 2 The time constants obtained from this analysis is plotted as a function of baking time The initial increase in time constant of decay suggests that during first 30 minutes of baking, trapped solvents are being driven out leading to increased laser induced degradation resistance

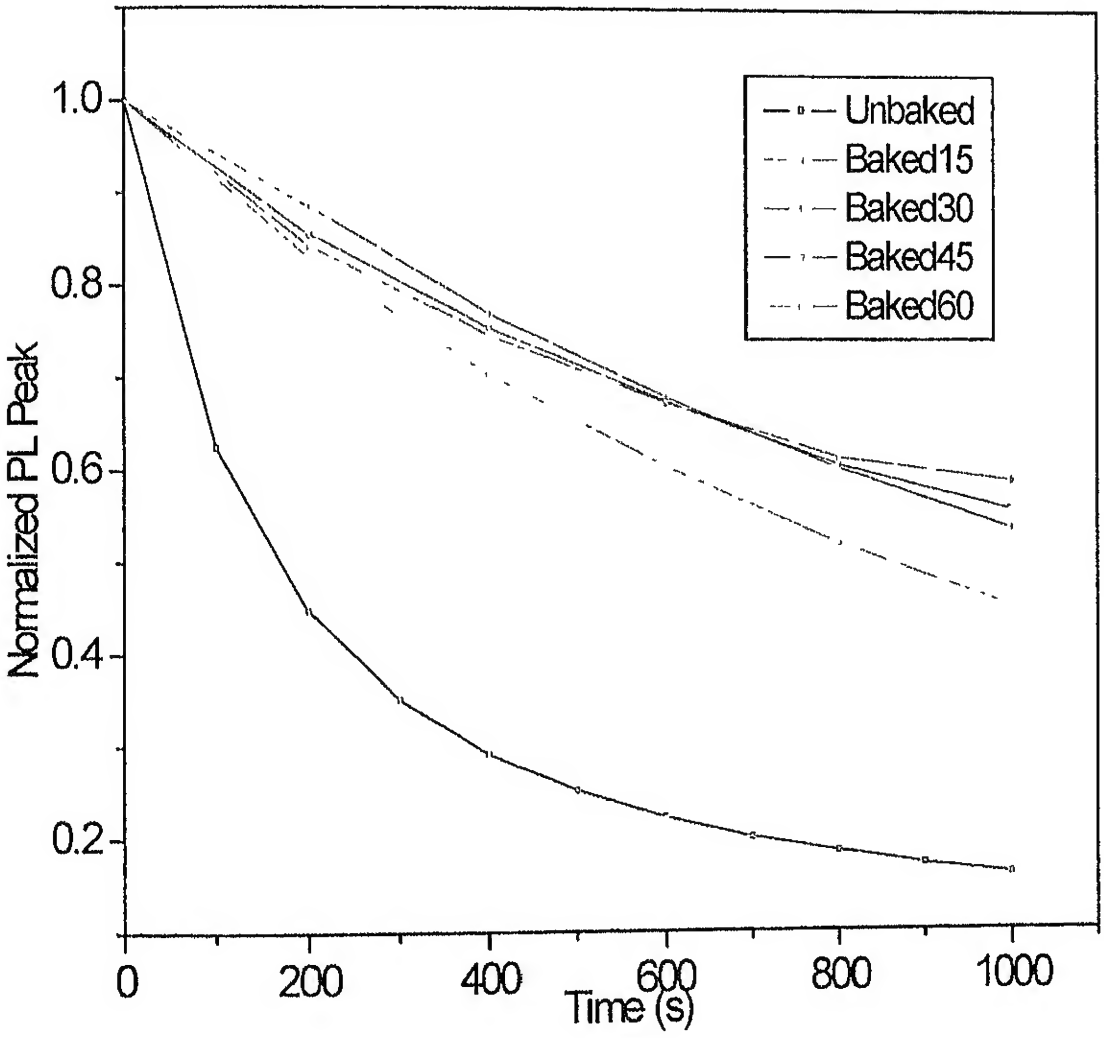

Fig 6.2.4.2.1: PL decay for CNPPV on glass with different baking times under laser

The exponential decay fitting of the baked samples are shown below

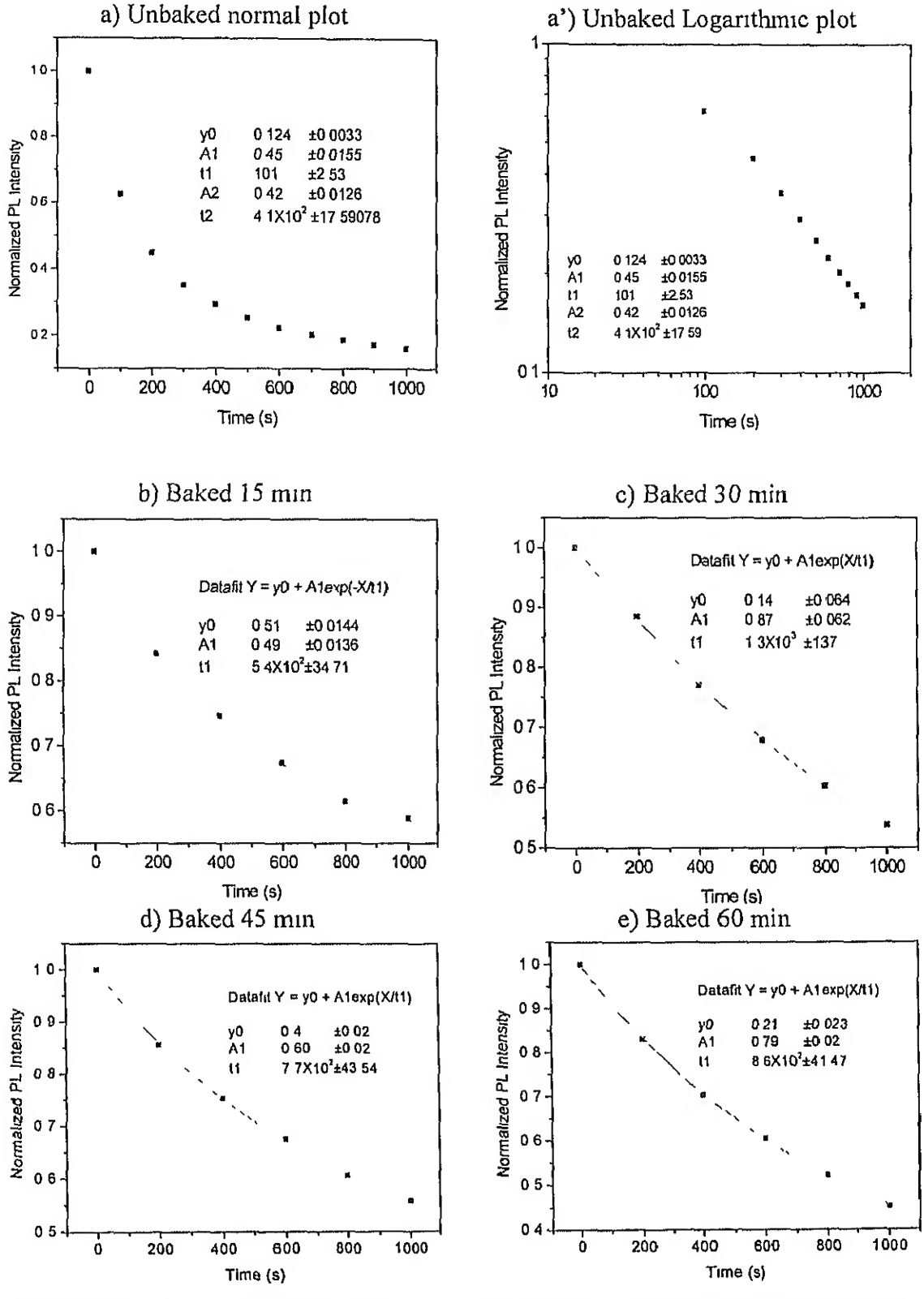

Fig 6.2.4.2.2: Exponential fit of the decay of the different time baked CNPPV samples

The driving out of solvents and degradation due to oxygen in the ambient are competing process giving rise to an optimum baking time in air For long duration baking transport of oxygen into the film and the subsequent oxidation seem to be dominant The time constant for the degradation can be summarized in Figure 6 2 4 2 3

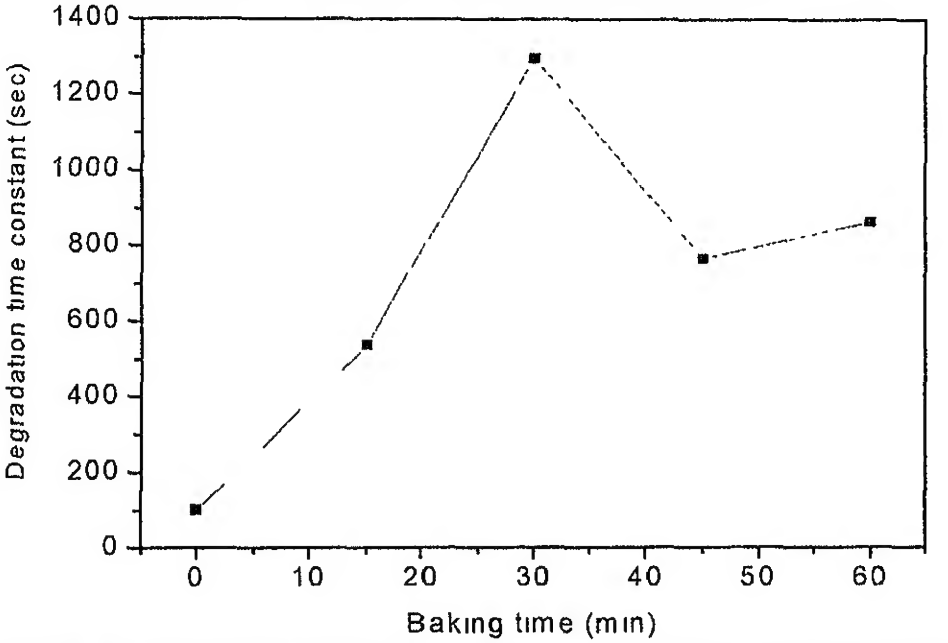

Fig 6.2.4.2.3: Variation of degradation time constant with baking time for CNPPV film

The FWHM of the normalized spectrum increases with the increase of laser irradiation time Also an effective blue shift is observed The normal and normalized PL spectra for different exposure time processed in air ambient is shown in Figure 6 2 4 2 4

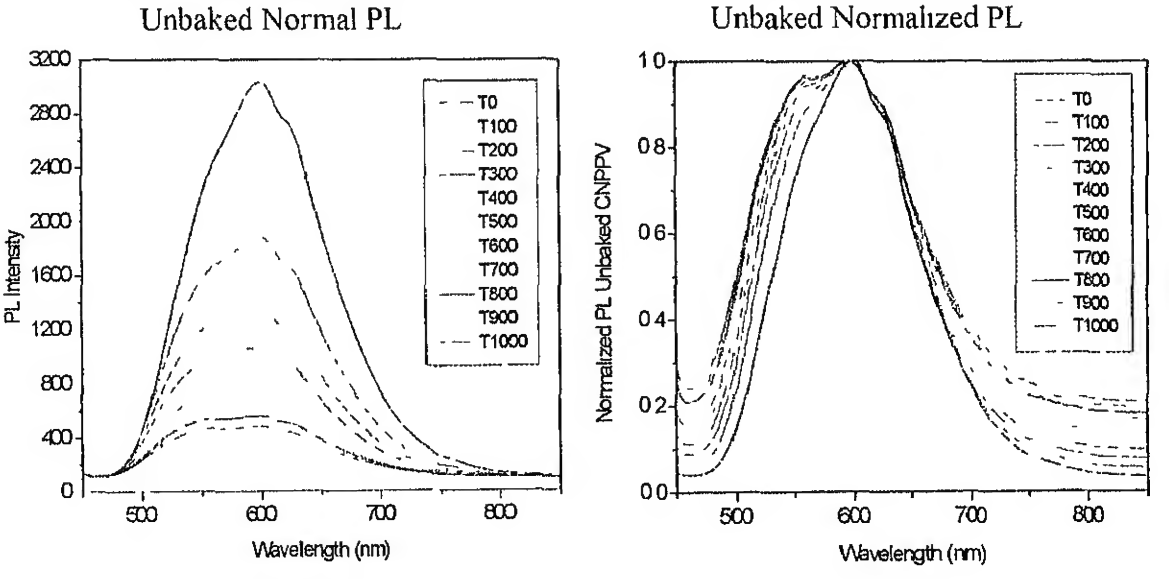

Baked 15 min Normal PL

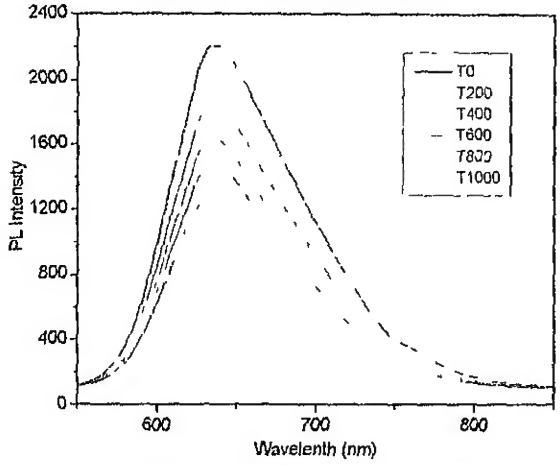

Baked 15 min Normalized PL

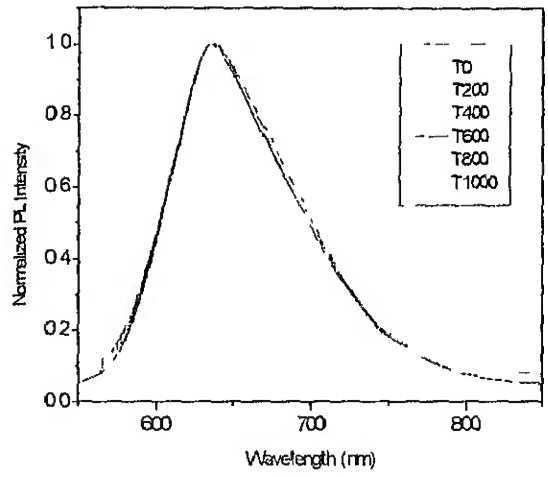

Baked 30 min Normal PL

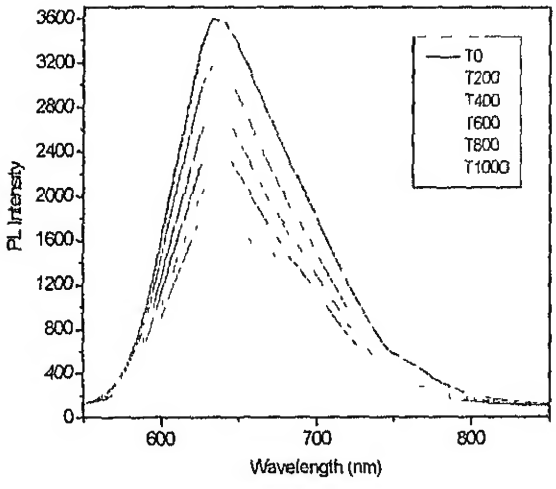

Baked 30 min Normalized PL

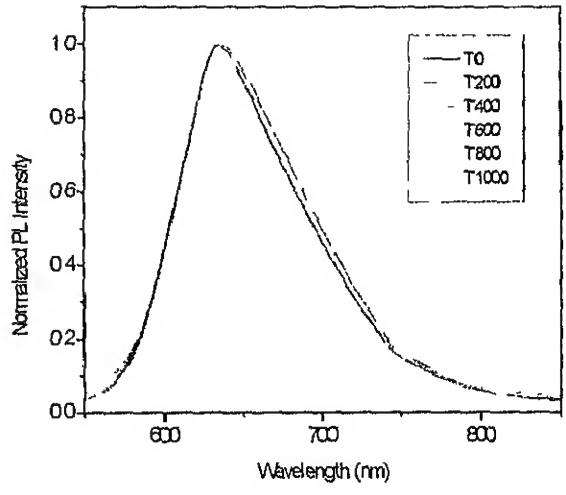

Baked 45 min Normal PL

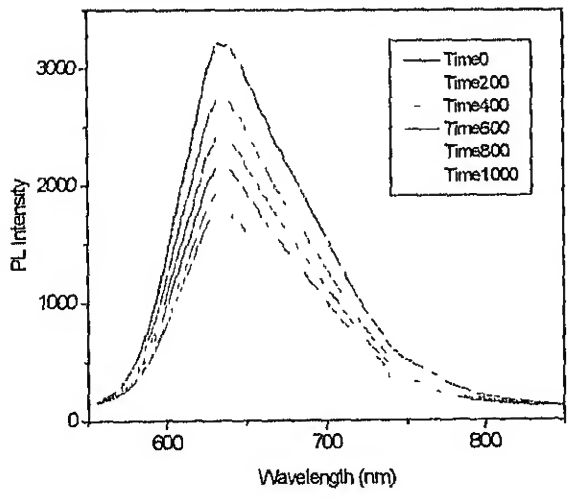

Baked 45 min Normalized PL

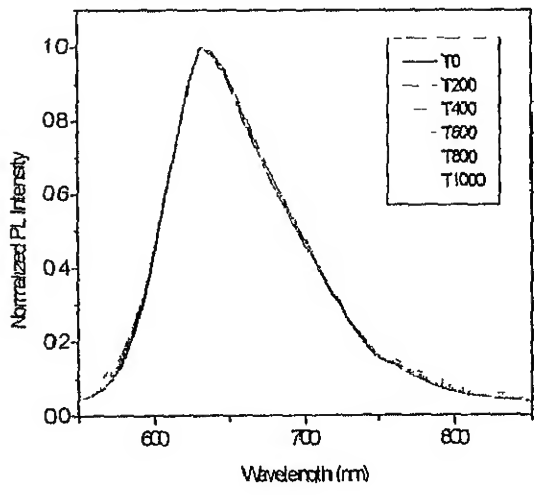

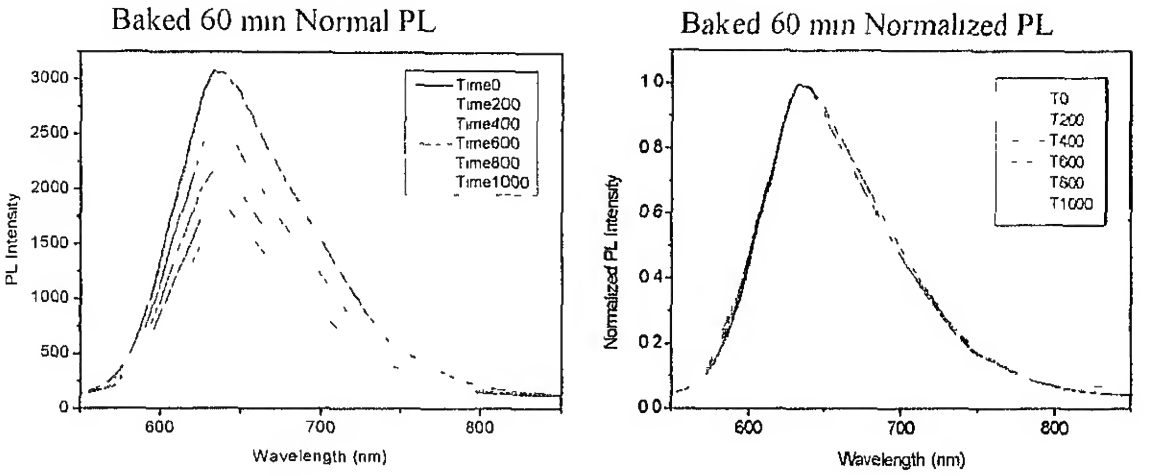

Fig 6.2.4.2.4: PL variation of air baked and spin-coated CNPPV sample under laser

Both blue shift and significant increase of width of the unbaked CNPPV spectra is observed on laser light irradiation indicating occurrence of photoxidation leading to disorder in chemical environment of chromophores

6.2.4.3 Effect of laser on unbaked films spin-coated in air

As shown in Figure 6 2 4 3 1, PL spectrum of the unbaked sample red shifts after laser irradiation for few seconds The intensity of constituting peaks also undergo changes This shows occurrence of baking of the unbaked sample during laser irradiation The plot is shown in Figure 6 4 2 3 1

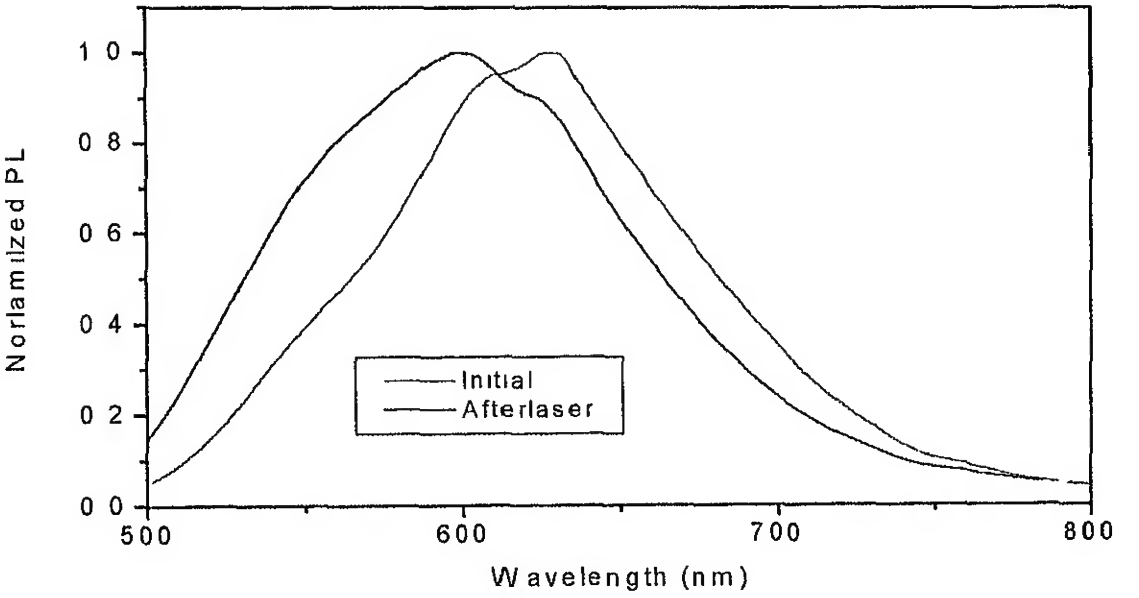

Fig 6.2.4.3.1: Effect of laser on PL spectrum of unbaked air spin-coated CNPPV sample

The observation of effective red shift may be due to the fact that the first peak (lower wavelength peak) is decaying at a faster rate compared to the second one with laser exposure time The origin of the lower wavelength peak has not been ascertained but can be traced to trapped solvents

6.2.4.4 Effect of air baking on transmittance of CNPPV

Figure 6 2 4 4 1 shows transmittance spectra for unbaked and baked samples With baking a red shift in the transmittance spectrum is observed, but the baked samples have almost same characteristics Transmittance minima shifts from 480nm to about 500nm from unbaked to baked sample This indicates changes in optical properties of the film as baking progresses The changes may include film properties and thickness However monitoring changes through PL seems a better option than transmittance

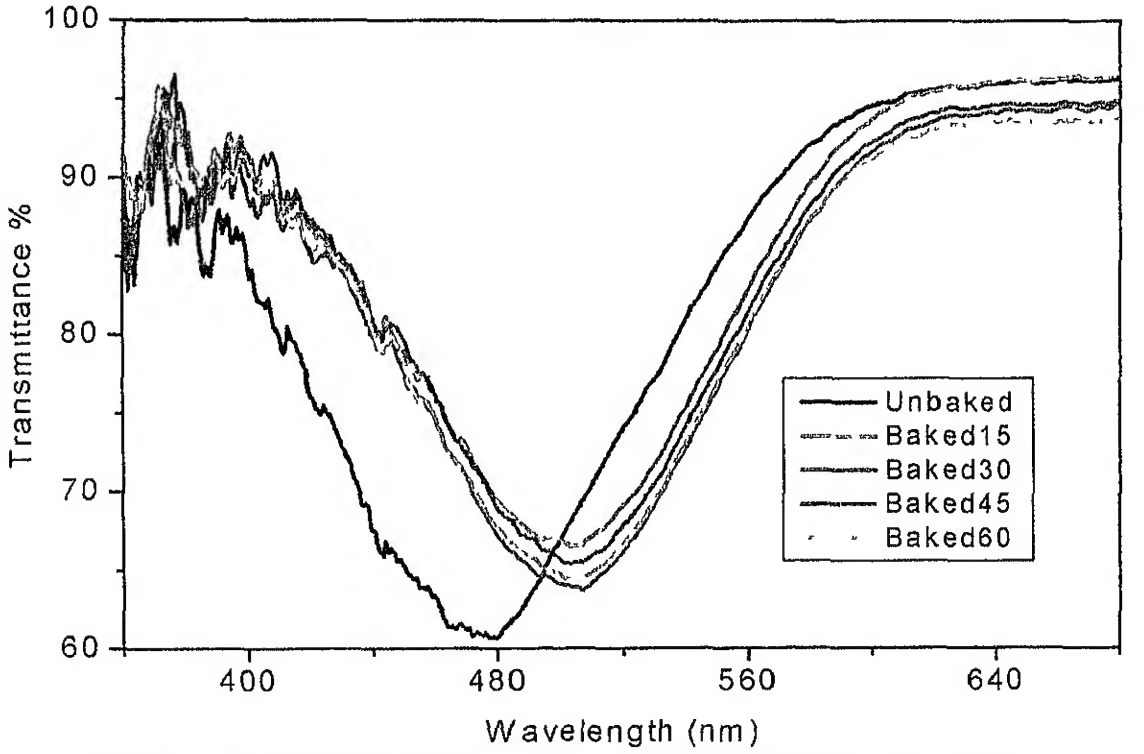

Fig 6.2.4.4.1: Variation of transmittance of air baked CNPPV with baking

6.2.5 Degradation of CNPPV spin coated and baked under nitrogen

In the last section, baking in air and its monitoring through laser induced degradation of PL intensity established its efficiency as a tool for studying process variation In this section we use ambient and baking conditions typically employed in device fabrication in our laboratory at present

6.2.5.1 Effect of nitrogen baking on photoluminescence

Figure 6 2 5 1 1 shows the normalized PL spectrum of a thin film prepared from a solution of CNPPV spin-coated at 1000 rpm under nitrogen environment The PL spectra stabilize after 15 min of baking and shows no further changes in the spectrum With baking of CNPPV in nitrogen ambient, the peak red shifts by about 15 nm and the peak gets narrower than the unbaked sample but degree of narrowing is less compared to air baked sample

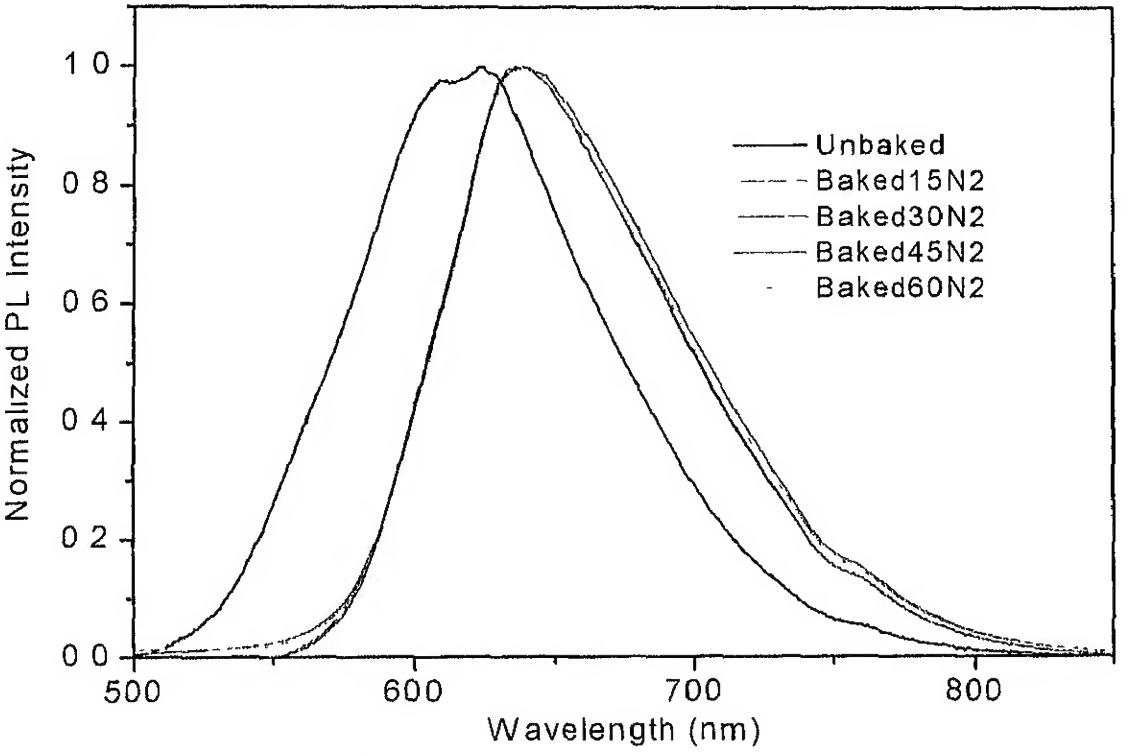

Fig 6.2.5.1.1: PL intensity variation with baking time

As in the case of air baking, the luminescence at the lower wavelength peak disappears with baking and must originate from solvent trapped in film during spin-coating This study clearly shows that 15 minutes of baking is enough as far as luminescence is concerned

6.2.5.2 Effect of duration of baking in nitrogen on degradation

Baking significantly improves the degradation resistance of CNPPV under laser irradiation However after prolonged baking for 45 min, enhancement in PL intensity is observed for the 45 min & 60 min baked samples as shown in Figure 6 2 5 2 1

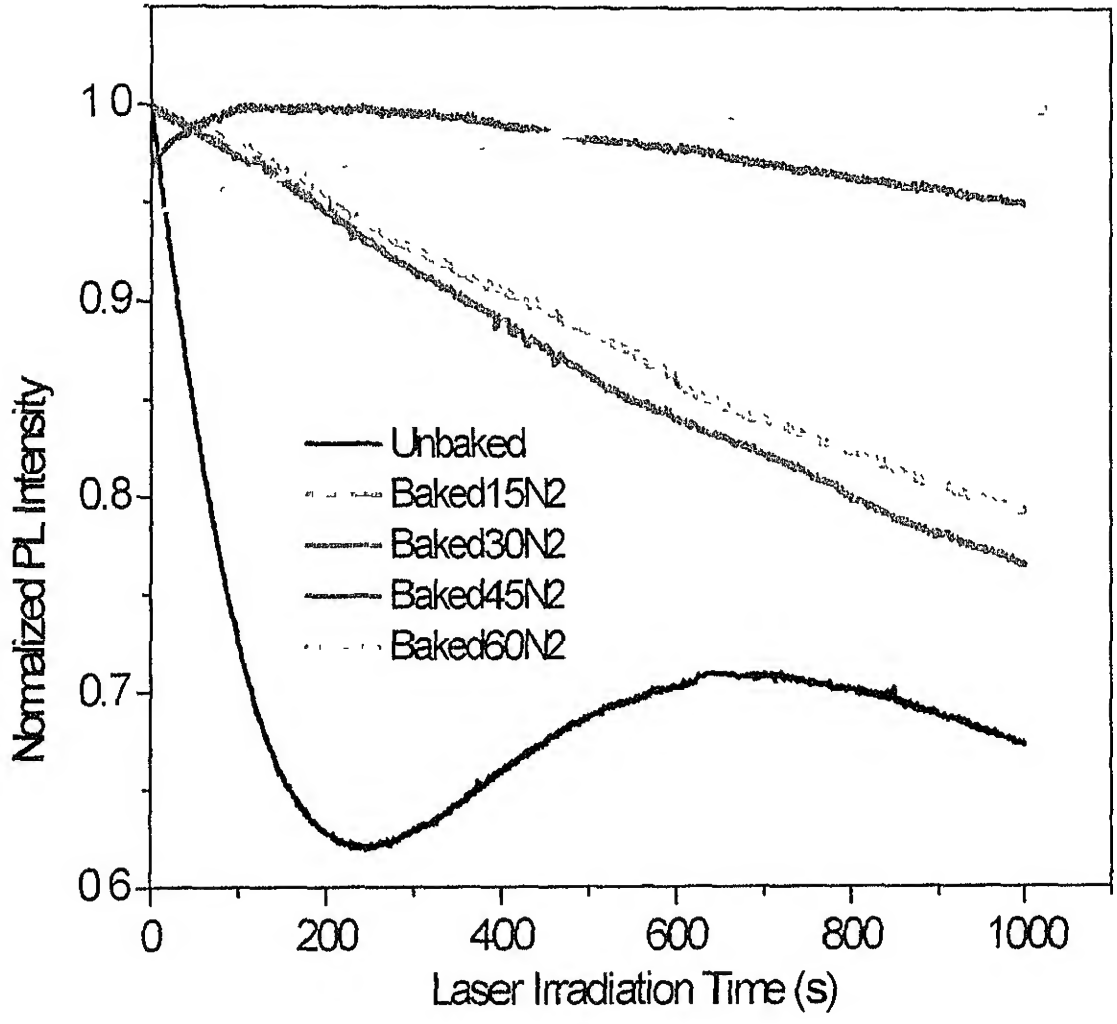

Fig 6.2.5.2.1: Normalized PL intensity degradation under laser with baking time

The unbaked sample shows severe laser induced degradation but with slower rate as compared to air baked sample Surprisingly however it shows increase after about 200 sec of irradiation Degradation resistance clearly increase with baking time For the case of curve corresponding to 45 min baking in Figure 6 2 5 2 1, note that there is initial enhancement and then gradual decrease at much longer exposure times This indicates that the process responsible for enhancement is an independent process competing with that responsible for decrease Once degradation resistance saturates with baking time, enhancement of PL is observed Hence the increase observed at long time for unbaked samples is due to degradation resistance achieved due to in-situ baking occurring with laser irradiation during measurement

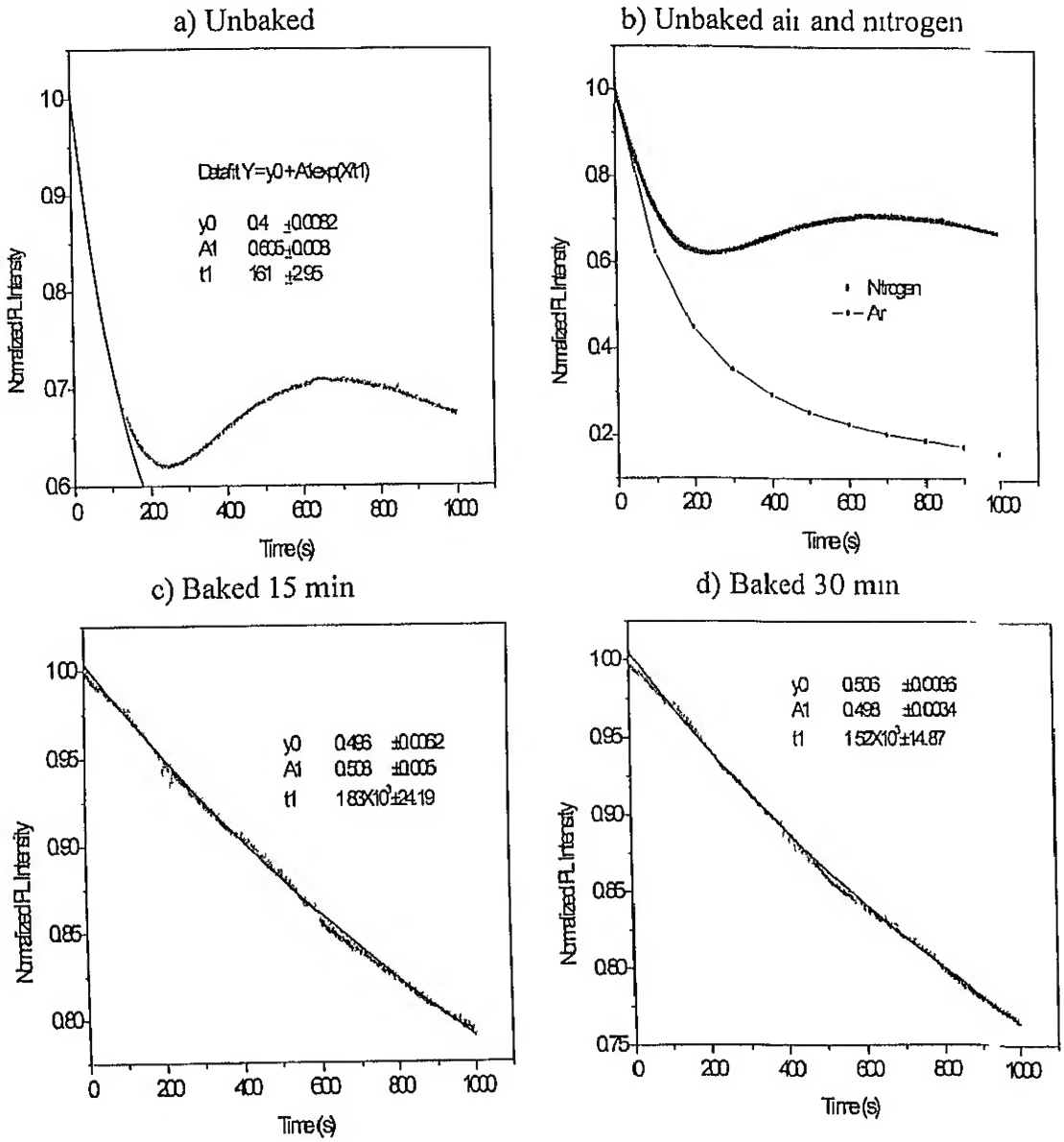

Fig 6.2.5.2.2: Degradation of unbaked and 15 and 30 min nitrogen baked samples

Figure 6.2.5.2.2 show fit to first order exponential decays for the case for 15 min and 30 min baking time. Degradation time constants are lower compared to air baked samples for each case. Changes in spectral features for baking in nitrogen for different duration is tracked by showing normal and normalized spectra in Figure 6.2.5.2.3. Each figure consists of spectra for progressive laser exposure times The difference in degradation resistance in unbaked samples processed under air and nitrogen comes out by Figure 6.2.5.2.2 b).

Unbaked Normal PL

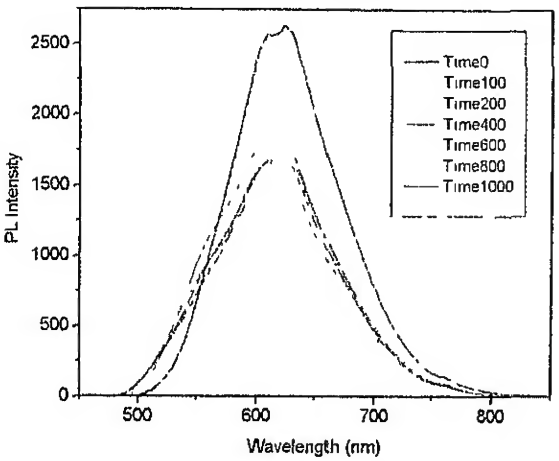

Unbaked Normalized PL

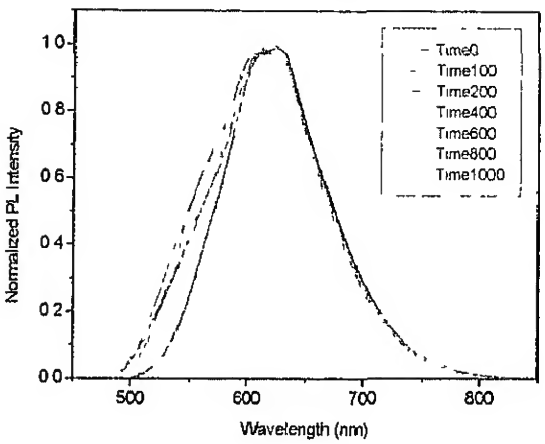

Baked 15 min Normal PL

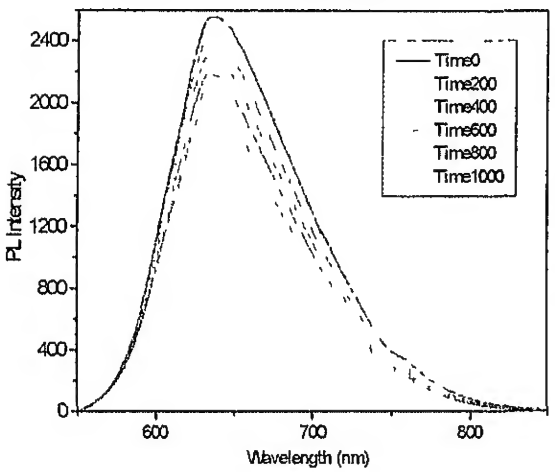

Baked 15 min Normalized PL

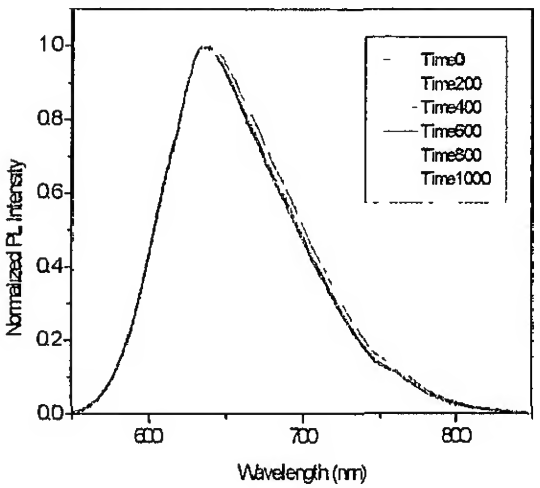

Baked 30 min Normal PL

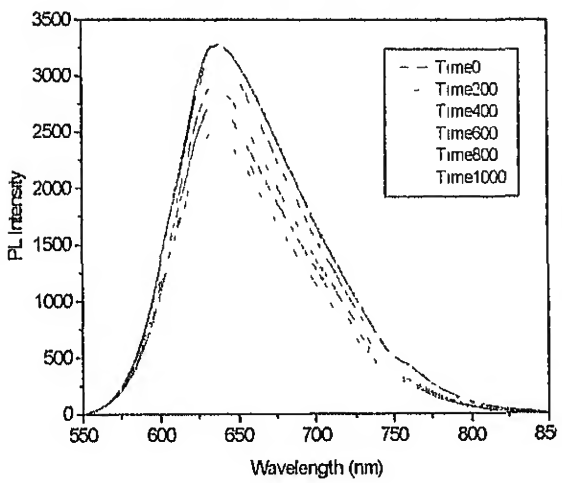

Baked 30 min Normalized PL

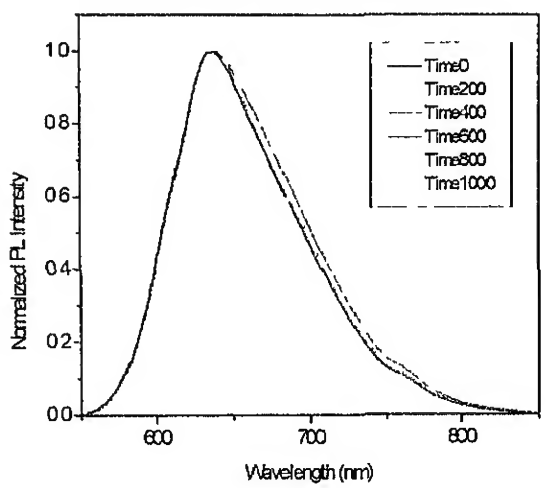

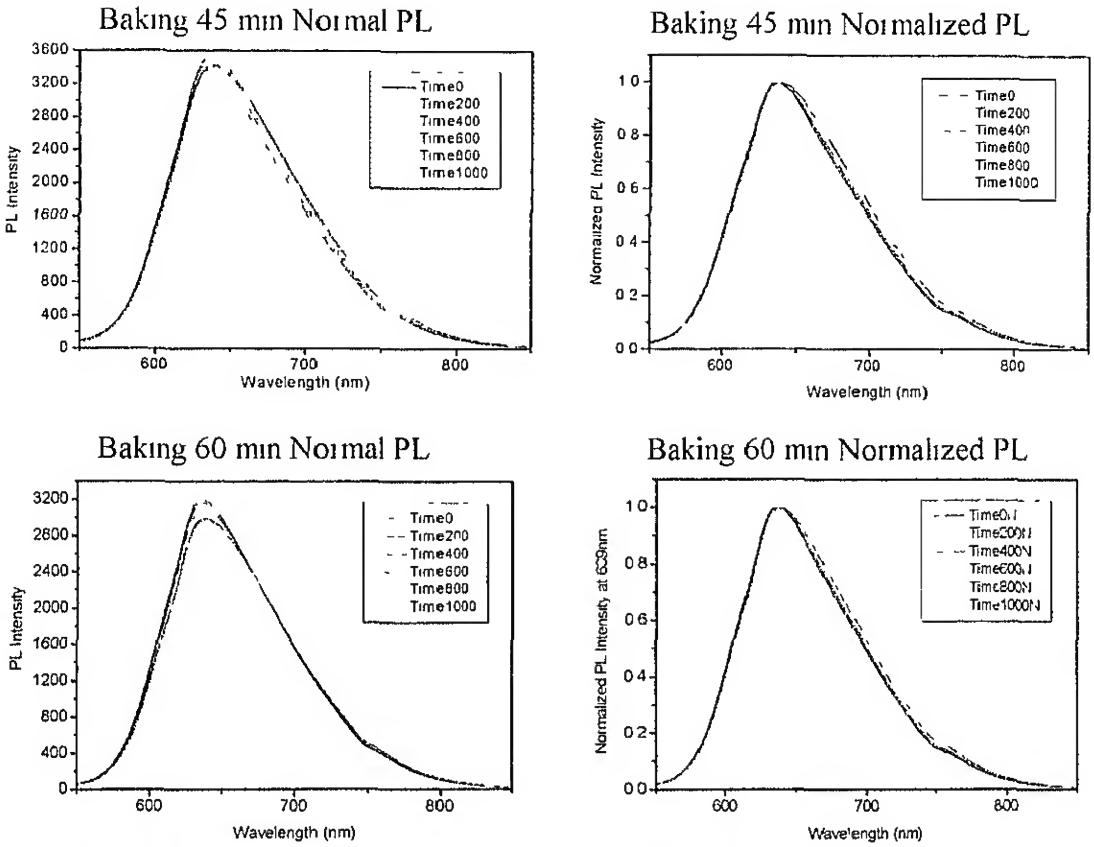

Fig 6.2.5.2.3: PL spectra of nitrogen baked CNPPV samples with irradiation time

Slight blue shift along with decrease of width of spectra is observed with increase in time irradiation of laser

6.2.5.3 Effect laser irradiation side on degradation

Effect on degradation with polymer and glass side irradiation is shown in Figure 6 2 5 3 1

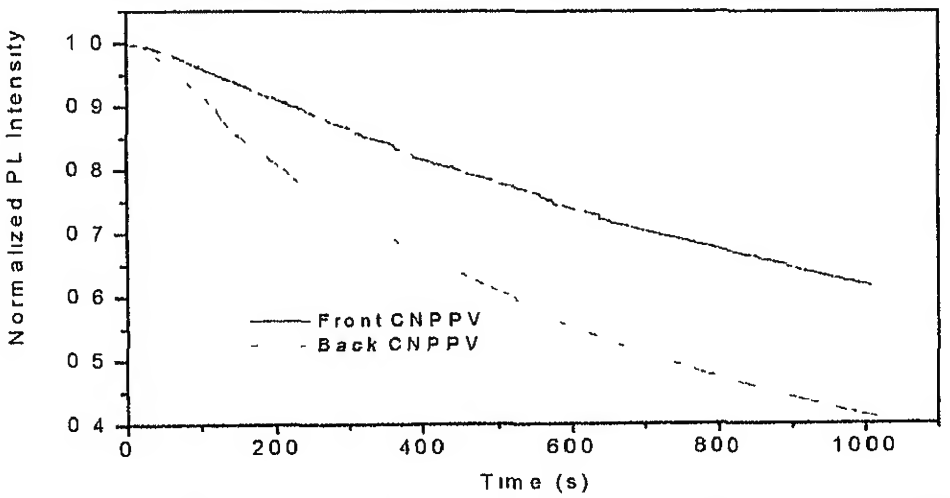

Fig 6.2.5.3.1: Effect of side of polymer and glass side irradiation on degradation

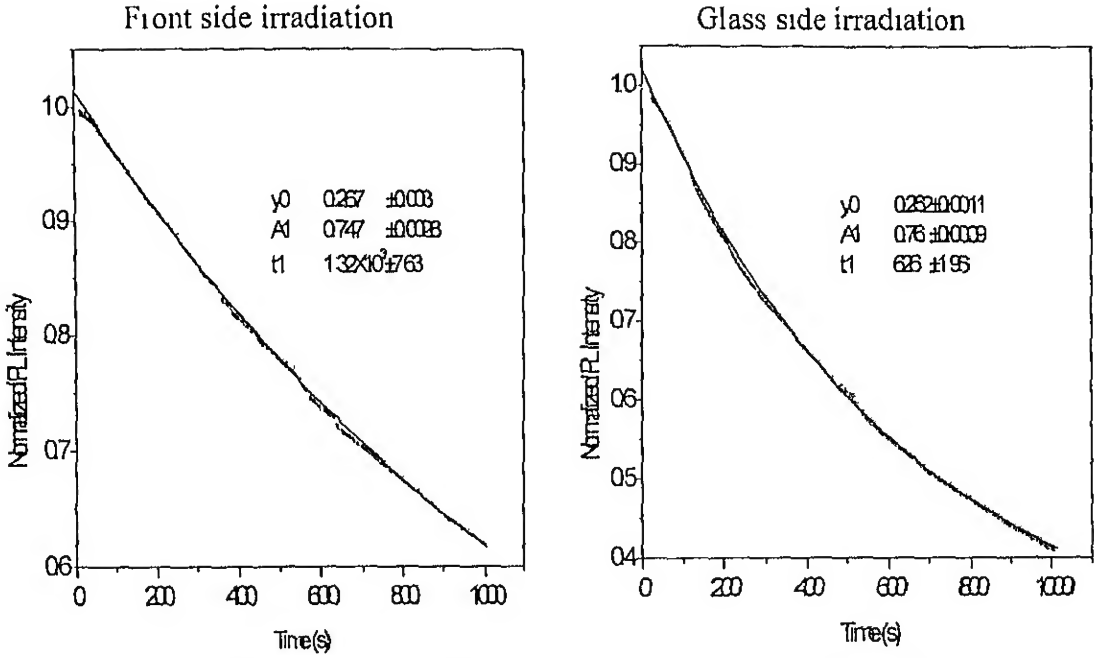

Fig 6.2.5.3.2: Exponential fitting for different side of irradiation decay curves

The degradation in the glass side irradiation is much faster with almost twice the decay rate. This can be simply understood by the fact that light is reflected more at the air/polymer interface (about 16% for normal incidence considering refractive index of polymer to be approximately 2 3), while it is only 4% at the glass polymer interface. The decay rate would be proportional to the light intensity. Therefore in employing comparative measurements of this type, it is important to keep the illumination side same among other experimental conditions. Since the intensity of light is very high and the samples transmit most of the light, sample volume or thickness or inhomogenity doing thickness should not play a role in this manifestation of this difference

6.2.5.4 Effect of vacuum on degradation

The effect of carrying out laser irradiation in vacuum on the degradation of CNPPV is shown in Figure 6.2.5.4.1. PL enhancement is observed for laser irradiation under vacuum and then subsequently when the same measurement is carried out in air, the PL intensity decays. All the measurements were done at the same spot in the polymer sample. Spot was formed when laser was irradiated in air, but no such spot was formed by just laser irradiation under vacuum.

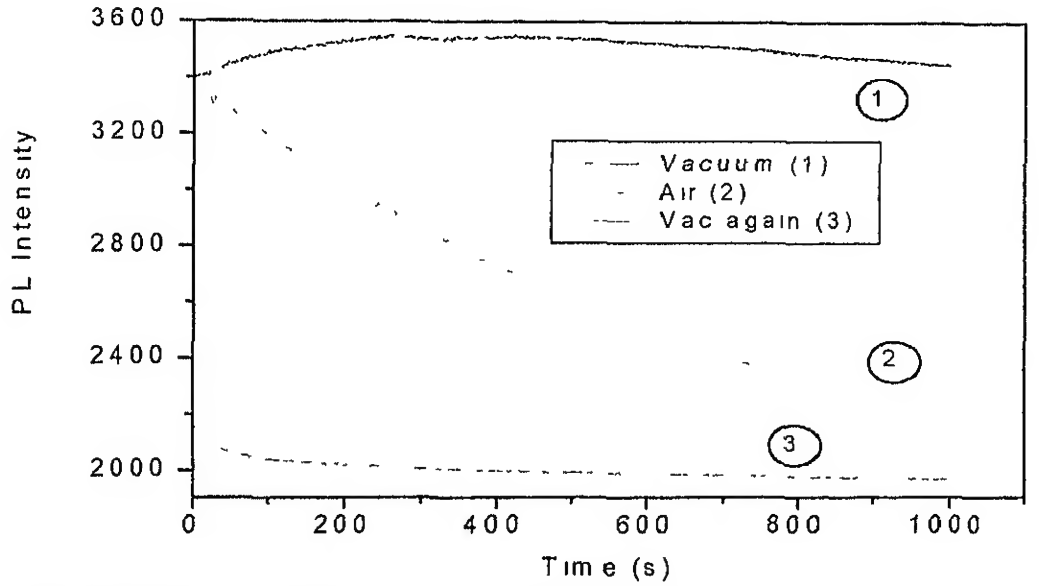

Fig 6.2.5.4.1: PL intensity variation under vacuum, air and again under vacuum

Curve 3 in the figure 6 2 5 4 1 shows a subsequent measurement after recreating vacuum in the sample chamber Again there is some degradation with laser irradiation This suggests that on measuring the degradation in air, some oxygen is getting entrapped within the film The trapped oxygen is responsible for an initial degradation under vacuum till it is then either consumed during irradiation or driven out of the film under vacuum The PL decay of CNPPV under an ambient showed second order exponential decay compared to first order for earlier CNPPV without vacuum experiment The fitted decay plots and the comparison with direct air degradation are shown in Figure 6 2 5 4 2

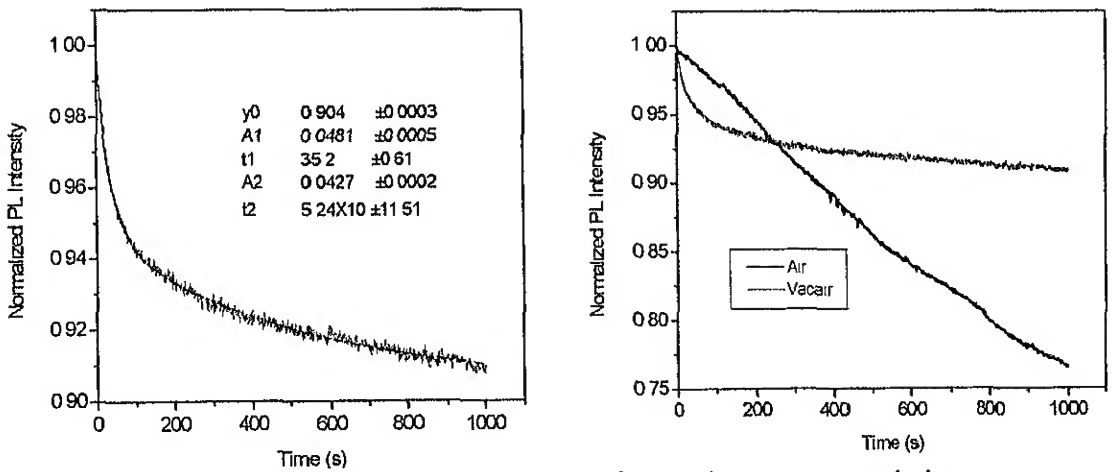

Fig 6.2.5.4.2: Fitting and comparison of degradation in air and nitrogen

The comparison shows that the initial rate of decay for air degradation after vacuum laser irradiation is initially faster, but in a larger time scale it stabilizes and the net

degradation is slower This signifies some degradation resistance initiated by laser under vacuum that still needs to be properly understood Also enhancement is shown under vacuum under laser irradiation, which shows some mechanism involved with laser radiation creating some change in the polymer itself This cannot be due to increase in temperature by laser irradiation since it is known from experiments conducted in our laboratory that an increase in temperature leads to decrease in PL intensity accompanied by changes in FWHM of spectra This also proves that laser and oxygen both are required for the degradation and any one of them is not good enough for the degradation to occur Since light cannot be avoided in an OLED device, so there is requirement of proper encapsulation so that oxygen can be avoided

The plots of PL spectra for sample under vacuum and then in air followed by the plots under vacuum again is shown in Figure 6 2 5 4 3

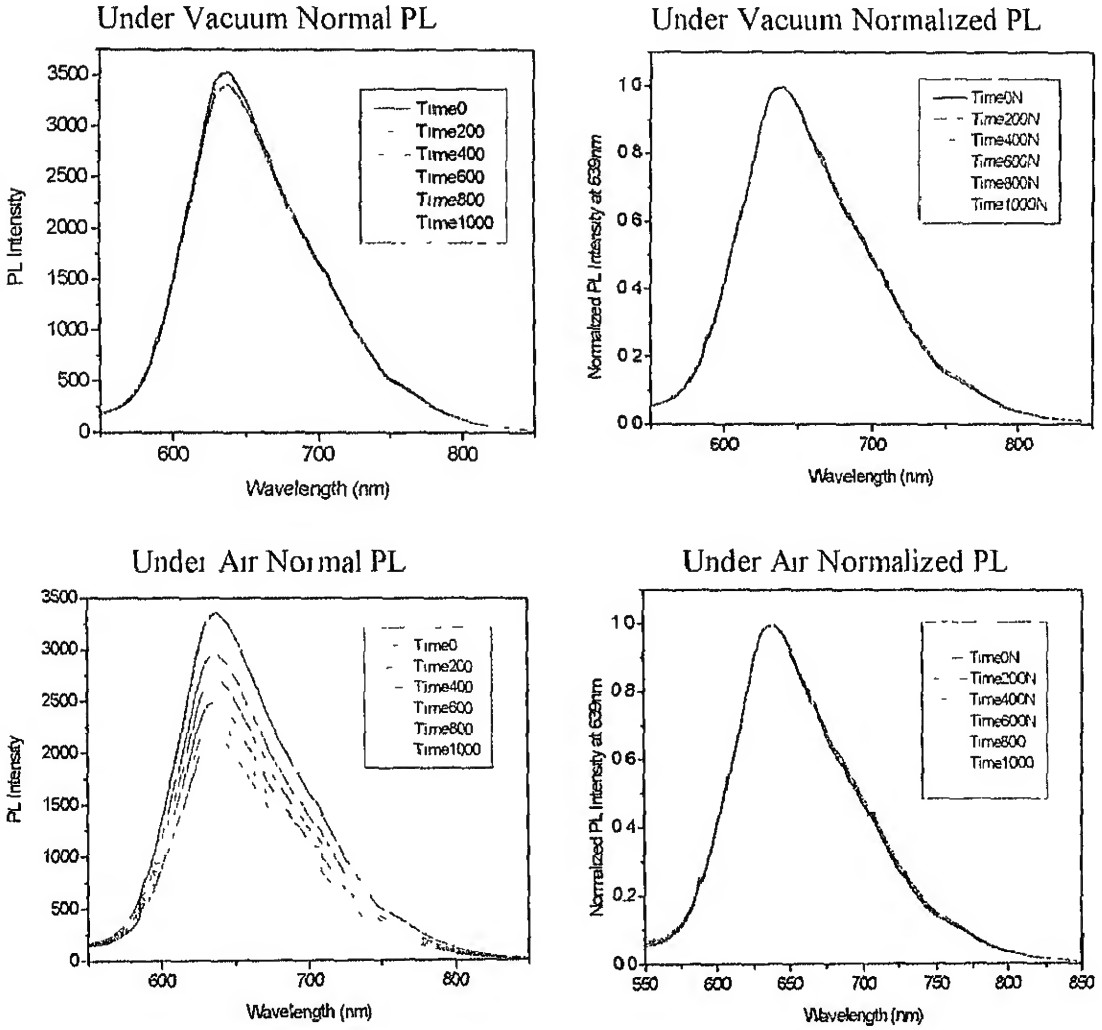

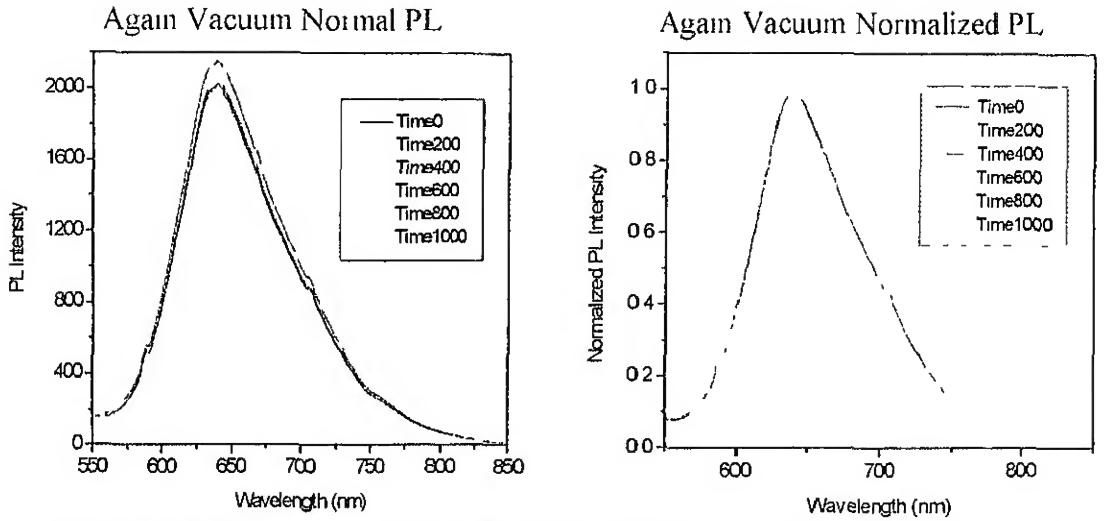

Fig 6.2.5.4.3: PL spectra of vacuum baked CNPPV samples with irradiation time

There is minute decrease in the width of the PL spectrum with laser, but after air, when again laser is irradiated, there is no change in the width of the PL spectrum

6.2.5.5 Effect of laser intensity on degradation

The degradation rate is studied at different intensities of 1, 0 5 and 0 3 respectively The intensities were varied with neutral density filters For lower fractional intensities there was inadequate PL to detect The effect of laser intensity on PL degradation rate is shown in Figure 6 2 5 5 1 The time constants corresponding to first order decay kinetics is obtained as a function of fraction of input light intensity as shown in the Table 6 2 5 5 1

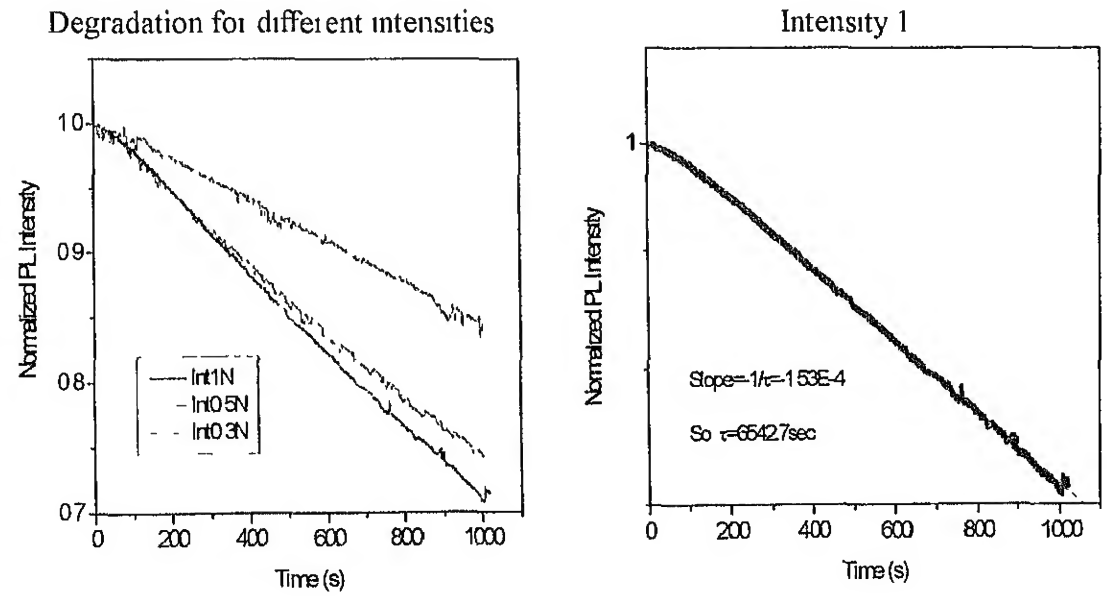

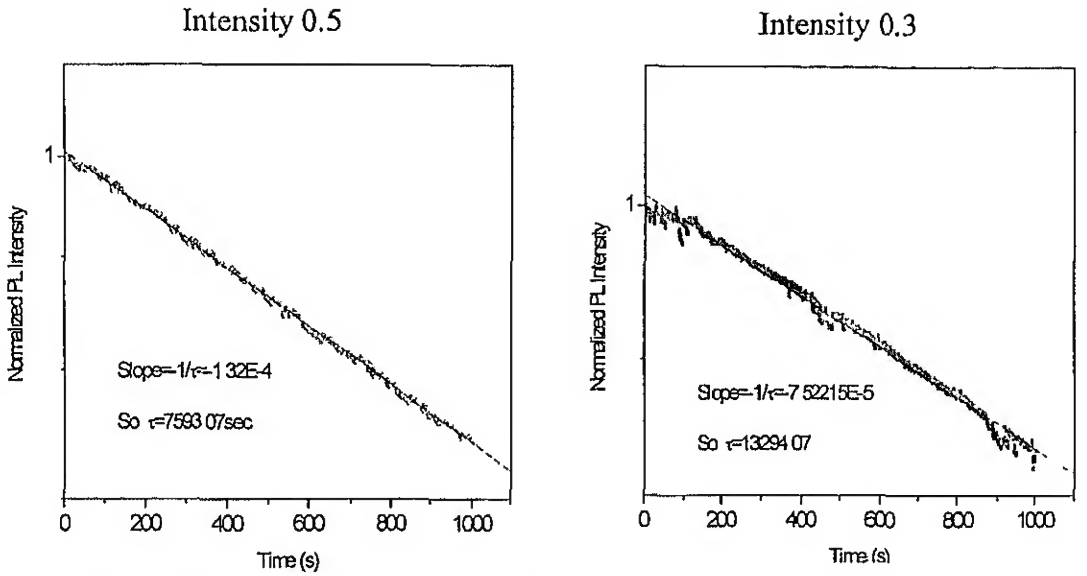

Fig 6.2.5.5.1: Degradation rate variation with intensity with their fittings

I/I_0	$1/\tau$
1	$1\ 53 \times 10^{-4}$
0.5	$1\ 32 \times 10^{-4}$
0.3	0.75×10^{-4}

Table 6.2.5.5.1: Variation of decay time constant with intensity

Though the decay rate is dependant on photo flux, it is not a linear function. It is not possible to guess the functional form of this dependence with this limited data However further studies of this dependence can give insight into this degradation mechanism

6.3 Electrical Characteristics

Ultimately the aim of any degradation studies of material is to establish relationship of material degradation to device lifetime. However in this work the focus has been on ability to characterize material oxidation. Nonetheless, experiments were carried out to study electrical characteristics of devices fabricated from materials studied in earlier sections

Apart from laser induced degradation of luminescence, a device is susceptible to degrade by many other routes. We give below an indicative list of instabilities found during this work to aid future systematic correlation and diagnostics during the process of material

development. A typical I-V characteristic of an ITO/PPV/Al device is shown in Figure 6.3 1 The turn-on voltage for this device is particularly low and slope of logI-logV show two slopes of 1 and 2.5 respectively. The slope 1 corresponds to ohmic regime, but we get the other slope to be 2.5 instead of 2 expected for space charge regime. A subsequent measurement of I-V changes the I-V characteristics indicating possible degradation of contacts or charge accumulation in the device These features are currently being studied more thoroughly by others in our laboratory.

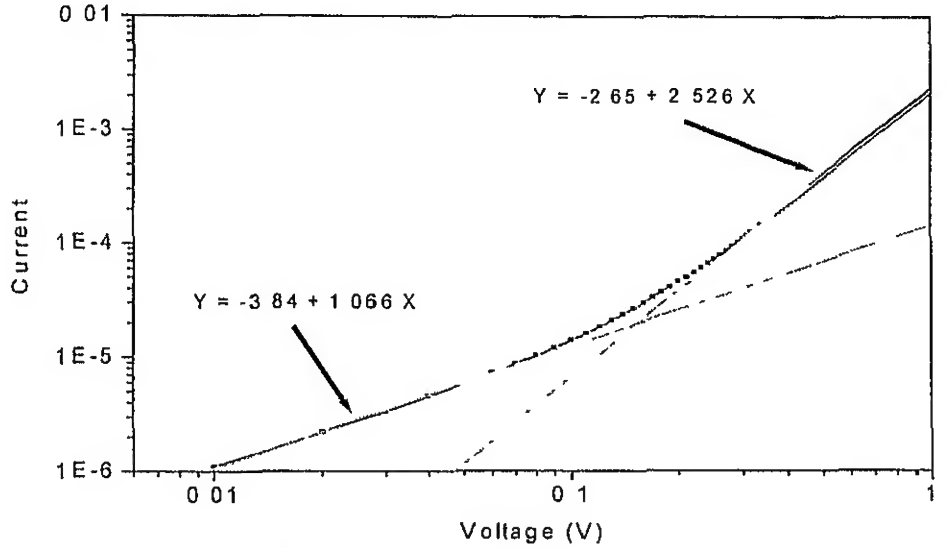

Fig 6.3.1: I-V characteristics of a PPV device

The reverse bias affects the forward I-V of a PPV device after application of reverse-bias as shown in Figure 6 3.2

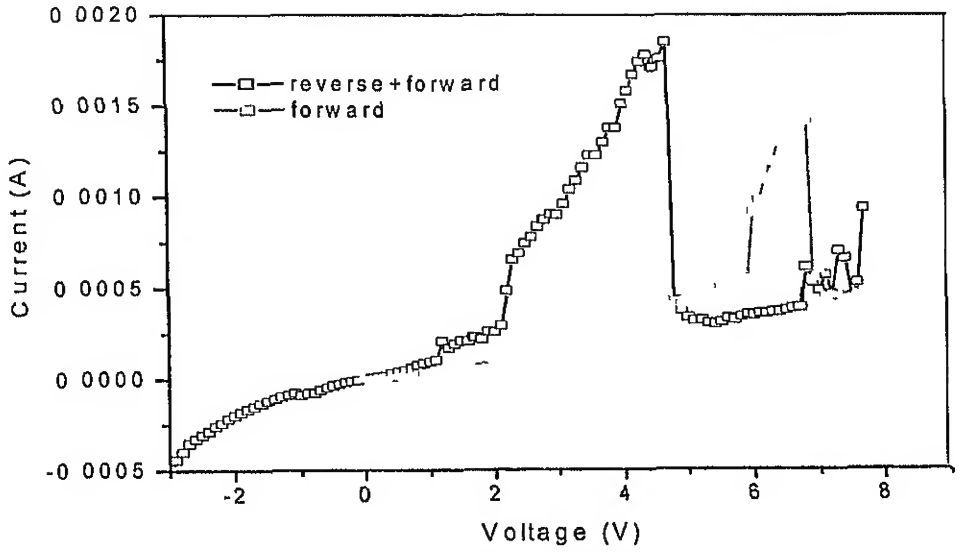

Fig 6.3.2: Reverse bias behaviour of a PPV device

First the I-V characteristic of the device is checked for proper diode characteristics Then after waiting for 20 sec at –3 V reverse bias, the voltage is swept from –3 V to 8 V at a sweep rate of 0 1 V/sec A peak appears in the forward I-V at around 4 V This may be due to suspected space charge accumulation near the electrodes resulting in the increased injection and hence a higher current density After 4V, it appears that the accumulated space charge during reverse bias gets dispersed due to forward bias resulting change in charge polarity

Reverse Bias Forward Bias

Accumulation of charges at the electrode either due to interface polarization or barrier formation with reverse bias During subsequent forward bias, the current is lower and the voltage at which peak occurs is also higher Then at higher voltages the current levels again returns to lower current state This may be attributed to lower space charge concentration in second sweep

The current density of the device increased with successive sweeps ultimately leading to a shorting of device After keeping the device for three months, there is no significant change in current levels Then on applying reverse bias, again a peak appears in the I-V characteristics The I-V is shown in Figure 6 3 3

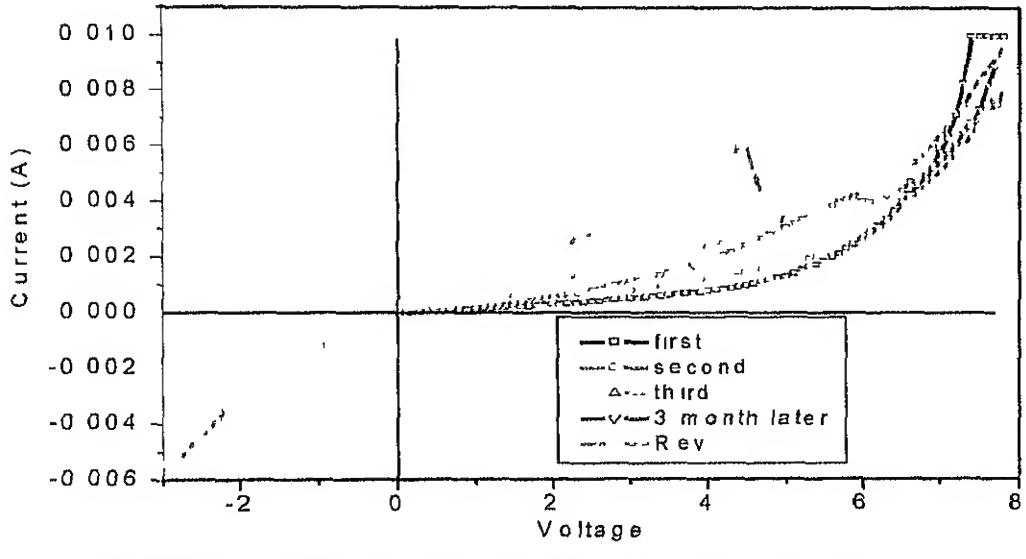

Fig 6.3.3: I-V sweeps on a PPV device and the reverse bias behaviour

Following this measurement, it was suspected that such instabilities can be due to impurities The PPV polymer was further purified and then the I-V characteristics of fresh devices were measured as shown in the Figure 6 3 4 Now under forward bias, there is decrease in current levels on successive sweeps for higher voltages, which may be due to degradation

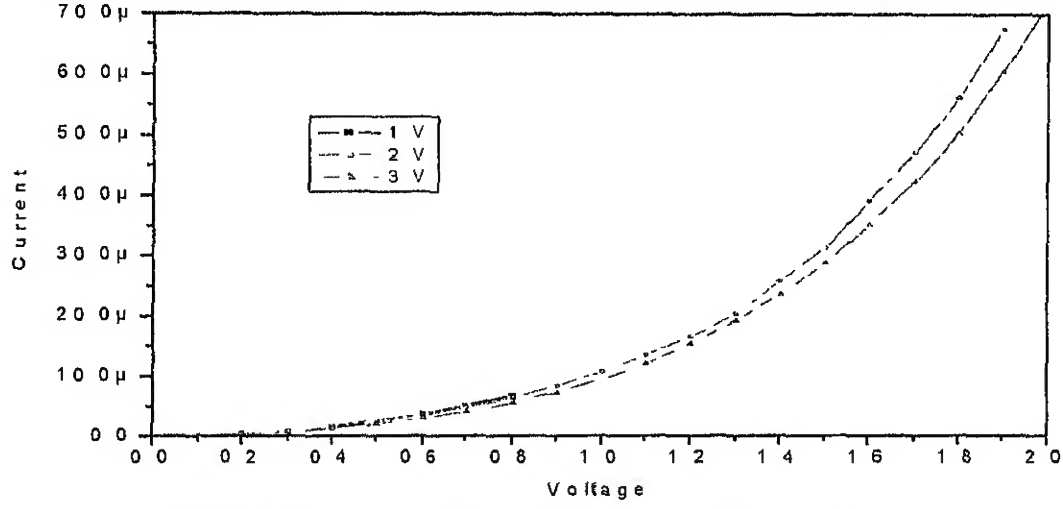

Fig 6.3.4: Variation of I-V with voltage for PPV device

Hence I-V was measured keeping the sweep levels of voltages constant from 0 to 2 V, to separate out the contribution of degradation Figure 6 3 5 summarizes I-V changes over five sweeps Clearly electrical characteristics are sensitive to sources of charge process in the material and interfaces Devices made out of purer material gave better I-V characteristics However it still depends on number of measurement sweeps Hence it can be inferred that higher turn-on voltage with higher voltage may be actually due to degradation rather than due to increase of voltage

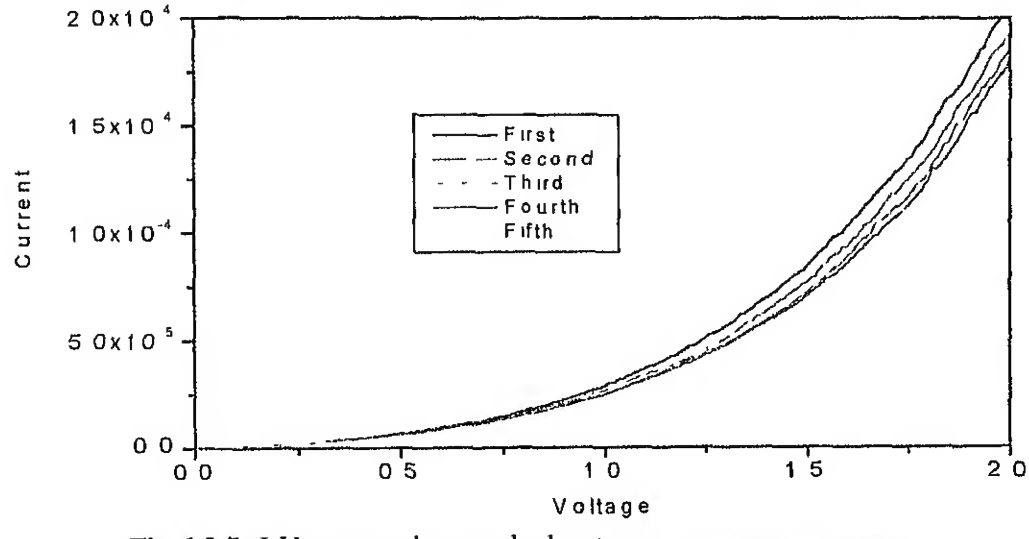

Fig 6.3.5: I-V sweeps showing higher turn on successive sweeps

During the course of this work, impedance spectroscopy was attempted to separate out the factors of degradation and to distinguish between degradation due to contacts and degradation due to material. However it was observed that application of sinusoidal voltage to the device during the measurements changes I-V characteristics of the device as shown in Figure 6.3.6 indicating that AC voltage may lead to either accumulation of charge or polarization in the device

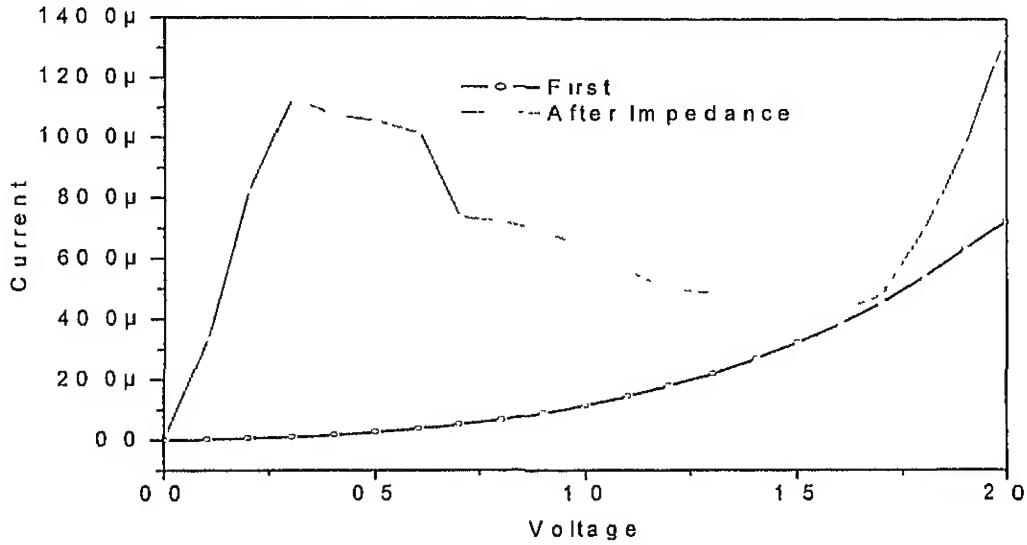

Fig 6.3.6: I-V before and after impedance spectroscopy on device

When impedance spectroscopy was attempted in vacuum, it also showed instability during I-V measurements, which in turn became almost linear. But surprisingly it recovered partly in keeping the device without applying bias for one day in vacuum

6.3.1 Electroluminescence and its degradation of Bilayer Device

Electroluminescence from single layer PPV device was very short-lived for performing the experiments. So ITO/PEDOT/PPV/CNPPV/Al device was used for this study. Double layer increases the stability of the device and increases the efficiency by providing charge balance and avoiding quenching of electrons and holes. Encapsulation under nitrogen environment with a glass plate was also tried with UV curable epoxy. The encapsulation gave better results with more brightness and higher lifetime

As we have seen that device characteristics are also very sensitive to process other than material degradation. In order to get an idea of device lifetime, intensity can be monitored as a function of time. The EL spectrum of the device is shown in Figure 6.3.1.1

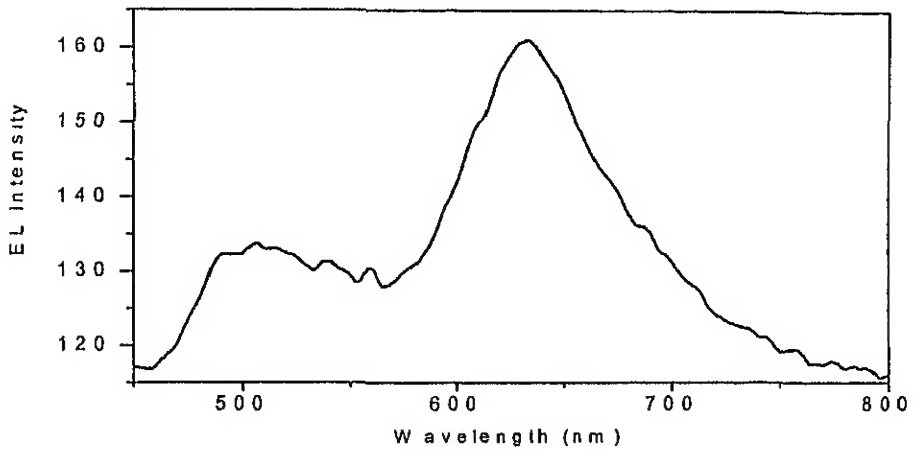

Fig 6.3.1.1: EL spectrum of Bilayer Device

The spectrum shows contribution from the PPV as well. The recombination mainly takes place in the CNPPV region as the electron injection and transport becomes the bottleneck in the process. There was degradation in the EL intensity when the device was kept under electrical stress even when encapsulated. The plot showing the decrease in the EL intensity for a typical device is shown in Figure 6.3.1.2

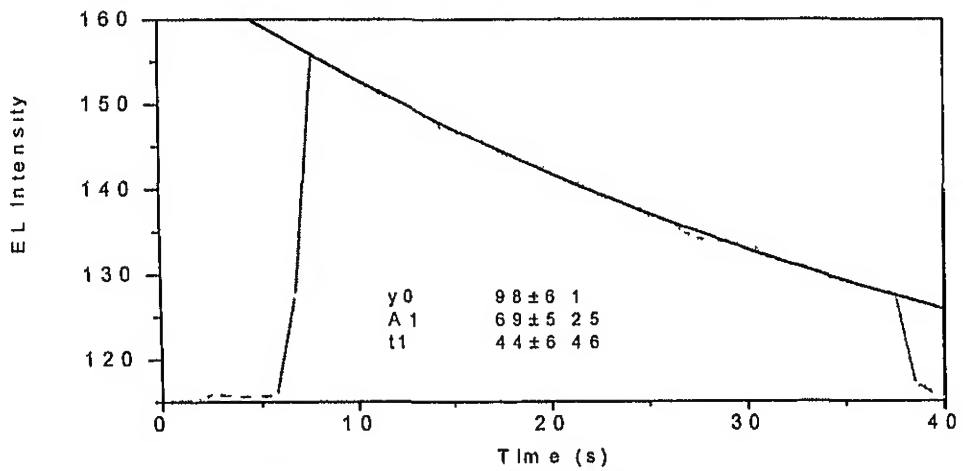

Fig 6.3.1.2: EL decay of Bilayer Device

The EL showed first order exponential decay with time constant of around 44 sec However it is not possible to isolate at this stage the step that limits lifetime Our studies suggest that at the photon densities of operation of the device, material degradation being not the rate-limiting step. The material degrades in air at much higher photon densities in thousands of seconds. Hence device characteristics or injection mechanisms seem to limit EL rather than photo-oxidation of material in present study.

Summary

Though degradation of luminescence due to photo-oxidation in the light emitting polymers is by now a well known fact as is clear from our review in Section 4.3, there are several significant features of the phenomena that are yet to be coherently understood. In this study, we have described laser induced degradation of PL as a method of evaluating process and material quality. This has been used to study the effect of preparation ambient and baking conditions on degradation resistance of thin films of PPV and CN-PPV. We also show that at the present stage of our device development effort in the Laboratory, the device lifetime is limited by a faster process than material degradation due to photo-oxidation, and that devices are unstable and sensitive to charge accumulation processes.

We report for the first time significant systematic similarities and differences between laser induced degradation of PPV and CN-PPV. The PL intensity degradation in air for PPV shows two rate constants for all samples, whereas baked CN-PPV shows only one characteristic decay rate constant. In addition, we observe significant changes in spectral feature for PPV with degradation in contrast to the case of CN-PPV. Both these facts taken together suggest that defects created in PPV by photo-degradation influence the environment of the chromophores. In contradistinction to this, in CN-PPV there seems to be diffusion of carriers or excitons from degraded chains to undegraded chains, and hence PL intensities decrease without observable changes in spectral features. This has been invoked by Gobato et al. (2002) in PPV to explain their findings regarding PL intensity dynamics due to laser induced effects in air. They have also reported observation of PL enhancement for thick films (few microns), while for films thinner than the penetration depth of the laser both initial increase and then decrease of PL intensities have been observed. Note that in this work all films were thinner than the penetration depth of the laser and we only observe intensity decay for all cases in air, while enhancement is observed for all cases in vacuum. More work is required to understand the origin of PL enhancement, and increased degradation resistance due to laser irradiation in vacuum. Specifically a correlation of surface modification using microscopy (AFM), and changes in absorption coefficient using transmittance and ellipsometric studies are needed to unravel mechanisms underlying these effects.

7. Conclusions

The display technology based on organic or polymer light emitting diodes provides a good prospect of becoming the dominant technology of flat and possibly flexible displays in the near future due to its many advantages. However, the major problem with PLED/ OLED is the degradation and lifetime of the devices. Hence there is at present extensive research in this field to control the degradation of OLED, which prevents widespread commercialization of OLED/ PLED technology In this work, UV laser induced degradation of polymers such as PPV and CN-PPV is studied under different conditions of preparation such as ambient and baking schedule.

In the current study, thin films of PPV and CN-PPV were spin-coated on glass plates, and primarily their photoluminescence degradation was studied with 442 nm line of He-Cd laser under vacuum and ambient conditions Preliminary observations on instabilities associated with electrical measurements of devices fabricated from same material have also been pointed out.

A summary of the results obtained are listed below:

1. Reflectance and photoluminescence: effect of optical geometry of samples

   This work involved monitoring PL spectra, and PL intensity as a function of time; during the course of this work several useful features in optical characterization of these thin films on glass substrates were encountered e.g

   - Reflectance of polymer film changes with back metallization and hence PL intensities show an approximate four times increase in photoluminescence with back metallization.
   - Double coated PPV films at 800 rpm from a Xanthate precursor solution of 18mg/cc gives around 0.5 microns thickness; and this is the order of thickness, which we could reliably characterize by spectral reflectance measurements. Most films studied in this work are an order of magnitude smaller, and can be considered thin as compared to the penetration depth of the 442nm laser light used for excitation and photodegradation.
   - PL intensities are higher when laser is irradiated from the glass side than when irradiated from the film side since reflectivity of air/polymer interface is more than glass/polymer interface.

2. PL intensity varies linearly with excitation intensity till the maximum intensities used ($0.5mW/mm^2$).

3. Laser induced degradation in air of PPV films
   - PPV thin film PL intensity degrades with time in air with laser irradiation at 442nm with power $0.5mW/mm^2$ showing second order exponential decay with time constants of the order of approximately 110 and 900 seconds
   - PL spectrum fits with four Gaussian peaks observed at 508, 543 1, 580.9, 603 6 nm respectively with 508nm peak corresponding to the HOMO-LUMO gap and others as well resolved phonon replicas.
   - Peak2 at 543nm blue shifts by 5.4 nm while peak4 red shifts by 45.6 nm
   - Peak1 decays fastest and peak2 decays slowest.
   - Except for Peak 2FWHM of all other peak decrease slightly with increase in exposure time; FWHM of peak2 increases from 35nm to 51nm
   - Red shift and FWHM increase for Peak 4 at 603nm taken together suggests that it is associated with torsional mode of vibration which is hindered by carbonyl or formation of other PL quenching centers with laser exposure in air

4. Laser induced PL degradation for vacuum dried PPV films
   - PL enhancement was observed with laser irradiation in vacuum, however, in contrast PL decay was observed when irradiated in air.
   - Both the dominant peaks at 508nm and 543nm display second order exponential decay of PL intensity with exposure time.
   - Slight blue shift of the peak2 is observed showing that it is the peak at 540nm that is most sensitive to changes in conjugation length
   - Degradation in air is slower for vacuum dried samples as compared to oven dried samples in nitrogen demonstrating efficacy of vacuum drying in reducing oxygen content of processed films
   - No peak shift occurs when laser irradiation is carried out under vacuum clearly indicating absence of productionof quenching centers which affect conjugation length of polymer chains
   - Partial recovery of PL intensity occurs in vacuum following laser irradiation in air.

5. Laser induced PL degradation in air of CNPPV films coated and baked in air
   - CNPPV film PL spectrum red shifts with baking along with narrowing in spectrum
   - PL Unbaked sample degrades very fast which decreases on baking but again increases for baking for higher time.
   - Unbaked sample shows blue shifting along with increase of width of the spectrum.
   - No peak shift observed in CNPPV with decrease in PL intensity showing that degraded chains do not give rise to PL, most probably owing to diffusion of carriers from degraded to undegraded chains.
   - First order exponential decay is observed with laser induced degradation in air for baked samples, while the decay is second order for unbaked sample The time constants of degradation due to retention of solvents and due to oxidation from the ambient are different giving rise to two time constants for unbaked samples.
   - Red shift in transmittance minima is observed for baked samples as compared to unbaked samples.

6. Laser induced PL degradation of CNPPV films processed in nitrogen ambient
   - CNPPV film PL spectrum red shifts with baking along with narrowing in spectrum
   - PL intensity shows initial decay, and then enhancement observed for unbaked sample suggesting competition between degradation and in-situ drying
   - Degradation is observed, but enhancement is also observed for higher times in baked samples
   - Degradation rate for samples baked in nitrogen ambient is slower compared to air baked samples indicating the role of oxygen or moisture in the film in degradation
   - First order exponential decay both for baked and unbaked samples in contrast to second order decay for PPV in all cases
   - Slight blue shift of longer wavelength is observed accompanied by decrease in width is observed
   - The degradation rate is dependent non-linearly on photon flux and nearly halves when intensity of the laser is reduced by a factor of 0.3

7. Laser induced PL in vacuum of CNPPV films prepared in nitrogen ambient:
   - PL enhancement followed by a slight decay is observed under vacuum
   - However, decay is observed when laser irradiated in air, though significant resistance to photo-degradation is observed following laser irradiation in vacuum

- A small second order exponential decay is again observed when put in vacuum and then irradiated with laser suggesting entrapment of oxygen during laser irradiation in air
- Slight blue shift and spectrum narrowing is observed laser exposure in vacuum, and these changes are more pronounced for exposure in air
- Under subsequent laser irradiation in vacuum, no further change in spectral lineshape is observed

8 Electrical Characteristics of typical sample devices

- Accumulation is space charge seen in the forward I-V after application of reverse bias, and degree of accumulation decreases with subsequent sweeps
- No significant change is observed in I-V with storage for about three months
- Proper processing of polymer reduces space charge showing degradation with sweeps
- Electroluminescence decay of typical bilayer PPV-CNPPV (nominally encapsulated under dry nitrogen) device with a time constant of 44 sec is observed
- The observed EL decay is not limited by material degradation due to light emission since this work shows that it occurs on much longer time scale for as high intensity as $0.5 mW.mm^2$; device parameters for current devices are degrading faster than material properties.

In short we demonstrate the importance of laser induced accelerated degradation tests, and also show that the resistance to degradation of light emitting polymers can be increased by UV laser irradiation under vacuum.

Future scope of Work

- This work opens up heuristics for further work on degradation characterization in course of development of polymers Hence this can be used to optimize processing conditions and more importantly to elucidate underlying mechanisms of degradation in air and PL enhancement under vacuum.
- Correlated studies on FTIR for vibration modes and ellipsometry for progressive changes in optical constants and thickness would be extremely useful in identifying structural changes both at the level of chain and aggregation in thin film form.
- The functional dependence of decay time on light flux would be useful in defining rates and characterizing degradation reactions.
- Needless to say, correlation of material degradation to device degradation is an urgent task, which was out of scope of this work. Electrical characterization based on impedance spectroscopy is needed to distinguish between contact and bulk degradation, and the role of interfaces in determining device characteristics and ultimately lifetime of PLEDs.

References

1. Antoniadis, H.; Hsieh, B. R.; Abkowitz, M. A.; Jenekhe, S A and Stolka, M. (1994), *Synth. Metals* **62**, 265

2. Antoniadis, H.; Miller, J N., Roitman, D. B and Campbell, I H (1997), *IEEE Trans. Electron Devices* **44**, 1289

3. Aziz H. and Xu, G. (1996), *Synth Met.* **80**, 7

4. Bao, Z. (2000), *Adv Mater.*, **12**, 227

5. Berntsen, A.; Weijer, P. V. D ; Croonen, Y.; Liedenbaum, C and Vleggaar, J. (unpublished)

6. Birmstock, J.; Biassing, J.; Hunze, A.; Scheffel, M. and Winnacker, A. (2001) *Appl. Phys. Lett* **78**, 3905

7 Brabec, C. J ; Padinger, F ; Hummelen, J C., Janssen, R. A. J. and Sariciftci, N. S. (1999), *Synth Met* , **102**, 861

8. Brabec, C J.; Sariciftci, N. S. (2000), *Semiconducting Polymers – Chemistry, Physics and Engineering*, Hadziioannou, G., van Hutten, P F., Eds.; Wiley-VCH, Weinheim, Germany.

9. Brabec, C. J ; Sariciftci, N. S. and Hummelen, J C. (2001), *Adv Funct. Mater* , **11**, 15

10. Braun, D. and Heeger, A. J. (1991), *Appl. Phys. Lett.* **58**, 1982

11. Bredas, J L., Cornil, J. and Heeger, A. J. (1996), *Adv Mater* **8**, 447

12. Buchanan, M.; Webb, J. B and Williams, D. F. (1980), *Appl. Phys. Lett.* **37**, 213

13. Bulovic, V., Burrows, P. E. and S. R. Forrest, S R. (2000), *Molecular Organic Light-Emitting Devices, Semiconductors and Semimetals*, Vol **64**

14. Burroughes, J. H.; Bradley, D. D. C.; Brown, A. R.; Marks, R. N.; Mackay, K.; Friend, R. H ; Burns, P. L. and Holmes A. B (1990), *Nature* **347**, 539

15. Burrows, P. E.; Bulovic, V.; Forrest, S. R., Sapochak, L S.; McCarty, D M. and Thomson, M. E. (1994), *Appl.Phys. Lett.* **65**, 2922

16. Cacialli, F.; Friend, R. H.; Moratti, S. C. and Holmes, A B. (1994), *Synth Met.* **67**, 157

17. Carter, S. A.; Angelopoulos, M.; Karg, S.; Brock, P. J. and Scott, J. C. (1997), *Appl. Phys. Lett* **70**, 2067

18. Chao, C. L ; Chuang K R. and Chen, S. A. (1996), *Appl Phys Lett.* **69**, 2894

19. Chayet, H., Pogreb, R and Davidov, D. (1997), *Phys Rev* B **56**, R12707

20. Chen L K. P and Chua, S J. (2002), *Appl Phys. Lett* , **80**, 697

21. Chen, S. and Chang, E C. (1998), *Macromolecules*, **31**, 4899-4907

22. Chen, Y.; Huang, Z. E.; Cai, R. F. and Yu, B. C. (1998), *Eur Polym J* , **34**, 137

23. Chiang, C. K.; Fischer, C. R ; Park, Y. W.; Heeger, A. J., Shirakawa, H.; Louis, E.J ; Gau, S. C and MacDiarmid, A G., (1995) *Phys Rev. Letters*, **39**, 1098

24. Cole K. S. and Cole, R. H (1941), *J Chem Phys* **9**, 341

25. Coutal, C , Azema, A and Roustan, J. C. (1996), *Thin Solid Films* **288**, 248

26. Cumpston B. H. and Jensen, K F. (1995), *Synth. Met* **73**, 195

27. Cumpston, B H., Parker, I. D. and Jensen, K. F. (1997), *J Appl. Phys* **81**, 3716

28. Do, L M.; Han, E. M ; Niidome, Y.; Fujihira, M.; Kanno, T.; Yoshida, S.; Maeda, A. and Ikushidma, A. J. (1994), *J Appl Phys* **76**, 5118

29. Do, L. M.; Oyamada, M.; Koike, A.; Han, E. M.; Yamamoto, N and Fujira, M. (1996), *Thin Solid Films* **273**, 209

30. Dolabalapur, A. (1998), *Appl Phys. Lett* **73**, 142

31. Echegoyen, L. and Echegoyen, L. E (1998), *Acc. Chem. Res.*, **31**, 593

32. Friend, R H.; Gymer, R. W.; Holmes, A. B.; Burroughes, J. H.; Marks, R. N.; Taliani, C.; Bradley, D. D. C.; Dos Santos, D A ; Brédas, J. L.; Lögdlund, M.and Salaneck, W R. (1999), *Nature*, **397**, 121

33. Fujihira, M ; Do, L. M.; Koike, A. and Han, E. M. (1996), *Appl. Phys. Lett.* **68**, 1787

34. Gao, J.; Hide, F. and Wang, H. (1997), *Synth Met.*, **84**, 979

35. Geckeler, K. E. and Samal, S (1999), *Polym. Int* , **48**, 743

36. Gobato, Y. G.; Marletta, A.; Faria, R. M ; Guimaraes, F. E. G.; de Souza J. M and Pereira, E. C. (2002), *Appl. Phys. Lett.* **81**, 942

37. Greenham, N. C.; Moratti, S. C.; Bradley, D D. C.; Friend R H and Holmes, *A. B. (1993), Nature* **365**, 629

38. Gundlach, D. J., Kuo, C. C.; Nelson, S. F., Jackson, T. N. (1999), *57 Device Research Conference Digest*, **164**

39 Hadziioannou, G ; Van Hutten, P F. and Malliaras, G. G (1997), *Macromol. Symp* , **121**, 27

40. Hamaguchi, M. and Yoshino, K. (1996), *Appl. Phys Lett.* **69**, 143

41. Han, L. M. Do, Nidome, Y. and Fujihira, M. (1994), *Chem Lett* 969

42. Ho, P K. H.; Kim, J S.; Burroughes, J. H.; Becker, H., Li, S F Y , Brown, T. M.; Cacialli, F. and Friend, R. H. (2000), *Nature*, **404**, 481

43. Hung, L. S.; Tang, C W amd Mason, M. G (1997), *Appl. Phys Lett.*, **70**, 152

44. Ishii, H and Seki, K (1997), *IEEE Trans. Electron Devices* **44**, 1295

45. Karg, S.; Riess, W ; Dyakonov, V. and Schwoerer, M. (1993), *Synth Metals* **54**, 427

46. Karg, S ; Scott J C. and Salem, J R. (1996), *Synth. Met.* **80**, 111

47. Ke, L.; Chua, S. J.; Zang, K. and Chen, P. (2002), *Appl. Phys Lett* **80**, 171

48. Kim, H.; Pique, A.; Horwitz, J. S.; Mattoussi, H ; Murata, H , Kafafi, Z H and Chrisey, D. B. (1999), *Appl. Phys Lett* **74**, 3444

49. Kim, J. S.; Granström, M., Friend, R. H ; Johanssen, N.; Salaneck, W. R., Daik, R.; Feast, W. J. and Cacialli, F. (1998), *J. Appl Phys.*, **84**, 6859

50. Klauk, H. and Jackson, T. N. (2000) *Solid State Technology* **63**, March

51. Koch, A. T. H.; Harrison, N. T.; Haylett, N.; Daik, R ; Feast, W. J and Friend, R. H. (1999), *Synth Met.*, **100**, 113

52 Kumar, S,; Biswas A K., Shukla V. K ; Awasthi, A., Anand R. S. and Narain J (2003), *Paper presented at OP2003, 5th International Topical Conference on Optical Probes for Conjugated Polymers and Organic & Inorganic Nanostructures: (To appear in Synthetic Metals, Nov 2003)*

53 Kuzina S. I and Mikhailov, A. I. (1993), *Eur Polym J.* **29**, 1589

54 Lee, J G , Kim, Y.; Jang, S H.; Kwon, S. N and Jeong, K (1998) *Appl. Phys Lett* **72**, 1757

55. Malliaras, G. G ; Salem, J R.; Brock, P. J and Scotta, J C. (1998), *J. Appl Phys* **84**, 1583

56. Marks, R. N ; Halls, J. J. M., Bradley, D D C.; Friend, R. H. and Holmes, A. B. (1994), *J. Phys Condens Matter* **6**, 1379

57. Maruyama T and Fukui, K. (1991), *Thin Solid Films* **203**, 297

58. May, P. (1995), *Phys. World*, **8(3)**, 52

59. McElvain, J.; Antoniadis, H , Hueschen, M. R , Miller, J N., Roitman, D. M.; Sheats, J. R. and Moon, R. L (1996), *J Appl. Phys.* **80**, 6002

60. Milliron, D. J.; Hill, I G., Shen, S., Kahn, A and Schwartz, J. (2000), *J Appl. Phys* **87**, 572

61 Nath, P ; Bunshah, R. F ; Basol, B. M and Staffsud, O. M. (1980), *Thin Solid Films* **72**, 463

62. Nguyen, T. P.; Molinie', P.; Le Rendu, P. and Tran, V. H. (1997), *Synth. Met.* **84** 679

63. Nguyen, T. P.; Spiesser, M.; Garnier, A.; de Kok, A. M. and Tran, V. H (1999), *Mat Sc. & Engg.* **B60**, 76

64. Ohmori, Y.; Uchida, M.; Muro, K. and Yoshino, K. (1991), *Jpn. J Appl Phys.***30**, L1941

65. Onada, M. and Yoshino, K. (1995), *Jpn. J Appl. Phys* **30**, L260

66 Padro, D. A.; Jabbour, G. E. and Peyghambrian, N. (2000), *Adv Mater.* **17**, 1249

67. Papadiamitrakopoulos, F.; Yan, M.; Rothberg, L. J.; Katz, H. E.; Chandross, E. A. and Galvin, M. E. (1994), *Mol. Cryst. Liq Cryst.* **256**, 663

68. Papadimitrakopoulos, F., Zhang, X. M.; Thomsen, D. L. and Higginson, K. A. (1996), *Chem. Mater* **8**, 1363

69 Parker, I. D. (1994), *J Appl. Phys.* **75**, 1656

70. Paıker, I. D. (1994), *J. Appl Phys.* **78**, 930

71 Pıchler, K. (1997), *Philos. Trans. R. Soc London, Ser* A **355**, 829

72. Roman, L. S., Hummelgen, I. A.; Nart, F. C.; Peres L. O. and Sa, E L. (1996), *J Chem Phys.* **105**, 10614

73. Rothberg, L. J.; Yan, M.; Papadiamitrakopoulos, F.; Galvin, M. E.; Kwock E.W. and Miller, T. M. (1996), *Synth. Met.*, **80**, 41

74. Saınova, D.; Miteva, T.; Nothofer, H G.; Scherf, U.; Glowacki, I.; Ulanskı, J., Fujikawa, H. and Neher, D (2000), *Appl. Phys. Lett* **76**, 1810

75. Salbeck, J. and Bunsenges. B. (1996), *Phys. Chem.* **100**, 1667

76 Saıcıftci, N. S.; Braun, D ; Zhang, C.; Srdanov, V. I.; Heeger, A. J.; Stucky, G.and Wudl, F. (1993) *Appl Phys Lett* , **62**, 585

77. Sariciftci, N. S ; Smilowitz, L ; Heegeı, A. J and Wudl, F., (1992) *Science*, **258**, 1474

78. Sarker, A. M.; Dıng, L.; Lahti, P M. and Kaıasz., F. E. (2002), *Macromolecules* **35**, 223

79. Schlatmann, A. R ; Floet D. W. and Hilberer, A. (1996), *Appl. Phys. Lett.* **69**, 1764

80. Scott, J. C.; Kaufman, J. H.; Brock, P. J ; DiPietro, R ; Salem, J. and Goitia, J. A (1996), *Appl. Phys.* **79**, 2745

81. Scurlock, R. D.; Wang, B., Ogılby, P R., Sheats, J. R. and Clough, R. L. (1995), *J Am Chem. Soc* **117**, 10194

82. Seguıa, J. L. (1998), *Acta Polym* , **49**, 319

83 Shasheen, S. E.; Brabec, C. J.; Saıiciftcı, N. S., Padinger, F.; Fromherz, T. and Hummelen, J. C. (2001), *Appl. Phys Lett.*, **78**, 841

84. Shim; H. K ; Murase; I ; Ohnishi; T.; Noguchi T. and Hiıooka, M. (1984), *Polym. Commun.* **25**, 327

85. Shimizu, J. A. (2000), Single Panel Reflective LCD Optics (Philips Research)

86. Shirakawa, H.; Louis, E. J.; MacDiarmid, A. G.; Chiang, C K. and Heeger, A. J., (1977) *J Chem. Soc. Chem Commun.*, 578

87. Skordoulisa, C D., Brouwerb, H J. and Hadziioannoub, G. (1999), *Optics and Laser Technol*, 259

88. Son, S.; Dolabalapur, A.; Lovinger, A. J. and Galvin, M. E (1995), *Science* **269**, 376

89. Sutherland, D. G J ; Carlisle, J. A., Elliker, P ; Fox, G ; Hagler, T. W.; Jimenez, I.; Lee, H. W., Pakbaz, K.; Terminello, L. J., Williams, S. C., Himpsel, F. J.; Shuh, D. K.; Tong, W M.; Jia, J. J., Callcott, T. A and Ederer, D. L. (1996), *Appl. Phys. Lett.* **68**, 2046

90. Talaie, A ; Lee, Y K.; Huh, G.; Kim, K M.; Jeong, H Y , Choo, D J ; Lee, J. Y. and Jang, J. (2001), *Materials Science and Engineering* **B85**, 177

91 Tang, C W and Vanslyke, S A. (1987), *Appl. Phys. Lett* **51**, 913

92 Tessler, N. (1999), *Adv. Mater* , **11**, 363

93. Vasu V. and Subrahmanyam, A. (1990), *Thin Solid Films* **193/194**, 696

94 Vaz, A.; Queiroz, K. S.; Cavalcanti, G. B ; Lins, R. V.; Santos, C G.; Nascimento, M. P. and Melo, C. P. (2001), *Synth Met.* **121**, 1727

95. Wang, W.; Lim, S. F. and Chua, S. J. (2002), *J Appl. Phys.* **91**, 5712

96. Watanabe, T ; Nalwa, H. S. and Miyata, S., *Organic Electroluminescent Materials and Devices*

97 Wessling R. A. and Zimmerman, R. G. (1962) *U.S Patent* **3401**,152

98. Wu, W. F.; Chiou, B. S. and Hsieh, S T (1994), *Semicond Sci Technol* **9**, 1242

99. Xing, K. Z.; Fahlman, M.; Chen, X. W.; Inganàs, O and Salaneck, W R (1997), *Synth Met* , **89**, 161

100. Xu, B.; Zhang, J. and Peng, Z. (2000), *Synth Met.* **113**, 35

101. Yakimov, A. V.; Davidov, D. and Progreb, R. M. (1997), *Appl. Phys. Lett.* **71**, 3344

102. Yan, M. (1994), *Phys. Rev. Lett* **73**, 744

103. Yu, G.; Pakbaz, K. and Heeger, A. J. (1994), *Appl. Phys. Lett.* **64**, 3422

104. Yu, G.; Zhang, C and Heeger, A. J (1994), *Appl. Phys. Lett* **64**, 1540

105. Zhao, J.; Yang, Z., Han, S., Ye, L. and Xie, S (2001), *Displays* **22**, 101

106 Zheng J P. and Kwok, H. S (1993), *Appl. Phys. Lett.* **63**, 1

107. Zhou, X., He, J ; Liao, L. S.; Lu, M., Xiong, Z. H.; Ding, X M ; Hou, X. Y., Tao, F G.; Zhou C E. and Lee, S. T. (1999), *Appl Phys. Lett* **74**, 609

108. Zyung T and Kim, J J. (1995), *Appl Phys. Lett* , **67**, 3420

Appendix

PPV peakfit results and conclusions

Time(s)	Peak1				Peak2				Peak3				Peak4				Total Area
	Pos	Int	FWHM	Area	Pos	Int	FWHM	Area	Pos	Int	FWHM	Area	Pas	Int	FWHM	Area	
0	508	1	29 05	1	543.1	1	35 37	1	580 9	1	44 4	1	603 6	1	113 4	1	1
100	507.7	0 80	29	0.8	542 6	0 83	36 55	0 86	580 8	0.8	44 33	0.84	606.4	0.83	112.79	0.82	0.83
200	507 4	0.68	29.26	0 68	542 4	0 72	37 39	0 76	581 2	0 7	43 35	0.71	607 8	0.73	114 65	0 73	0.73
300	507.2	0 59	29 28	0 6	541 6	0 64	37 64	0.68	579 6	0.7	45 98	0.68	610.1	0.63	112 78	0.55	0.65
400	506 9	0.52	29.43	0 52	541.4	0 58	38 88	0 64	580 5	0 6	44 79	0 61	612 7	0 57	111 59	0 56	0.59
500	506.7	0 45	29.61	0.46	540 6	0 51	38 88	0 56	578 5	0 6	47 07	0 59	614.8	0.49	113 86	0 50	0 52
600	506 7	0 42	29 96	0 43	540.8	0 49	39 51	0 54	579 8	0 5	46 31	0 56	619.3	0 44	109 44	0 43	0 49
700	506 4	0 37	29 76	0 38	540 5	0 45	40 47	0 52	580	0 5	45 48	0 49	618 7	0 41	111 68	0 41	0 45
800	506	0 33	29 21	0 33	540.2	0 42	42.33	0 51	581 2	0 4	45.58	0 45	624 4	0 35	101 68	0 32	0 41
900	506 1	0 3	29 51	0 31	540 1	0 4	42 31	0 47	581 4	0 4	43 8	0 38	619.8	0 37	115 57	0 37	0 40
1000	505 7	0 27	28 96	0 27	539 8	0 37	43 7	0 46	582	0 3	42 82	0 33	621	0 34	114.32	0 34	0 37
1100	505 9	0 26	29 66	0 26	539.7	0 35	43.13	0 43	581 2	0 3	44 95	0 35	625 9	0 31	112 82	0 31	0.35
1200	505.9	0.24	29 47	0.24	539.7	0.34	43.91	0 42	581 9	0.3	42 2	0 30	627 3	0 30	110 84	0 29	0.33

1300	506	0 22	29 43	0 23	539 6	0.32	43 82	0 39	581 5	0 3	43 61	0.29	628 7	0 28	112 9	0 28	0 31
1400	505.5	0.2	29 19	0 2	539.5	0 31	46.6	0 41	583.7	0.3	41.71	0.25	631 8	0 26	107.61	0 25	0 30
1500	506	0.2	29.29	0 2	538 6	0 28	43 42	0.35	579 3	0 3	48 13	0.34	638 1	0 23	97 26	0.20	0 28
1600	505.5	0 17	28 82	0 16	538 9	0 28	47 33	0 37	583 5	0.2	41.87	0.22	634.8	0 23	107.47	0.22	0 26
1700	506	0.16	28 12	0.16	538.8	0 26	45 87	0 34	582.6	0.3	44 31	0 25	642 6	0.20	90 14	0 20	0.24
1800	505.8	0.15	28.55	0.15	539	0.25	47.35	0.34	584	0 2	42 02	0.21	641.8	0.21	100.72	0 18	0.24
1900	505.5	0 14	27 97	0.13	538.7	0 25	49 05	0 34	584 9	0.2	40 9	0 18	642.7	0 20	101 09	0.18	0.23
2000	506	0 13	28 82	0 13	538 9	0.23	48 42	0 32	584 7	0 2	41 05	0.18	645 7	0 2	95.79	0 17	0.22
2100	506	0 12	28 18	0.11	538 3	0 23	49 58	0 32	584 9	0.2	42 08	0 17	646 4	0 19	103 67	0 17	0 21
2200	506	0.11	27.83	0 10	538 4	0.22	50.89	0.32	586	0 2	39 31	0.14	645 8	0.19	101.38	0 17	0 20
2300	505.6	0 1	27 15	0.1	538	0 21	50.59	0 30	585 4	0.2	40.82	0.16	649 5	0 18	84.92	0 13	0.19
2400	505.7	0 09	27 49	0.09	537 7	0.21	51.75	0 30	586 3	0.1	41 22	0 14	648.7	0 18	96 76	0.15	0.19

Degradation Conclusions

1. Intensity and area of all the peaks decreasing exponentially with time
2. FWHM of peak1 is almost constant, but for peak2 it is almost monotonously increasing and for peak4 monotonously decreasing.
3. Peak2 is blue shifting by around 4nm in 1000 sec.